International Scientific-Technical and Production Journal

CONTENTS

COMPARATIVE EVALUATION OF SENSITIVITY OF WELDED JOINTS ON ALLOY INCONEL 690 TO HOT CRACKING

**K.A. YUSHCHENKO, V.S. SAVCHENKO, N.O. CHERVYAKOV, A.V. ZVYAGINTSEVA,
G.G. MONKO** and **V.A. PESTOV**

E.O. Paton Electric Welding Institute, NASU, Kiev, Ukraine

Sensitivity of metal of the welds made with wires Inconel® 52 and Inconel® 52MSS to hot cracking was evaluated. The machine testing methods (Varestraint-Test and PVR-Test), which provide for forced deformation of test specimens during welding, were used. The welds made with wire Inconel 52MSS were shown to be more resistant to ductility dip cracking, but several times more sensitive to solidification cracking. Evaluation of ductile properties of the weld metal using the «Ala-Too» machine showed that the Inconel 52MSS type weld metal had no ductility dip, whereas the Inconel 52 type weld metal was characterized by a pronounced decrease in the elongation values.

Keywords: *TIG welding, nickel alloys, filler wire, weld metal, evaluation of crack resistance, ductility dip range, grain boundary, forced deformation*

Welded joints on high-alloy steels with a stable austenitic structure and nickel alloys are known to be characterised by high sensitivity to hot cracking during fusion welding. As to their nature, hot cracks can be subdivided into two types (Figure 1): solidification (type 1) and underbead (type 2) cracks that form in the process of thermal-force loading of the multi-pass weld metal zones [1]. The temperature range of formation of the solidification cracks depends on the range of the solid-liquid state of metal during solidification of the weld. The lower limit of this range is determined by the value of solidus temperature at the end of solidification, T_S. The ductility dip temperature range is determined by an approximate ratio of $(0.6–0.8)T_S$ [2]. In this range the cracks initiate and propagate along the boundaries of high-angle austenitic grains [3].

The sensitivity to hot cracking is determined by the following factors [4–8]:

• chemical composition of the weld metal in terms of the content of main and impurity elements, having a limited solubility in solid solution and determining the solidification temperature range;

• value and rate of the growth of strain in solidification of the weld and its subsequent cooling;

• presence of conditions for redistribution of impurity elements, such as carbon, sulphur, oxygen etc., characterised by a high diffusivity under the thermal-force impact on metal by the fusion welding process;

• formation of the fine weld structure in one- and multi-pass welding, which determines the process of plastic deformation in metal of the polycrystalline welds;

• cohesive strength of grain boundaries in the welds with a stable austenitic structure, which determines conditions for initiation of hot cracks.

The purpose of this study was to perform comparative evaluation and investigation of the sensitivity of welds and welded joints on alloy Inconel 690 made by using welding wires Inconel 52 and Inconel 52MSS to hot cracking.

Special specimens are available for simulation of conditions of deformation of the deposited metal in multi-pass welding of real structures. Evaluation of the sensitivity to hot cracking, including in the multi-pass welds, is performed on the test specimens simulating the thermal-force impact exerted by the welding process on formation of the weld structure and initiation of hot cracks. Also, the use is made of the machine testing methods with the graduated forced deformation. In this case the most efficient methods are Varestraint-Test and PVR-Test (Programmierter Verformungs-Riss Test) [9]. So, these methods were employed to evaluate the sensitivity to solidification cracking, as well as to ductility-dip cracking in multi-pass welding of nickel alloy Inconel 690 by using welding wire Inconel 52MSS characterised, according to the preliminary data, by high crack resistance in the low-temperature ductility dip range. Investiga-
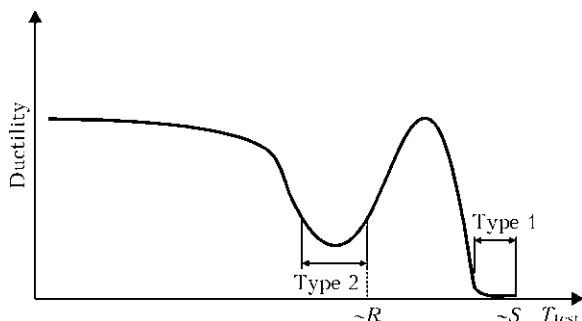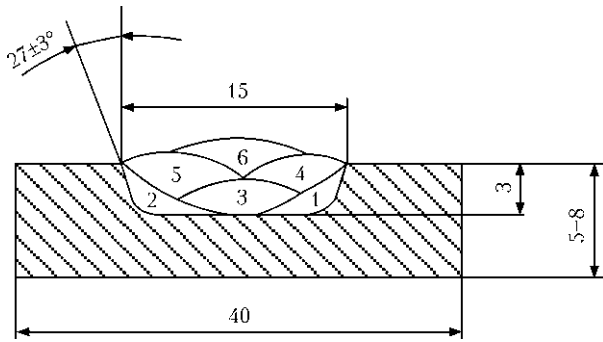

Figure 1. Temperature ranges in which low ductility leads to formation of two types of the cracks during welding [1]: S — solidus; R — recrystallisation

Figure 2. Schematic of filling of the groove with beads (deposition welds) in test specimens according to the Varestraint-Test and PVR-Test procedures

Figure 3. Appearance of composite specimen for evaluation of high-temperature properties of multi-pass welds: *1* — gauge section of composite specimen of the Inconel 690 joint made with wires Inconel® 52MSS and Inconel® 52; *2* — grip of 304 type steel

tions provided for plotting of brittle temperature ranges and determination of the critical value of strain ε_{cr} in fusion welding. In addition, the critical deformation rate was determined (PVR-Test), thus allowing evaluation of the sensitivity to formation of both solidification and ductility-dip cracks.

Chemical composition of the base metal and welding wires is given in the Table.

Microstructure of alloy Inconel 690 is fine-grained, non-textured, and consisting of austenitic grains and annealing twins located inside the grains. No substantial amounts of redundant phases or boundary precipitates was detected.

Specimens for investigation of weldability by the Varestraint-Test and PVR-Test procedures were prepared by making a groove in the Inconel 690 specimens measuring $8 \times 40 \times 170$ and $8 \times 50 \times 200$ mm. This groove was preliminarily filled up with a multilayer weld using wires Inconel 52 and Inconel 52MSS. Elements of the edge groove and sequence of deposition of the beads are shown in Figure 2.

Welding was performed by the TIG method in argon atmosphere using 0.9 mm diameter wires Inconel 52 and Inconel 52MSS. The stable weld formation was achieved by weaving the tungsten electrode and filler wire at a preset amplitude and frequency under optimal welding conditions. Test specimens were cut out from the weld-deposited plates: specimens measuring $170 \times 70 \times 3.5$ mm for Varestraint-Test, and specimens measuring $200 \times 40 \times 3.5$ mm for PVR-Test. In addition, specimens (Figure 3) for evaluation of ductility of the deposited metal in the ductility dip temperature range were cut out from the weld metal [10].

The machine testing methods with forced deformation of a specimen welded, providing the deformation of a graduated value and rate, hold promise for evaluation of weldability of metallic materials.

The evaluation method is implemented by performing TIG welding of a flat plate without filler and by simultaneously subjecting this plate to the time-variable deformation in a direction that is longitudinal with respect to the welding direction.

The principle of implementation of the PVR-Test procedure is shown in Figure 4 [11]. A characteristic feature of this procedure is ensuring the required range of the value of the forced deformations of a test specimen during welding and the rate of their variations. In this case it is required that the following two deformation dependences be fulfilled:

$$\frac{\Delta l}{\Delta t} = v, \quad \frac{\Delta v}{\Delta t} = \text{const},$$

where l is the displacement of grips *2* (see Figure 4); v is the speed of displacement of the grips; and t is the time of the displacement.

Critical deformation rate v_{cr} at which the first cracks form serves as a criterion of the sensitivity to cracking. During welding the cracks may simultaneously form in the weld and in the HAZ metal. These two types of the cracks are of a different nature [12] and, as a rule, form at a different rate of critical deformation v_{cr}. The solidification cracks are caused by development of the segregation process and formation of intergranular liquid interlayers in a temperature range close to T_S. They are located along the grain boundaries in the weld metal. The ductility-dip cracks form as a result of a loss of ductility of metal. They are located at some distance from the fusion line in the HAZ metal, the temperature of which has not yet reached the melting temperature. This makes it possible to quantitatively characterise the sensitivity

Chemical composition of base metal and welding wires Inconel® 52 and Inconel® 52MSS, wt.%

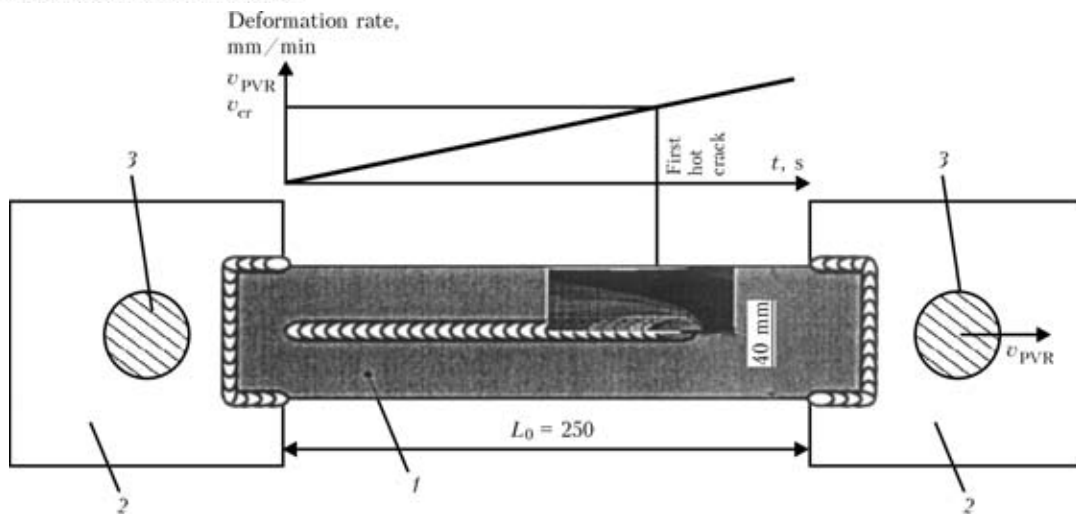| Material	C	Mn	Ni	Cr	Fe	Nb	Mo	Ti	S	P	Al	Si
In 690	0.020	−	Base	29.72	10.30	−	−	0.28	0.002	0.005	0.87	0.32
In 52MSS	0.024	0.29	54.55	30.30	7.24	2.52	3.45	0.25	0.002	0.0055	0.22	0.15
In 52	0.021	0.24	59.17	29.19	9.99	−	0.01	0.51	0.001	0.003	0.72	0.12

Figure 4. Schematic of the principle of implementation of PVR-Test [11]: *1* — specimen; *2* — grips; *3* — fastening pins for loading of specimens

to a certain type of the cracks. Position of a specimen after welding and its surface appearance are shown in Figures 5 and 6.

The diagram of displacement of grips of the PVR-Test machine depending on the time is fixed during an experiment, and the rate of deformation of metal in each of the eight regions is determined based on the diagram data. Such measurements make it possible to plot dependence of the quantity of the investigated type of the cracks on the deformation rate, and determine the value of critical deformation rate v_{cr} from the plot by way of extrapolation at intersection of the straight line with the abscissa axis.

The quantity of the cracks classified as the ductility-dip ones was counted by choosing the cracks that began and ended in the HAZ metal. This was done by using an optical microscope with ×50 magnification.

The cracks that formed in the weld were regarded as the solidification ones. Some of them stopped in the HAZ metal by forming a characteristic plastic strain in the stopping location. Analysis of the sensitivity to hot cracking was carried out by counting the quantity of the ductility-dip cracks located at some distance from the fusion line, as well as the solidification cracks that formed, as a rule, in the reference weld. The scheme accepted for classification of the cracks (Figure 7) was similar to that given in study [13].

Investigation of weldability by the Varestraint-Test procedure was performed by subjecting a metal plate during welding to forced bending deformation. In this case the deformation rate should exceed the welding speed to minimise displacement of the weld pool during the deformation time. Parameters of the brittle temperature range, as well as the critical value of strain ε_{cr} at which no cracks have yet formed served as a weldability evaluation criterion. Crack resistance of the wires was investigated on a series of plates measuring $170 \times 60 \times 3.5$ mm. The chosen forced deformation values ranged from 0.2 to 2.0 %, this corresponding to the mandrel radii ranging from 850 to 85 mm. Welding parameters for the Varestraint-Test procedure were as follows: $I_w = 90$ mm, $U_a = 9.7$ V, $v_w = 8$ m/h, and argon flow rate — approximately 8.5 l/min.
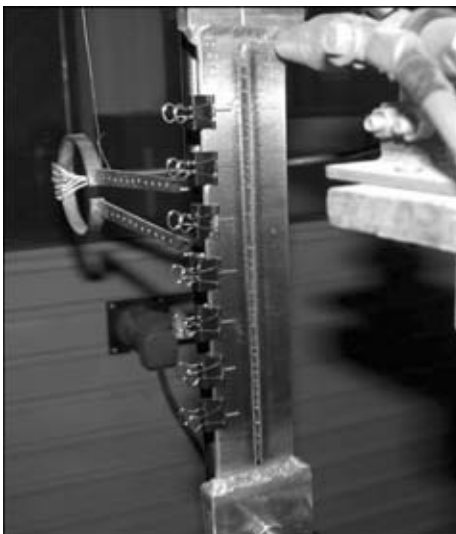

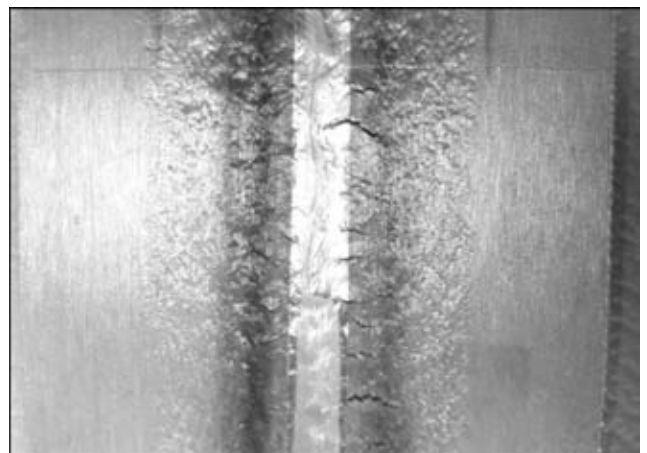**Figure 5.** General view of specimen after welding using the PVR-Test machine

Figure 6. Surface of specimen after weldability tests by the PVR-Test procedure
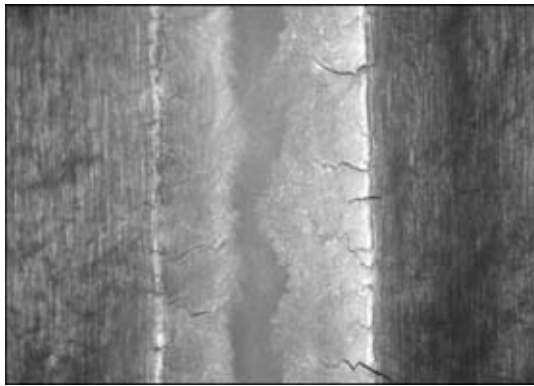
Figure 7. Solidification cracks in welds made with wire Inconel® 52MSS (×10)

Figure 9. Schematic of preferential location of cracks in welds after tests by the PVR-Test procedure

The tests were conducted to determine the values of tensile strength and elongation δ of the investigated metal in a temperature range from 20 to 1100 °C by using the «Ala-Too» testing machine (of the Gleeble type). The software provided maintaining of the preset temperature, fixing of the loading, and calculation and graphical representation of the load-displacement curve.

The loading systems of the «Ala-Too» machine allow evaluation of metal ductility in a wide temperature range in vacuum (10^{-5} mm Hg) (Figure 8).

The investigation results revealed substantial differences in the sensitivity to solidification and ductility-dip cracking between the weld metals obtained with wires Inconel 52 and Inconel 52MSS. The welds made with wire Inconel 52 had a minimal sensitivity to solidification cracking, and were sensitive to ductility-dip cracking. The ductility-dip cracks were located in regions of the HAZ metal whose temperature during welding did not reach T_S at a distance of 100 μm to 2 mm from the fusion line.

And on the contrary, the welds made with wire Inconel 52MSS were very sensitive to solidification cracking and almost insensitive to ductility-dip cracking. This dependence is schematically shown in Figure 9.

The results obtained were confirmed by the brittle temperature ranges (BTR) plotted by using the

Varestraint-Test procedure (Figure 10). Wire Inconel 52 was shown to have two brittle temperature ranges — high- and low-temperature ranges.

Testing of wire Inconel 52MSS with a forced deformation of up to 2.3 % revealed no low-temperature range, this being indicative of a higher resistance of these welds to ductility-dip cracking.

Microstructure of metal of the investigated welds with a face-centred cubic lattice was polycrystalline, consisting of grains of a different crystallographic orientation within each grain, separated by boundaries. Hot cracks, and first of all the ductility-dip cracks, may form along the grain boundaries under the corresponding conditions. According to the solidification conditions, the welds had either a directed cellular or cellular-dendritic structure, determining the mechanism of formation of the solidification cracks. The ductility dip temperature range was present in the Inconel 52 welds and absent in the Inconel 52MSS welds over the entire range of the deformations applied.

Based on the results obtained, it can be considered that the solidification cracks initiate mainly along the high-angle boundaries of elongated austenitic grains in the process of their formation during solidification (Figure 11).

Metallographic examinations of the multilayer welds made by TIG welding with filler wire Inconel 52MSS and of the reference weld made by TIG welding

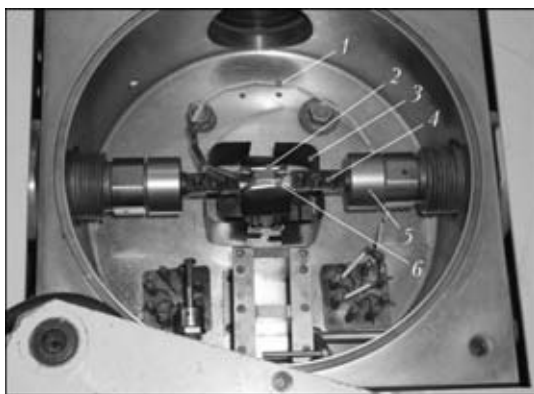**Figure 8.** Vacuum chamber of the «Ala-Too» machine with device for deformation of specimens: *1* — platinum-rhodium thermocouple; *2* — radiation heating device; *3* — thermal shield; *4* — grip; *5* — draw bar; *6* — specimen
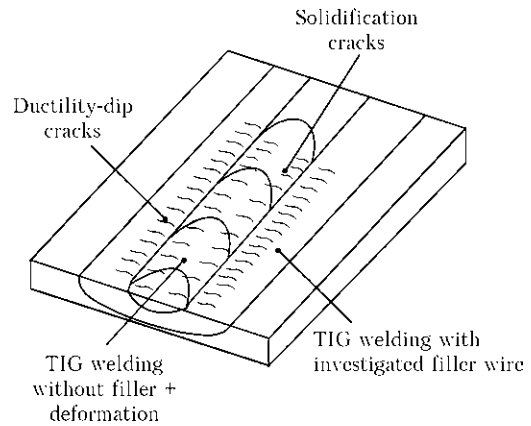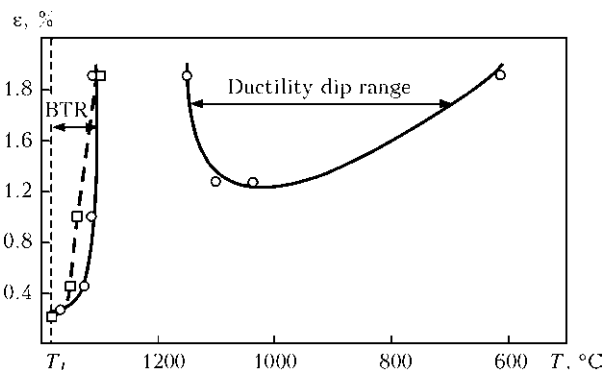

Figure 10. Brittle temperature ranges of the welds made with wires Inconel® 52 (solid line) and Inconel® 52MSS (dashed) in evaluation of weldability by the Varestraint-Test procedure
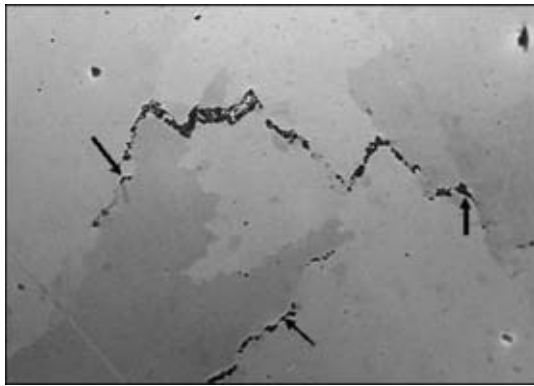
Figure 11. Character of propagation of solidification cracks (indicated by arrows) in weld metal obtained with wire Inconel® 52MSS (×200)
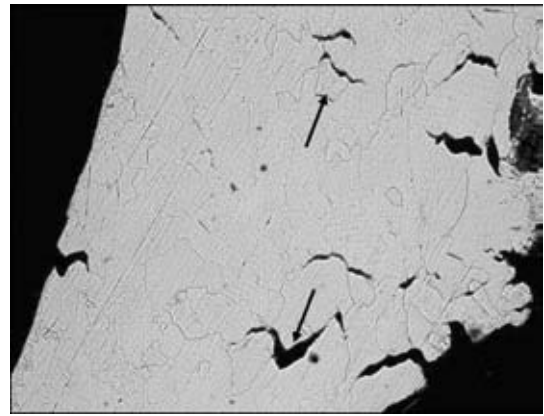
Figure 13. Microstructure (×100) of metal of the multi-pass weld made with wire Inconel® 52 at ductility dip temperature (intergranular fracture is shown by arrows)
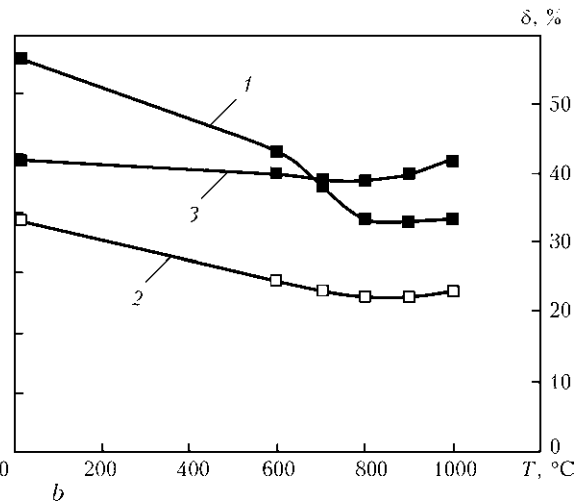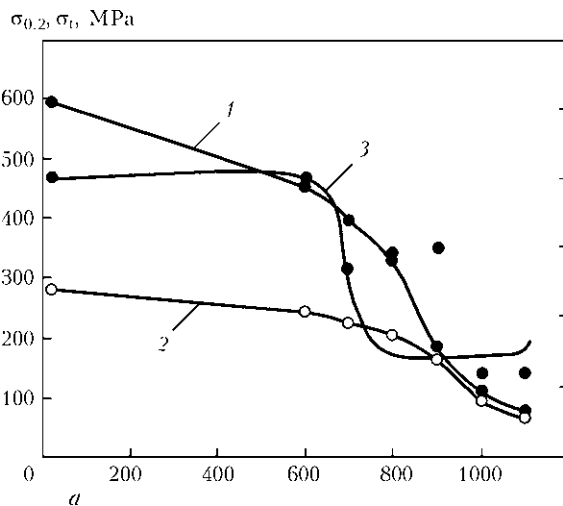
Figure 12. Temperature dependence of strength and ductility of specimens of the welded joint made with wires Inconel® 52 (*a*) and Inconel® 52MSS (*b*): *1* — σ_t; *2* — $\sigma_{0.2}$; *3* — δ

without filler during the forced deformation by the PVR-Test procedure confirmed the data that metal of the investigated welds is practically insensitive to formation of the ductility-dip cracks, which are the main type of microcracks forming in the multi-pass welds with a stable austenitic structure.

Results of investigation of temperature dependence of ductility of metal of the welds made with wires Inconel 52MSS and Inconel 52 are shown in Figure 12.

In contrast to specimens of the joints welded with wire Inconel 52, the dip in the characteristic temperature range is only slightly discernible in the curve of ductility of the joints welded with wire Inconel 52MSS (Figure 12, *b*), which is attributable to peculiarities of composition of this wire.

Analysis of microstructure of weld metal specimens showed that brittle intergranular fracture occurred in the Inconel 52 welds as a result of loading (Figure 13).

Therefore, the main cause of formation of the ductility-dip cracks in welds with the stable austenitic structure is migration of a number of impurity elements to grain boundaries in the multi-pass welds, this migration being accelerated by thermoplastic deformation.

Analysis of the published data [15], as well as the obtained investigation results allow putting forward a hypothesis on the probable mechanism of formation of cracks in multi-pass welding of austenitic high-alloy steels and nickel alloys. According to this hypothesis, the cracks form along the high-angle grain boundaries because of segregation of impurity elements, such as carbon, oxygen, sulphur and phosphorus, which actively diffuse to the boundaries [16, 17]. The mechanism of the effect of the impurities on embrittlement of the grain boundaries in the ductility dip temperature range requires additional investigation, which is planned to do in further studies.

CONCLUSIONS

1. The machine testing methods (Varestraint-Test and PVR-Test) providing for the forced deformation of test specimens during welding, as well as the technological test, i.e. multilayer welding, were used for the investigations.

2. Brittle temperature ranges were plotted for the welds in tests by the Varestraint-Test procedure. It was shown that welding with wire Inconel 52MSS in all shielding atmospheres resulted in formation of only

solidification cracks in the welds. In this case, the critical strain value was $\varepsilon_{cr} \approx 0.43$ %. Ductility-dip cracks were absent in all variants of the welds in a temperature range of 700−1000 °C.

3. As shown by using the PVR-Test procedure, the sensitivity to formation of the ductility-dip cracks was very low. At the same time, the solidification cracks were observed in the Inconel 52MSS welds under certain deformation conditions.

4. Evaluation of ductile characteristics of metal of the welds made with the investigated wires using the «Ala-Too» machine showed that the Inconel 52MSS type weld metal had no ductility dip, whereas the Inconel 52 type weld metal was characterised by a pronounced decrease in the elongation values. The data obtained prove a high resistance of the Inconel 52MSS welds to ductility-dip cracking (type 2) and sensitivity to solidification cracking in the brittle temperature range (type 1).

5. The probable cause of intergranular fracture of the welds is decrease in values of cohesive strength of the grain boundaries.

1. Hemsworth, W., Boniszewski, T., Eaton, N.F. (1969) Classification and definition of high temperature welding cracks in alloys. *Metal Constr. and British Welding J.*, **1**, 25, 5−16.
2. Torres, E.A., Peternella, F.G., Caram, R. et al. (2010) In situ scanning electron microscopy high temperature deformation experiments to study ductility dip cracking of Ni−Cr−Fe alloys. In: *In situ studies with phonons, neutrons and scattering*. Berlin; Heidelberg: Springer, 27−39.
3. Lippold, J.C., Kotecki, D.J. (2005) *Welding metallurgy and weldability of stainless steels*. John Wiley & Sons.
4. Collins, M.G., Lippold, J.C. (2003) An investigation of ductility dip cracking in nickel-based weld metals. Pt I. *Welding J.*, 82(**10**), 288−295.
5. Collins, M.G., Ramirez, A.J., Lippold, J.C. (2003) An investigation of ductility dip cracking in nickel-based weld metals. Pt II. *Ibid.*, 82(**10**), 348−354.
6. Collins, M.G., Ramirez, A.J., Lippold, J.C. (2004) An investigation of ductility dip cracking in nickel-based weld metals. Pt III. *Ibid.*, 83(**2**), 39−49.
7. Lippold, J.C., Nissley, N.E. (2007) Further investigation of ductility dip cracking in high chromium, nickel-based filler metals. *Welding in the World*, 51(**9/10**), 24−30.
8. Noecker, F.F., DuPont, J.N. (2009) Metallurgical investigation into ductility dip cracking in nickel-based alloys. Pt II. *Welding J.*, 88(**3**), 62−77.
9. Cross, C.E., Coniglio, N. (2008) Weld solidification cracking: critical conditions for crack initiation and crowth. In: *Hot cracking phenomena in welds II*. Berlin; Heidelberg: Springer.
10. Zvyagintseva, A.V., Yushchenko, K.A., Savchenko, V.S. (2001) Effect of structural changes in high-temperature heating on ductile characteristics of nickel alloys. *The Paton Welding J.*, **4**, 13−17.
11. Herold, H., Hubner, A., Zinke, M. (2004) Investigation of the use of nitrogenous shielding gas in welding and its influence on the hot-crack behaviour of high temperature resistant fully austenitic Ni- and Fe-base alloys. *IIW Doc. IX-2110−04*.
12. Yushchenko, K.A., Savchenko, V.S. (2008) Classification and mechanisms of cracking in welding high-alloy steels and nickel alloys in brittle temperature ranges. In: *Hot cracking phenomena in welds II*. Berlin; Heidelberg: Springer, 95−114.
13. Vallant, R., Cerjak, H. (2004) Investigation on the mechanical values and the hot crack susceptibility of Ni-base weld metals type 70/20 and 70/15 of different Nb contents. *IIW Doc. II-1535−04*.
14. Savage, W.F., Lundin, C.D. (1965) The Varestraint test. *Welding J.*, 44(**10**), 433−442.
15. Savchenko, V.S., Yushchenko, K.A. (1993) Mechanism of formation and ways of prevention of underbead cracks in welding of austenitic steels. *Avtomatich. Svarka*, **12**, 8−11.
16. Yushchenko, K.A., Savchenko, V.S., Chervyakov, N.O. et al. (2010) Probable mechanism of cracking of stable-austenitic welds caused by oxygen segregation. *The Paton Welding J.*, **5**, 5−9.
17. Trefilov, V.I., Majboroda, V.P., Firstov, S.A. et al. (1986) Investigation of influence of localised shear deformation on composition of surface steel fractured in vacuum. *Metallofizika*, 8(**3**), 78−83.

INFLUENCE OF TECHNOLOGICAL FACTORS ON RESISTANCE TO DELAYED FRACTURE OF BUTT JOINTS OF RAIL STEEL IN ARC WELDING

V.D. POZNYAKOV[1], V.M. KIRIAKOV[1], A.A. GAJVORONSKY[1], S.B. KASATKIN[1], A.V. KLAPATYUK[1], S.D. TARANENKO[2] and **V.A. PROSHCHENKO[2]**

[1]E.O. Paton Electric Welding Institute, NASU, Kiev, Ukraine
[2]OJSC «Dnepropetrovsky Strelochny Zavod», Dnepropetrovsk, Ukraine

The results of study of the effect of technological factors and groove shape on deformability and cyclic fatigue life of welded joints of rail steel are given. Dependences of variations in deformability h_{cr} of butt joints with the V- and U-shaped grooves on the welding heat input, preheating temperature and conditions of cooling of the joints after welding are presented. The technology of arc welding of longitudinal joints in rail ends of railway frogs was developed.

The frogs of railroad switches are manufactured of high-manganese steel 110G13 (Hadfield steel). In Ukraine such frogs are manufactured at railway switch factories in Dnepropetrovsk and Kerch using casting technology. As the switch frogs have complicated shape the existing technological processes of their manufacture are labor-intensive and power consuming, thus increasing their cost. Also it should be noted that evaporation of manganese in casting of products of steel 110G13 deteriorates sanitary-hygienic conditions of labor and ecology of environment. It is possible to provide significant decrease in cost of frogs and to improve ecological conditions at production sites using the rail steel for manufacture of frogs. Here, the feasibility appears in replacement of bolted joints of frogs in railways by welded rails, which decreases dynamic loads on the road bed and increases speed of movement of trains [1]. Nowadays this way of modernization of railway infrastructure is being developed throughout the world.

Production of welded structures of frogs is most widely mastered in Europe at «Voest-Alpine» company (Austria). According to the proposed technology the welding of longitudinal weld of rail end, manufactured of rail steel, is performed using automatic method by solid wire of 3 mm diameter under flux layer. Further, the ready rail end, the length of which can vary from 1.5 to 3.6 m, is welded on to a core (steel 110G13) by a flash-butt welding method using insert of steel 10Kh18N10T.

The test specimens of welded frogs with end of rail steel of domestic production (Figure 1) were manufactured at Murom Railway Switch Factory and tested at the test grounds «Koltso» (Shcherbinka, Moscow region, Russia). The tests carried out at load of 27 t per axis according to the procedure showed that only two of three frogs manufactured according to the Voest-Alpine technology of had successfully passed the test, whereas one of them fractured before the standard life (less than 80 mln t per running kilometer).

The fatigue crack in the given frog was formed in the end of a butt weld (crater zone) and propagated perpendicularly relative to the weld axis. This is probably connected with the fact that the increased heat input, characteristic for automatic submerged arc welding, caused the formation in welded joints of rail steel of a relatively wide HAZ, where structure is formed characterized by increased tendency to brittle fracture. Therefore, it was necessary to develop the new technology of welding longitudinal butt of switch frog ends, which will allow avoiding the mentioned disadvantages.

The aim of this work was evaluation of effect of technological factors (temperature of preheating and heat input of welding) and structural factors on deformability and service life of welded joints of rail steel under the conditions of static and cyclic loading.

The investigations were conducted on butt joints of high-carbon Si−Mn rail steel of M76 grade with 0.71−0.82 % C and 0.75−1.05 % Mn content.

Influence of technological factors and design shape of a groove on strength properties of joints of rail steel at static loading was studied under conditions of tests of welded specimens for three-point bending in the installation of Friedland. The specimens were loaded by the force of 3000 kg at the speed of 1 mm/min. The criterion for evaluation of these tests was the level of critical deformation of specimens h_{cr} at which the crack formation does not yet occur at the surface of welded joint. Welded specimens for tests represented the rail steel butt joints of 240 × × 85 × 18 mm size. The peculiarities of fracture of multipass joints of rail steel with V- and U-shaped grooves were investigated, the influence of value of heat input of welding (8.6 and 28.5 kJ/cm), preheat-
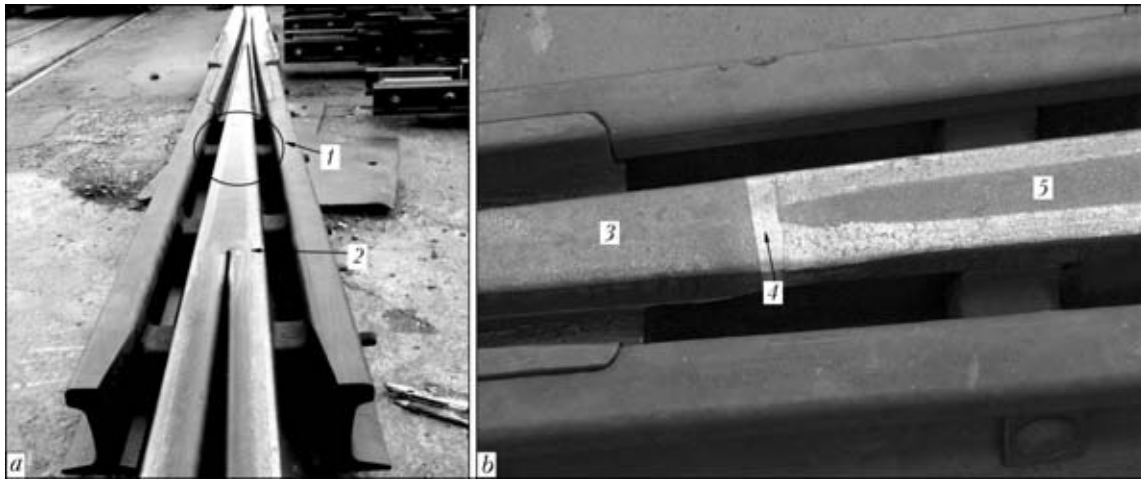
Figure 1. Welded railroad frog with rail end: *a* — general appearance; *b* — area in the site of welding of core with rail end; *1* — area of frog in the site of welding of core with rail end; *2* — place of fracture of rail end; *3* — core of steel 110G13; *4* — insert of steel 10Kh18N10T; *5* — rail end of steel M76

ing at temperatures 150 and 250 °C, and also conditions of cooling of joints after welding was evaluated. As the welding material the low-alloyed wire Sv-08G2S of 1.2 mm diameter was used. Mechanized welding of specimens was performed in mixture of shielding gases (Ar + 20 % CO_2).

In addition, the results of earlier performed works on evaluation of influence of thermodeformational cycle of welding on formation of structure, change of strength and ductile properties in HAZ metal of rail steel, as well as temperature of preheating and heat input of welding on resistance of welded joints to the formation of cold cracks [2, 3] were used.

The results of carried out investigations on evaluation of influence of technological factors and design shape of a groove on deformability of welded joints of rail steel, obtained during static bending test, are given in Figures 2–5.

As is seen from presented data, the shape of a groove considerably influences the values of critical deformation of specimens. For welded joints with U-groove h_{cr} is 1.5–2 times higher than that in welded joints with V-groove (Figure 2). The application of preheating at 250 °C in welding of joints of rail steel with U-groove contributes to increase in h_{cr} value by 1.5 times. Moreover, the character of fracture of welded joints itself changes as well. Formation of cracks and fracture of joints with V-groove occurred exclusively along the metal of fusion zone and near weld zone (area of coarse grain of HAZ). The surface of fracture of specimens was characterized by large crystal structure which was an evidence of brittle fracture (Figure 3). Fracture of welded joints with U-groove occurred in a tough way, mainly along weld metal. Surface of fracture was fine-crystalline.

The increase of heat input from 8.6 to 28.5 kJ/cm allows additional increasing of h_{cr} value of joints of rail steel practically by 1.3 times (Figure 4).

To increase the resistance of welded joints of high-carbon steels against cold crack formation, the tech-

nological process directed to delay of their cooling after welding is widely used. It favors relaxation of welding stresses in the joints and more complete proceeding of processes of hydrogen diffusion in metal. Thus, for example, wheels flanges of freight railway cars after restoration surfacing are cooled in special thermal chambers [4]. The evaluation of influence of this technological operation on resistance of welded joints of rail steel to static bending loading was the aim of further investigations carried out as-applied to butt joints of rail steel with U-groove of edges, welding of which was performed using wire Sv-08G2S of 1.2 mm diameter in mixture of gases at heat input of 28.5 kJ/cm with preheating of up to 250 °C. One part of specimens after welding was cooled in the air and another one was placed to thermal chamber. Thus, their cooling rate was delayed down to 50 °C/h. The results of carried out investigations, given in Figure 5, evidence that this technological operation allows increasing the critical deformation level of welded joints of rail steel as compared to specimens, the cooling of which was performed in the air, practically by 40 %.
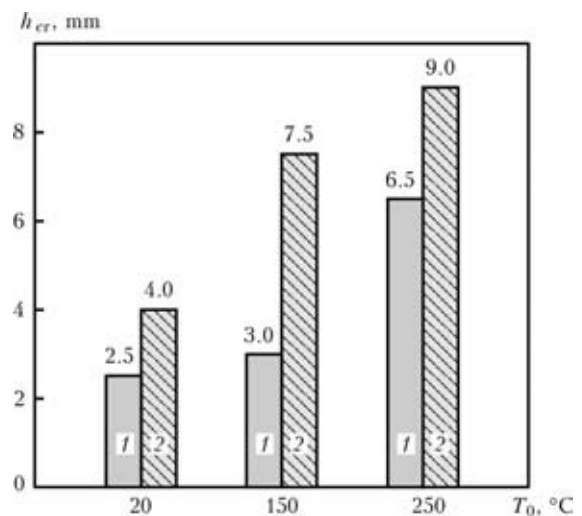
Figure 2. Influence of V- (*1*) and U- (*2*) grooves and temperature of preheating T_0 on critical deformation of welded joints h_{cr} of rail steel performed at heat input $Q_w = 8.6$ kJ/cm
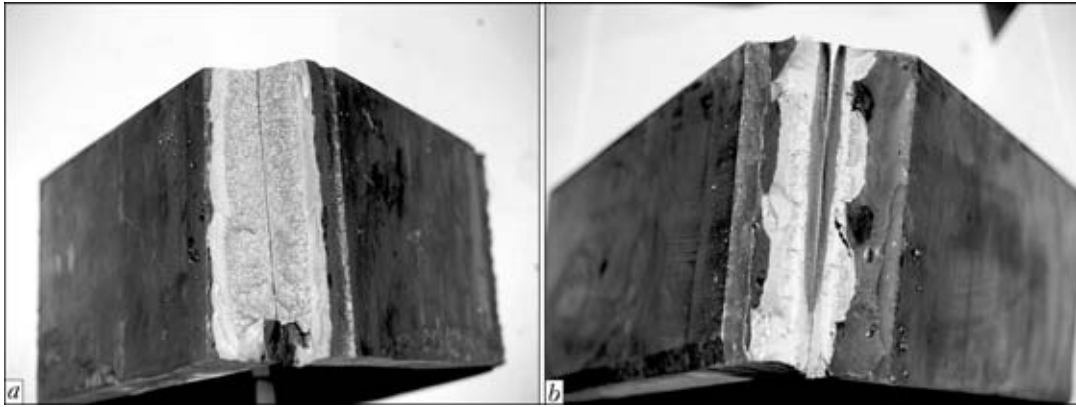
Figure 3. Characteristic fractures of welded joints of rail steel with V- (*a*) and U- (*b*) grooves performed at preheating of up to 150 °C at heat input of 8.6 kJ/cm after tests for three-point bending

The carried out investigations showed that due to transition from V- to U-groove of edges, the increase of heat input of welding from 8.6 to 28.5 kJ/cm, application of preheating of joints up to 250 °C and delay of cooling rate after welding down to 50 °C/h, the deformability of welded joints of rail steel can be more than 4 times increased.

Influence of shape of edge preparation on resistance of welded joints of rail steel to fatigue fractures was investigated according to generally-accepted methods of fatigue tests [5] in the installation UMP-1 at symmetric cycles of bend loading with 14 Hz frequency at loading cycle of 40 MPa. As specimens, the butt joints of rail steel of sizes 250 × 85 × 18 mm with V- and U-grooves without complete penetration were used, that allowed modeling the conditions for making the longitudinal weld of rail ends.

The specimens were welded without preliminary heating in mixture of shielding gases using wire Sv-08G2S of 1.2 mm diameter under the conditions providing heat input of 9.2 kJ/cm in making of weld root bead and 28.5 kJ/cm in filling of remaining part of the groove. This, on the one hand, allowed decreasing of volume of base metal in weld metal and, on the other hand, preventing of hot cracks formation in the joint.

It was established as a result of carried out investigations (Figure 6) that resistance to fracture at cyclic loading of welded joints with V-groove is twice lower than that of joints with U-groove (formation of fatigue crack of 3 mm length was observed, respectively, after 190,000 and 430,000 loading cycles).

Fracture of welded joints with V-groove occurred along the fusion line and HAZ metal. Fatigue crack in the joints with U-groove was also formed along the fusion line in the lack of penetration zone. Their further fracture occurred along the weld metal. Thus, from the position of static and cyclic life during producing of welded joints of rail steel the joints with U-groove should be preferred. As applied to these joints the investigations were carried out at their final stage.

As in previous case, welding of specimens was performed in mixture of gases using wire Sv-08G2S. Welding conditions remained unchanged. The difference was in fact that specimens were welded with complete penetration, before welding they were preheated up to 250 °C and placed after welding into the
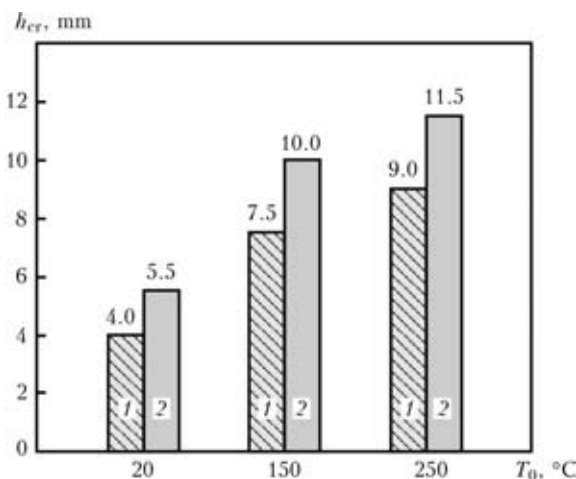
Figure 4. Influence of heat input and preheating temperature on critical deformation of welded joints of rail steel with U-groove: *1* — Q = 8.6; *2* — 28.5 kJ/cm
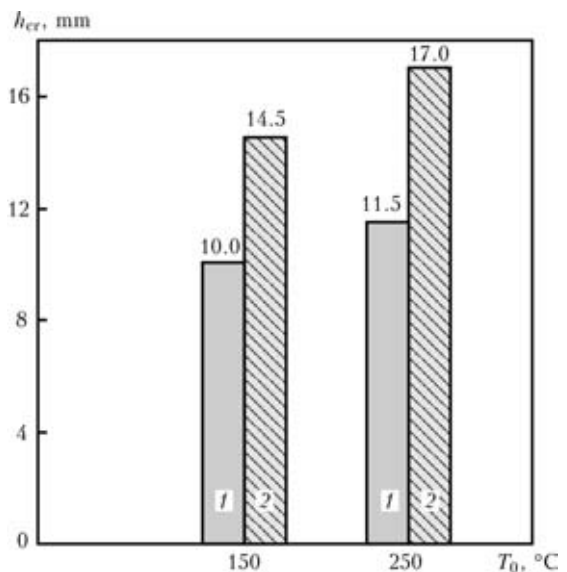
Figure 5. Influence of conditions of postweld cooling on critical deformation of welded joints of rail steel with U-groove, performed at heat input of 28.5 kJ/cm: *1* — cooling in the air at 20 °C; *2* — cooling in thermal chamber at 50 °C/h
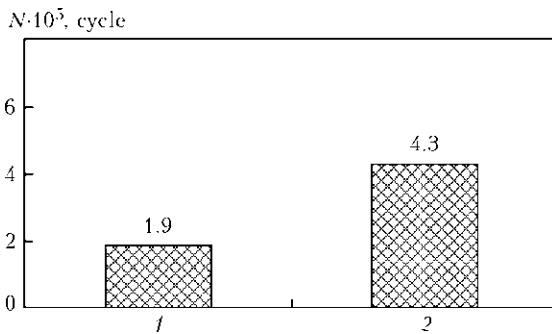
Figure 6. Influence of V- (*1*) and U- (*2*) groove on cyclic life of welded joints of rail steel
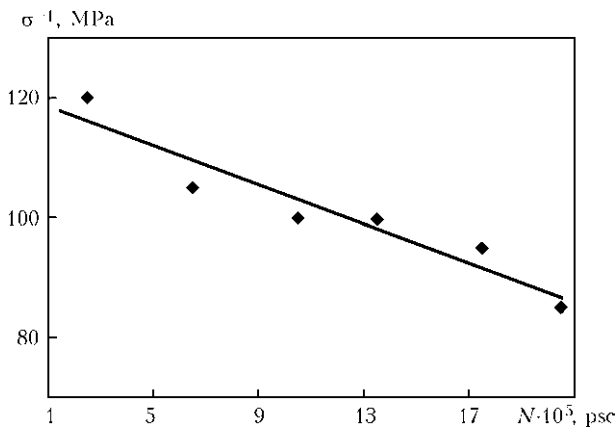
Figure 7. Influence of cycle stresses on cyclic life of welded joints of rail steel with U-groove, made with preheating of up to 250 °C at the heat input of 28.5 kJ/cm

Figure 8. Surface of fracture of welded joint of rail steel with U-groove, made with preheating of up to 250 °C at the heat input of 28.5 kJ/cm after cyclic loading by bending

thermal chamber to delay their cooling rate. Thus, technological process was reproduced when welded joints of rail steel acquired the highest ability to deformation.

The results of tests carried out at cycle stresses of 120, 105, 95 and 85 MPa are given in Figure 7. They showed that at the cycle stress of 120 MPa the fatigue cracks of 3 mm length were formed after approximately 220,000 loading cycles, after another 50,000 loading cycles the specimens were fractured completely. Initiation and primary development of crack occurred along the fusion line and then along the near weld HAZ metal. It was noted that after crack formation at 10 % of general area of section of specimen, its further development occurred in a brittle way (Figure 8).

At decrease of cycle stress down to 105 MPa the fatigue crack of 3 mm length formed after 643,000 cycles, and at 95 MPa — after 1,760,000 loading cycles.

In two of three specimens, the test of which was carried out at cycle stress of 85 MPa, after 2,000,000 cycles the cracks were not detected, therefore, the tests were interrupted. In one of the specimens the fatigue crack of less than 1 mm length was formed along the fusion line of a joint after 1,901,000 loading cycles, but as far as during further loading it did not propagate, the tests were interrupted. It gave grounds for us to consider the loading of 85 MPa as a conditional limit of endurance of rail steel welded butt joints, made using the offered technology.

The additional investigations on mastering of proposed technology of welding of joints of rail end were carried out during manufacture of a pilot batch of railway switches at the «Dnepropetrovsky Strelochny Zavod». The service tests of switches with rail ends, the electric arc welding of which was performed according to developed technology proved the high reliability and quality of products. Basing on these tests the technology of electric arc welding of rail ends was implemented in serial production, and a patent of Ukraine was granted for developed method of arc welding of longitudinal weld of a rail end [6].

CONCLUSIONS

1. It was established that the longitudinal weld of rail end should be performed by the design with U-shaped groove preparation.

2. It was shown that mechanized welding of rail ends should be performed at increased values of heat input in mixture of shielding gases under the conditions providing the process of spray transfer of the electrode metal.

3. It was determined that to provide high deformability and increase of life of welded joints of rail steel, they should be preheated before welding up to 250 °C and provide delayed cooling at the rate about 50 °C/h after welding.

1. Kuchuk-Yatsenko, S.I., Shvets, Yu.V., Kavunichenko, A.V. et al. (2008) Performance of flash butt welded joints on railway frogs. *The Paton Welding J.*, **9**, 30–33.
2. Sergienko, Yu.V., Sagirov, I.V. (2000) Prediction of formation of quenching structures in welding of rail steels. In: *Proc. of Sci. Seminar on Current Achievements in Welding, Surfacing and Related Technologies* (Mariupol, Nov. 2000). Mariupol: PriazovGU, 9–12.
3. Poznyakov, V.D., Kiriakov, V.M., Gajvoronsky, A.A. et al. (2010) Properties of welded joints of rail steel in electric arc welding. *The Paton Welding J.*, **8**, 16–20.
4. Sarzhevsky, V.A., Gajvoronsky, A.A., Gordonny, V.G. et al. (1996) Effect of technological factors on structure and properties of HAZ metal in repair-and-renewal cladding of flanges of solid-rolled rail wheels. *Avtomatich. Svarka*, **3**, 22–27, 33.
5. (1990) *Strength of welded joints under alternative loads.* Ed. by V.I. Trufyakov. Kiev: Naukova Dumka.
6. Taranenko, S.D., Proshchenko, V.A., Kiriakov, V.M. et al. *Method of electric arc welding.* Pat. 91938 Ukraine. Int. Cl. B 23 K 9/16, B 23 K 9/23. Publ. 10.09.2010.

FLASH-BUTT WELDING OF HIGH-TEMPERATURE NICKEL ALLOY USING NANO-STRUCTURED FOILS

V.S. KUCHUK-YATSENKO

E.O. Paton Electric Welding Institute, NASU, Kiev, Ukraine

The process of resistance flash-butt welding of high-temperature nickel alloy Rene 80 using nano-structured foils of Ti–Al and Ag–Cu system is considered. Features of welded joint formation and their microstructure are studied. Microhardness distribution in welded joints is shown.

Progress of science and technology is making ever higher requirements to high-temperature strength of materials in combination with ductility, thermal and low-cycle fatigue life, resistance to gas environment, and endurance. This stimulates activities on development and introduction of new alloys, in particular, high-temperature casting nickel-based alloys.

High-temperature casting nickel-based alloys are effectively used in industry as material for parts of gas turbine engines [1, 2]. Taking into account one of the methods to improve performance (alloying optimization) an experimental high-temperature casting nickel-based alloy is proposed, which has the following composition, wt.%: 0.17 C; 18 Cr; 8.5 Co; 1.8 Mo; 2.6 W; 0.9 Nb; 3.4 Ti; 3.5 Al; 1.75 Ta; $0.5 \leq$ Fe; Ni being the balance. A feature of this alloy is an increased content of aluminium, titanium (3.5 and 3.4 wt.%, respectively) and other alloying elements.

Metallographic investigations showed that the alloy structure is typical for cast metal (Figure 1). It is based on γ-phase dendrites, which are complex-alloyed nickel-based solid solution. Two kinds of phases are located in interdendritic space. These are, probably, γ'-phase based on $(Ni, Cr)_3(Ti, Al)$ compound and MeC type carbides, capable of creating such elements as titanium, tantalum and niobium. Location of these phases indicates that their precipitation occurred at solidification of interdendritic melt from γ'-phase and carbides. Isolated inclusions of these phases were also found in the dendrite volume.

Dimensions of γ'-phase and carbides are larger that those at dispersion precipitation from the solid solution. This, as well as the predominant location along the grain boundaries, changes their role in the alloy strengthening. Level of high-temperature strength determines the retardation of grain-boundary slipping.

Introduction of new alloys is complicated by the problem of producing their permanent joints with each other and other materials. Complex alloying by reactive elements and thermal instability at high temperatures cause certain difficulties in welding high-temperature alloys.

Resistance flash-butt welding (RFBW) provides local high-speed heat input into the joint zone [3]. Considering the experience of previous developments on RFBW of such difficult-to-weld materials [4, 5], it is proposed to perform welding of high-temperature nickel alloy using nano-structured foils.

Nano-structured foils of Ti–Al and Ag–Cu systems were used in this work. Production of such nano-structured foils based on vapor-phase technology has been mastered at PWI [6].

Ti–Al system foil is a multilayer composition of alternating layers of titanium and aluminium, corresponding to γ'-Ti–Al stoichiometric composition. Heating of such foil up to the temperature of about 300 °C, results in titanium and aluminium interaction with formation of intemetallic. Interaction reaction is
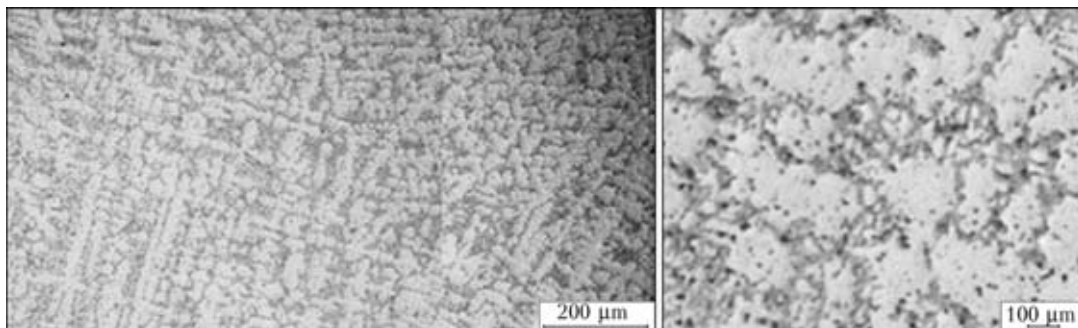
Figure 1. Microstructures of cast high-temperature nickel alloy Rene 80

Figure 2. Microstructure (*a*) and microhardness distribution in the joint of a high-temperature alloy produced using nano-structured foils (*b*)

developing at a high rate and is accompanied by evolution of addition heat.

Foil of Ag–Cu system in its composition is close to eutectic condition of Ag–Cu system alloys. Eutectic melting temperature is equal to 779 °C [7]. Melt formation at the contact boundary at the temperature lower than the alloy melting temperature, is favourable for joint formation.

RFBW was performed in an upgraded «Schlatter» machine. Maximum machine power was 25 kW·A and upsetting force was 800 MPa. Welding of samples of 10 × 10 × 100 mm size was performed in air at the pressure of 2 MPa, welding current of 4–5 kA and welding time of 3–5 s.

Analysis of microstructure and chemical inhomogeneity of the joints was conducted in optical microscope «Neophot 32» and scanning electron microscope ISM-840 with Link system microanalyzer.

To assess mechanical properties of welded joint microhardness distribution was determined on microprobe computerized «Micron-gamma» system.

At RFBW of the alloy in a similar joint without using foils such defects as lacks-of-penetration and microcracks were recorded in the welded joint zone (Figure 2). A probable cause for unsatisfactory formation of the joints is non-uniform heating of samples.

The following was noted in the HAZ of the produced joint (Figure 2). A region of equiaxed grains of γ′-phase is adjacent to base metal with arborescent dendrites. The quantity of carbides and γ′-phase is preserved here. In the region adjacent to the weld,

the quantity of carbides and γ′-phase decreases considerably. Isolated precipitates of these phases are found along the grain boundaries. Furtheron the dendritic structure and quantity of carbides and γ′-phase are restored.

Microhardness distribution was analyzed to assess the change of strength characteristics in the HAZ.

As is seen, microhardness lowering in the base metal from 3000 to 2500 MPa is recorded in the region with refined grains of the solid solution that forms along the joint line (see Figure 2). Microhardness increase above 3000 MPa occurs in the section of partial dissolution and, probably, further disperse precipitation of strengthening γ′-phase in the solid solution (see Figure 2).

At the next stage, welded joints of the alloy will be produced using nano-structured foils of Ti–Al, Ag–Cu system.

In the joint HAZ decomposition of oversaturated solid solution in interdendritic volumes of the metal and formation of strengthening γ′-phase were found (Figures 3 and 4). In the middle part the thermomechanical impact leads to structure refinement.

In the joint produced using foils of Ti–Al system arborescent dendrites are preserved and no foil fragments were found in the weld (see Figure 3), and in the joints produced using foils of Ag–Cu system equiaxed grains were observed (see Figure 4). In this case, microstructure is the result of solid-liquid interaction of the eutectic melt of Ag–Cu system with the alloy base metal.
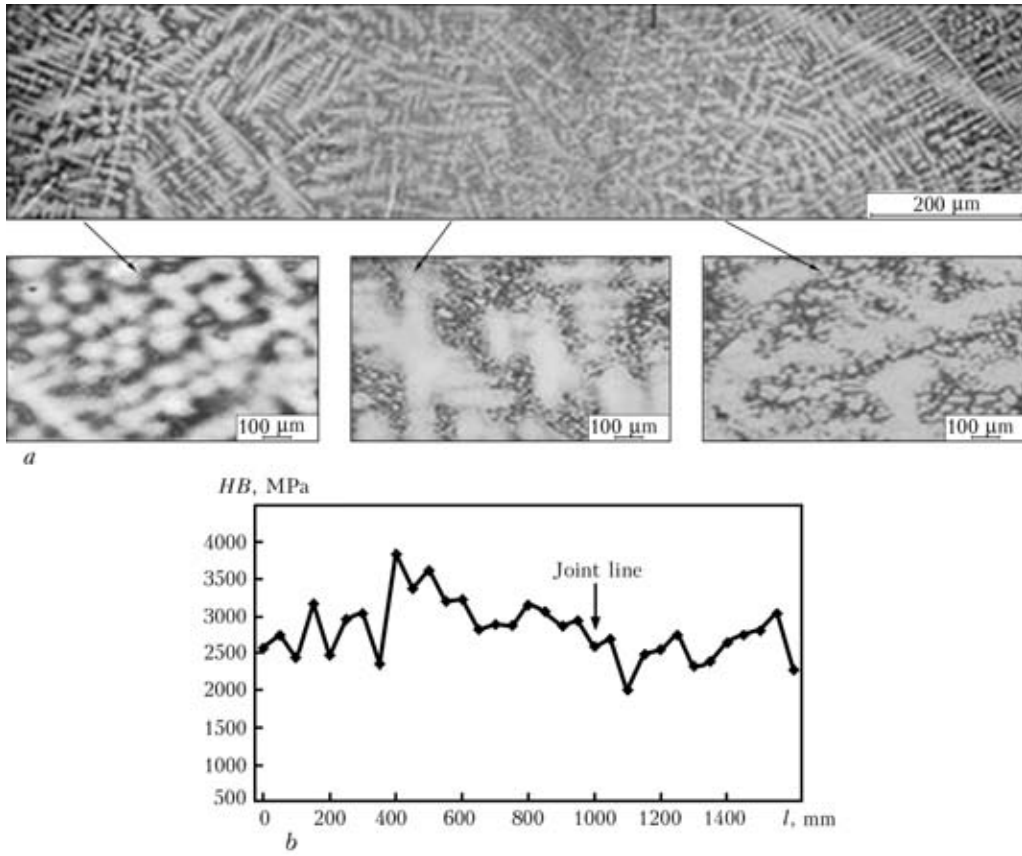
Figure 3. Mictrostructure (*a*) and microhardness distribution in the joint of high-temperature alloy produced using nano-structured foil of Ti–Al system (*b*)

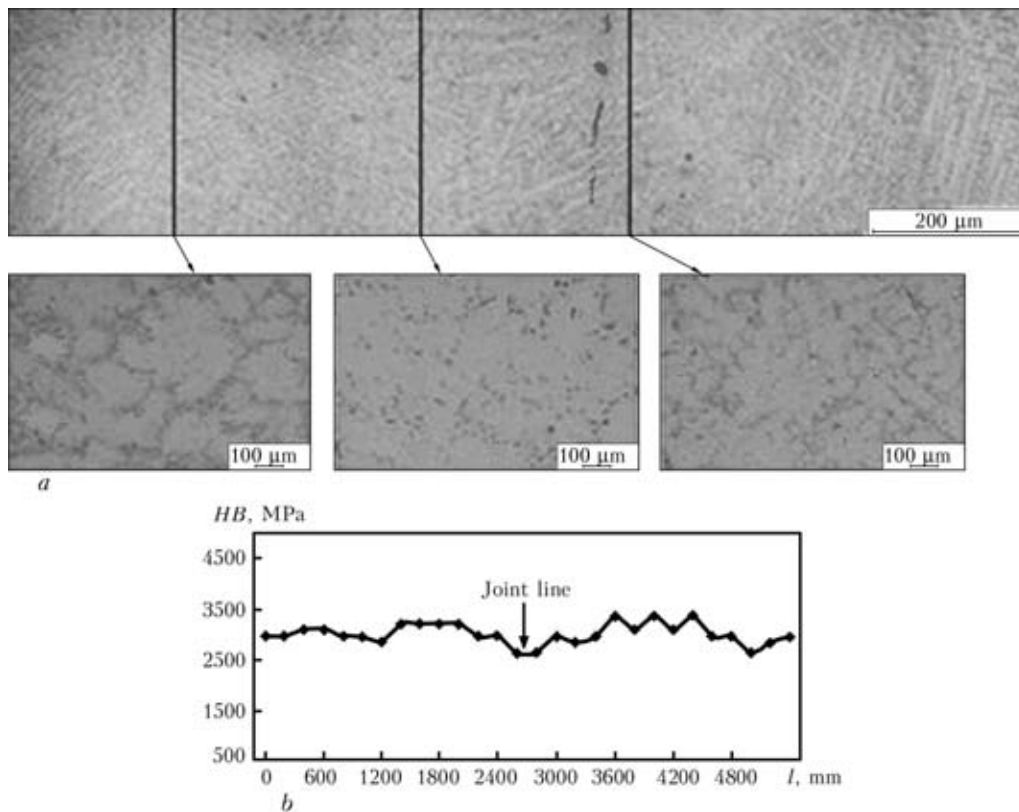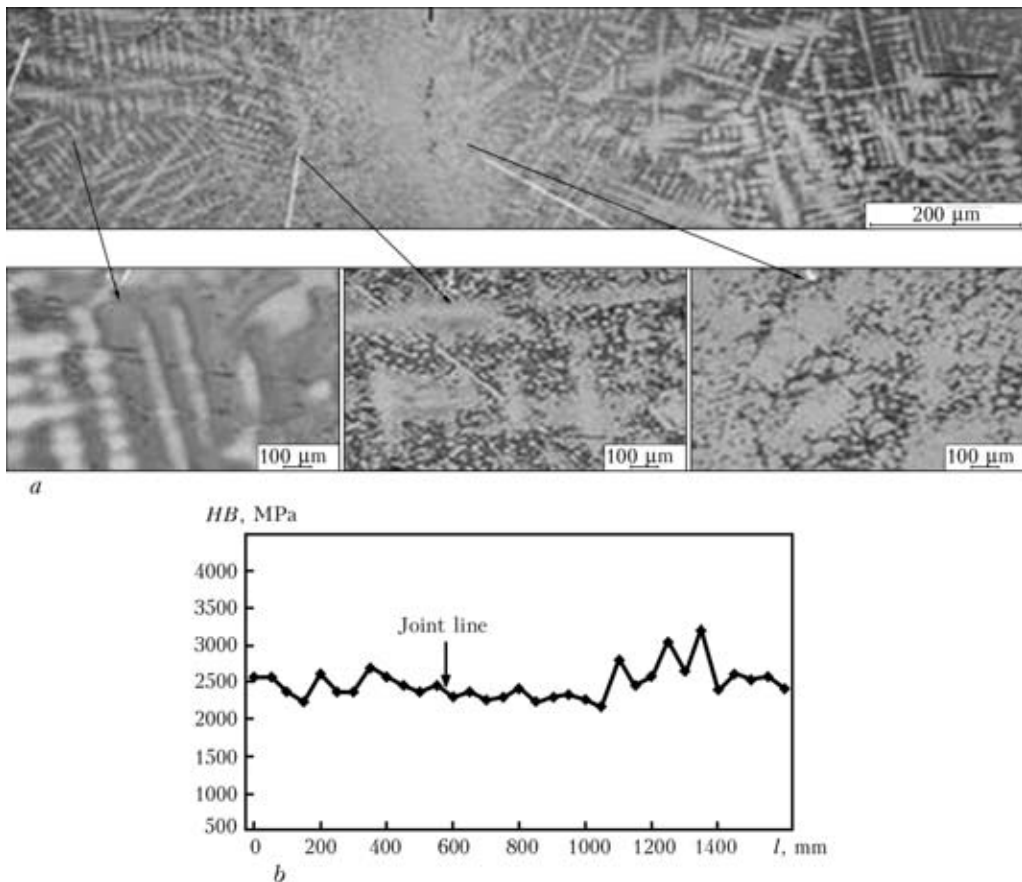**Figure 4.** Microstructure (*a*) and microhardness distribution in the joint of high-temperature alloy produced using nano-structured foil of Ag–Cu system (*b*)

Comparative analysis of microhardness distribution showed that in the middle part of the joint produced using foil of Ti–Al system microhardness rises relative to base metal and is equal to about 3000 MPa. On the other hand, in the middle part of the joint made with application of foil of Ag–Cu system microhardness is lower than in the base metal and is equal to 2250 MPa.

Therefore, application of nano-structured foil at RFBW of high-temperature nickel alloy will allow ensuring a uniform highly concentrated heating of the joint zone and lowering the process temperature, thus preventing base metal softening.

1. Khimushin, F.F. (1969) *High-temperature steels and alloys*. Moscow: Metallurgiya.
2. Paton, B.E., Stroganov, G.B., Kishkin, S.T. et al. (1987) *High-temperature strength of cast nickel alloys and their protection from oxidation*. Kiev: Naukova Dumka.
3. Kuchuk-Yatsenko, S.I. (1992) *Flash-butt welding*. Kiev: Naukova Dumka.
4. Kuchuk-Yatsenko, V.S., Shvets, V.I., Sakhatsky, A.G. et al. (2007) Specifics of flash-butt welding of aluminium alloys using nano-structured aluminium-nickel and aluminium-copper foils. *Svarochn. Proizvodstvo*, **9**, 12–14.
5. Kuchuk-Yatsenko, V.S., Shvets, V.I., Sakhatsky, A.G. et al. (2009) Features of resistance welding of titanium aluminides using nanolayered aluminium-titanium foils. *The Paton Welding J.*, **3**, 11–14.
6. Movchan, B.A. (1998) Inorganic materials deposited from vapor phase in vacuum. In: *Current materials science of XXI century*. Kiev: Naukova Dumka.
7. (1979) *Binary and multicomponent systems on the base of copper*. Ed. by S.V. Shukhardin. Moscow: Nauka.

DEVELOPMENT OF FLUX-CORED WIRE FOR ARC WELDING OF HIGH-STRENGTH STEEL OF BAINITE CLASS

V.N. SHLEPAKOV, Yu.A. GAVRILYUK and **S.M. NAUMEJKO**
E.O. Paton Electric Welding Institute, NASU, Kiev, Ukraine

Given are the results of investigation of the effect of alloying on formation of structure and mechanical properties of the weld metal in gas-shielded flux-cored wire welding, as well as of development of composition of a core of the wire providing the yield strength value of not less than 590 MPa and impact energy of more than 50 J at −50 °C. Optimal additional microalloying with zirconium was determined for the basic C–Si–Mn–Ni–Mo alloying system. This microalloying allows decreasing the volume fraction and size of non-metallic inclusions, as well as increasing the share of dispersed components in metal structure, and provides the required level of strength of the weld metal and its low-temperature tough-ductile properties.

Development of new welding consumables, meeting the high requirements made to mechanical property indices, in particular strength and impact toughness, was necessitated by expansion of production and application of low-alloy steels in building and industry.

The aim of the present paper is development of composition of a wire core providing obtaining of a weld metal with yield strength value of not less than 590 MPa and required values of low-temperature impact energy (more than 50 J at −50 °C) [1]. It is a complex task to achieve such a level of indices using traditional alloying systems.

Experience of development of low-alloy consumables, in particular, flux-cored wires, indicates an appropriateness of application of the alloying systems, close on composition to alloying system of steel to be welded, taking into account different conditions for formation of a metal structure at rolling and welding. As a rule, C–Si–Mn–Ni–Mo(Cr–Cu) system makes an alloying basis. Alloying of the metal in C–Si–Mn–Ni–Mo system due to solid-solution hardening [2, 3] provides necessary indices of strength. Regulation of the tough-ductile properties requires selection of alloying and microalloying system, providing formation of the dispersed structural components which have high resistance to brittle fracture [4, 5].

The investigations were carried out on the pilot batches of flux-cored wire of 1.2 mm diameter with slag-forming system of rutile-fluorite type during downhand welding of AB-1 steel grade plates (400 ×

Table 1. Content of alloying elements and additions in the weld metal, wt.%

Weld number	C	Si	Mn	Ni	Mo	Ti	Al	Zr	S	P
1	0.07−0.09	0.2−0.4	1.0−1.4	2.0−2.4	0.15−0.25	0.01−0.015	0.025−0.035	−	0.011−0.016	0.016−0.020
2								0.007−0.009	0.012−0.016	0.016−0.020
3								0.010−0.015	0.011−0.016	0.016−0.020
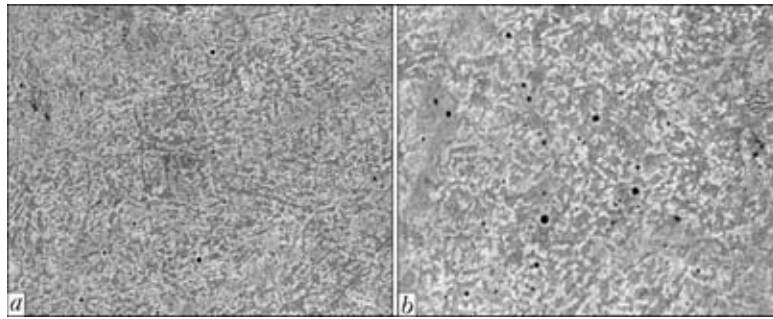
Figure 1. Microstructures of the weld metal alloyed by C−Si−Mn−Ni−Mo: a − ×1000; b − ×2000

Figure 2. Element composition (a), and size distribution of non-metallic inclusions in the weld metal of C−Si−Mn−Ni−Mo system (b)

× 200 mm size, 20 mm thick with V-groove preparation) in Ar + 15 % CO_2 gas shielding atmosphere at heat input 1.3−1.7 kJ/mm (welding current 180−200 A, arc voltage 28 V). A welded joint was cooled up to 90−110 °C before applying of each subsequent bead. Content of the alloying elements and additions in the weld metal varied in the limits, indicated in

Table 1. Zirconium microalloying by means of introducing of ferroalloy of Fe−Si−Zr system in the flux-cored wire was applied for obtaining of more high values of weld metal impact energy at low temperatures. Influence of the microalloying was investigated at zirconium content in the weld metal in the limits from 0.007 to 0.015 wt.% (see Table 1). Zirconium
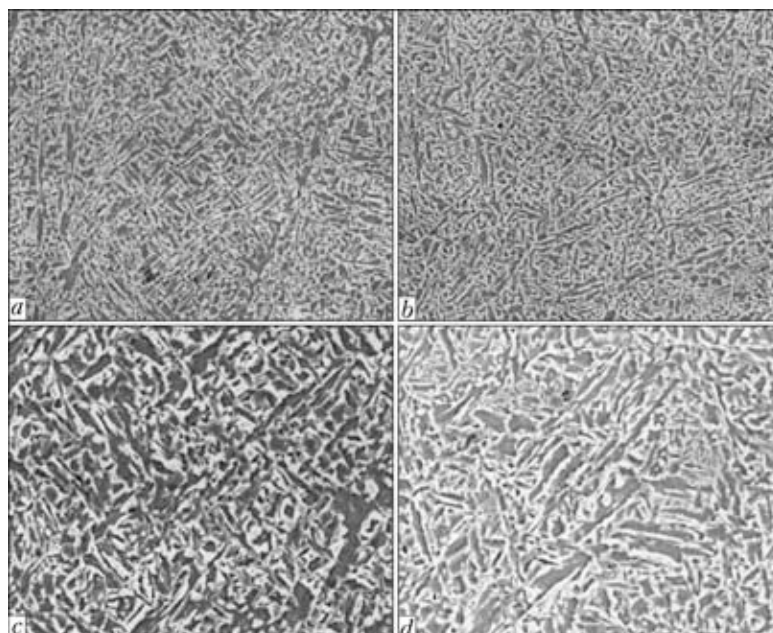
Figure 3. Microstructures of the Zr-microalloyed weld metal of C−Si−Mn−Ni−Mo alloying system: a, c − 0.007; b, d − 0.015 wt.%; a, b − ×1000; c, d − ×2000

acts as a deoxidizer and modifier of the weld metal due to formation of carbides, nitrides and oxides which have an influence on character of structural transformations in steel. The JEOL scanning electron microscope JSM-35CF equipped with energy dispersion analyzer was used for analysis of structure, composition and size distribution of the non-metallic inclusions.

Structure of the weld metal free from zirconium microalloying is a bainite with acicular ferrite areas (Figure 1). Size distribution of the non-metallic inclusions and their compositions are given in Figure 2 (average content of the elements being analyzed in non-metallic inclusions, wt.%: 44.89 O; 0.05 Mg; 14.62 Al; 5.94 Si; 3.58 S; 7.22 Ti; 23.7 Mn). As the analysis of chemical composition have showed, the non-metallic inclusions mainly consist of the oxides of manganese, silicon, aluminum and titanium (Figure 2, *a*). Small amount of oxysulfides, approximately to 3.6 wt.%, is also present in the inclusions.

Table 2. Mechanical properties of the weld metal

Weld number	$\sigma_{0.2}$, MPa	σ_t, MPa	δ, %	KV_{-50}, J
1	600−630	680−710	18−22	30−40
2	610−640	690−720	24−27	65−75
3	600−630	700−730	22−26	58−70

Values of impact energy KV_{-50}, obtained during the tests, make 30−40 J that is lower of the required ones (Table 2).

Fine-dyspersed ferrite of different modifications, i.e. acicular one with disordered second phase and polygonal (proeutectoid) ferrite in a form of fragments of ferrite rings (Figure 3), form the structure of the weld metal after zirconium microalloying. Volume fraction of the dispersed components (bainite) makes around 65 % in the structure of weld metal after zir-
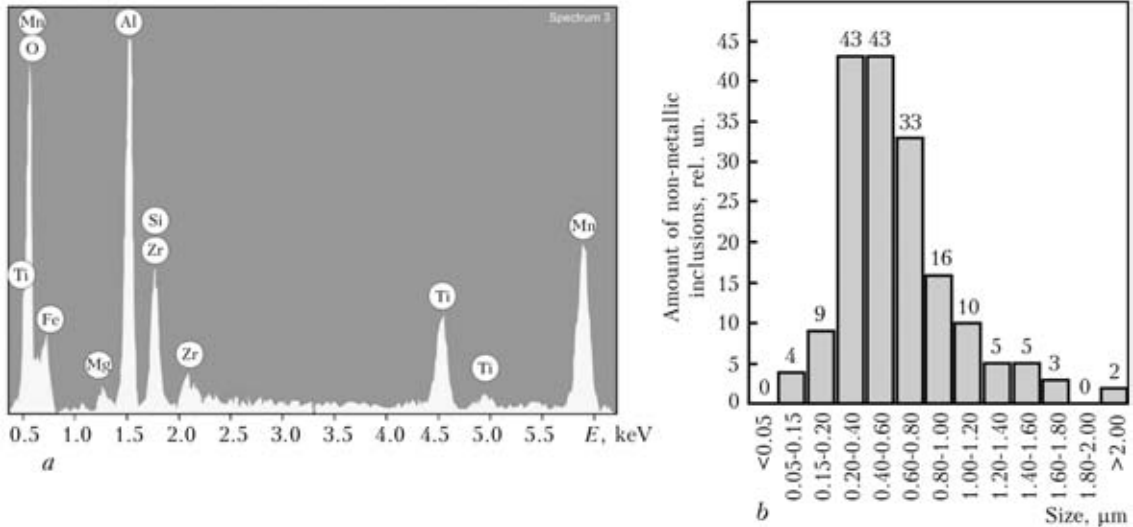
Figure 4. Element composition (*a*), and size distribution of non-metallic inclusions in the weld metal of C−Si−Mn−Ni−Mo system after 0.007 wt.% Zr microalloying (*b*)
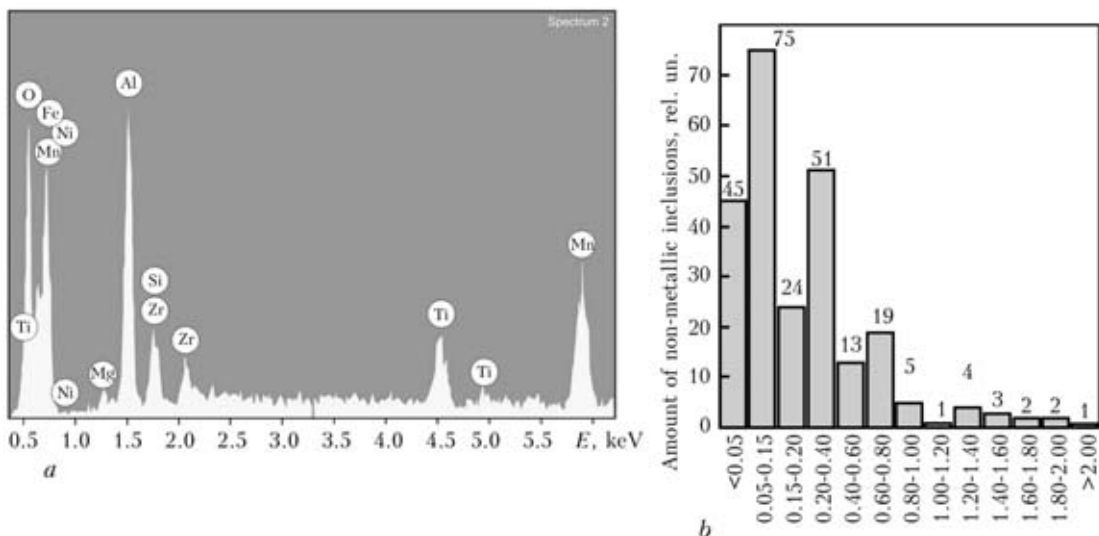
Figure 5. Element composition (*a*), and size distribution of non-metallic inclusions in the weld metal of C−Si−Mn−Ni−Mo system after 0.015 wt.% Zr microalloying (*b*)
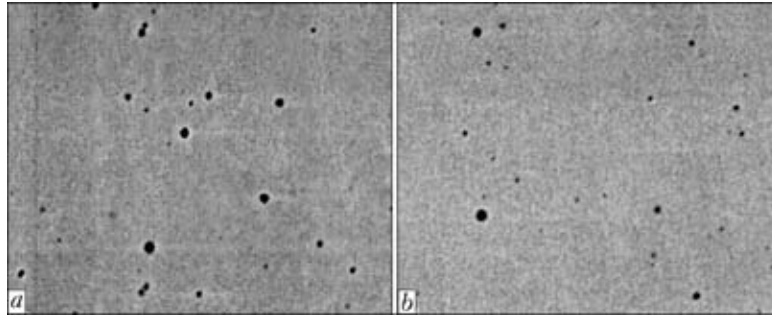
Figure 6. Typical distribution of non-metallic inclusions in the weld metal of C−Si−Mn−Ni−Mo alloying system (×3400): *a* − without zirconium microalloying; *b* − with zirconium microalloying on the level around 0.011 wt.%

conium microalloying on a level of 0.007 wt.%, and the rest is polygonal ferrite. Increase of zirconium microalloying up to 0.015 wt.% rises fraction of the dispersed structures up to 70 % and at that dimensions of the needles of the acicular ferrite decrease on average 1.5 times in comparison with the weld metal structure after zirconium microalloying on the level of 0.007 wt.%. Figures 4 and 5 show the compositions of non-metallic inclusions and their size distribution for the welds after zirconium microalloying. Average content of elements being analyzed in the non-metallic inclusions of the weld metal are (wt.%) 46.66 O; 1.45 Mg; 20.17 Al; 4.95 Si; 5.79 Ti; 19.08 Mn; 1.9 Zr after 0.007 wt.% Zr microalloying and 45.64 O; 1.17 Mg; 21.53 Al; 3.14 Si; 6.54 Ti; 16.91 Mn and 5.97 Zr after 0.015 wt.% Zr microalloying.

Volume fraction of the non-metallic inclusions reduces approximately 2 times due to formation of the zirconium oxysulfides which are removed in a slag phase at zirconium microalloying of the weld metal.

Average size of the inclusions itself also reduces approximately by 15 % at that. Zirconium microalloying of the weld metal promotes more uniform distribution of the non-metallic inclusions (Figure 6). Indices of impact energy of the welded joint, according to test results, make 65−75 J at −50 °C, that corresponds to the requirements (see Tables 1 and 2).

The flux-cored wire with the core of rutile-fluorite type was developed as a result of the investigations carried out. It is designed for shielded gas welding of metal structures from steel of not less than 590 MPa yield strength and provides achievement of the nec-essary level of tough-ductile properties of the weld metal.

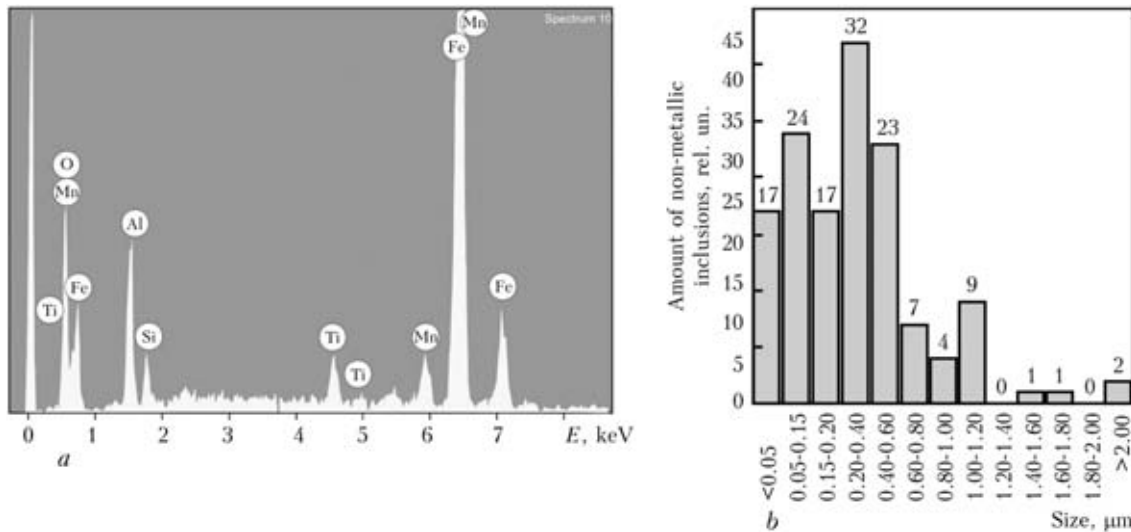**CONCLUSIONS**

1. Application of C−Si−Mn−Ni−Mo basic alloying with additional zirconium microalloying allows providing the necessary level of strength (yield strength more than 590 MPa) and impact toughness of the welded joint (impact energy more than 50 J at −50 °C test temperature).

2. 0.007−0.009 wt.% Zr is its optimum content in the weld metal at which reduction of the volume fraction and dimensions of non-metallic inclusions and increase of the fraction of dispersed components in the structure of metal can be achieved.

1. Gorynin, I.V., Malyshevsky, V.A., Legostaev, Yu.L. et al. (1996) High-strength steels for hulls, marine structures and deep-water technique. *Progres. Materialy i Tekhnologii*, **2**, 23−24.
2. Thomson, S.W., Krauss, G. (1996) Austenite decomposition during continuous cooling of HSLA-80 plate steel. *Metallurg. and Materials Transactions A*, 27(June), 1557−1571.
3. Tailor, D.J., Evans, G.M. (1983) Development of MMA electrodes for offshore fabrication. *Metal Constr.*, 15(**8**), 438−443.
4. Zhang, Z., Farrar, R.A. (1997) Influence of Mn and Ni on microstructure and toughness of C−Mn−Ni weld metals. *Welding J.*, 76(**5**), 183−190.
5. Wang, W., Liu, S. (2002) Alloying and microstructural management in developing SMAW electrodes of HSLA-100 steel. *Ibid.*, 81(**7**), 132−145.
6. Grabin, V.F. (1982) *Materials science of fusion welding.* Kiev: Naukova Dumka.
7. Grigorenko, G.M., Kostin, V.A., Golovko, V.V. et al. (2004) Effect of chemical inhomogeneity on the formation of acicular ferrite in high-strength weld metal. *The Paton Welding J.*, **4**, 2−7.

ANALYSIS OF SPECTRUM OF THE WELDING ARC LIGHT FOR MONITORING OF ARC WELDING (Review)

Ya.P. LAZORENKO, E.V. SHAPOVALOV and **V.A. KOLYADA**

E.O. Paton Electric Welding Institute, NASU, Kiev, Ukraine

The state-of-the-art in research activities in the field of spectral analysis of light of the welding arc is reviewed. The effect of welding parameters on the spectrum of the welding arc light, spectral diagnostics of the arc plasma, automation of the welding process based on spectral analysis of the welding arc light, monitoring of the welding process, and automatic detection of defects in the welds are considered.

Keywords: *arc welding, weld, spectrum of the welding arc, spectral analysis, automation of welding, monitoring of welding, diagnostics of welded joint, weld defects*

The idea of using spectral analysis for automation and monitoring of arc welding consists in the fact that optical spectrum of the welding arc light can serve as a basis for generation of valuable information on the welding process, e.g. detection of deviations of welding parameters from the rated ones. Potentially defective regions in the welded joints can be determined from the above deviations. Real-time fixation of the deviations of the welding parameters will make it possible to adjust and correct the welding process to assure the required quality of the welded joints. Therefore, the spectral analysis can be used for both monitoring and automation of the welding process.

Technical implementation of the commercial spectral analysis-based systems for monitoring and automatic control of welding is made possible now owing to the use of the advanced digital spectrometers, which allow measurement of the optical spectrum within a few milliseconds.

The purpose of this article is to generalise investigations dedicated to the spectral analysis of light of the welding arc.

Much research has been made up to now in this field [1–16]. The following areas have received further development:

• investigation of the effect of welding parameters on the arc light spectrum;

• spectral diagnostics of the welding arc plasma;

• monitoring of the welding process by analysis of the arc light spectrum;

• automation of welding based on the spectral analysis of the welding arc light.

Investigations into the effect of welding parameters on the welding arc light spectrum are reported in studies [1–4]. The spectrum includes a continuous component, spectral lines of shielding and active gases, and spectral lines of metal of the parts welded.

Studies [1, 2] describe experimental investigations of the effect of the welding current on the intensity of spectral lines of metal and shielding gas in TIG welding. Spectra of the welding arc at different values of the current were measured during the welding process. Argon [1, 2] and helium [1] were used as a shielding gas. Plates of low-carbon steel, as well as stainless steel, copper, aluminium and titanium were used for welding. As shown by analysis of the obtained spectra, the intensity of spectral lines of metal and shielding gas increases with increase in the current during welding in argon atmosphere. This dependence is of a non-linear character. In welding of different metals in helium atmosphere the intensity of their lines either increases or decreases, or first increases and then decreases.

Study [2] was dedicated to investigation of the effect of filler wire feed speed on the spectrum of the welding arc light in TIG welding. The experiments were conducted by making welds on low-carbon steel plates and measuring spectra of the welding arc light in a range of 480–860 nm at different deviations of filler wire feed speed $v_{f.w}$ from the rated value corresponding to the technological standard. Decrease in the intensity of the arc light over the entire range of the measured spectrum frequencies was fixed at $v_{f.w}$ in excess of the rated value. The intensity of the light substantially increased in all regions of the spectrum within the measurement range with delay of feeding of the wire ($v_{f.w} = 0$).

The effect of length of the welding arc on the optical spectrum was investigated in study [3], wherein a mathematical model determining the dependence of the intensity of the welding arc light on the arc length and welding current was suggested. Integrated arc light intensity B_{iv} within the preset spectral range can be determined from the following formula:

$$B_{iv} = G_1 L I^2 \left(e^{G_2/I} - \frac{1}{2} \right) + G_3 I^2 + G_4,$$

where I is the welding current; L is the arc length; and G_i are the coefficients that depend on the specific welding conditions. As seen, in this formula the relationship between radiation intensity B_{iv} and arc length L is linear.

The experiments were carried out to check the adequacy of the model, in which the integrated arc light intensity was measured in a spectral range of 500–1000 nm in TIG welding of steel in argon atmosphere at different values of the arc length and welding current. Coefficients G_i were calculated on the basis of the experimental data. Comparison of the measured data with the B_{iv} values calculated by using the above model proved its adequacy for the arc length values ranging from 1 to 5 mm.

In study [4] the adequacy of mathematical model (1) was checked for a wider range of the welding currents (50–300 A). The model was proved to be adequate for values of the current ranging from 50 to 150 A. At the currents higher than 150 A the values of the intensity calculated by using the model were substantially different from the measured values.

The mathematical model was synthesised on the basis of an artificial neural network (ANN) of the «multilayer perceptron» type, allowing estimation of the welding arc length [4]. Two parameters served as the input data for ANN: welding current and intensity of light of the specified spectral line of argon atoms. The model was developed for the process of TIG welding of copper in argon atmosphere. Teaching of ANN was done by using the BPE (Back Propagation of Error) algorithm. Checking the neural network model with the experimental data showed its adequacy for the welding currents of 50–300 A and arc length of 2–5 mm.

Diagnostics of the welding arc plasma is a set of methods for measurement of parameters of the plasma that characterise its state. Study [5] suggested a method for diagnostics of the welding arc plasma based on its light spectrum. This method can be used to measure temperature of the plasma and concentration of its components (atoms, ions and electrons). The temperature and concentration were calculated by using the synthesised mathematical model of the multicomponent plasma. The mathematical model allows performing calculations for any chemical composition of the welding arc plasma.

An important task of monitoring of the welding process is fixation of regions of a welded joint characterised by the highest probability of formation of defects. The weld diagnostics method based on the spectral analysis provides for extraction of some diagnostic features from the welding arc spectrum, with the help of which it is possible to assess the quality of the welded joint.

Results of the experimental investigations aimed at development of procedures and systems for monitoring of the welding process on the basis of the spectral analysis of the welding arc light are given in studies [2, 6–13]. The following types of the diagnostic parameters have been identified up to now: integrated intensity of the light within the preset spectrum frequency band [6–8], spectral line intensity [2, 9], temperature of the welding arc plasma [8, 10, 11], root-mean-square value of the spectrum signal [10], and integrated parameters of profiles of the spectral lines [13].

The method for monitoring of the welding process suggested in patent [6] allows assessment of the quality of the welded joints by registering and analysing signals of the integrated intensity of light of the welding arc in several spectral lines. The intensities are measured by using photodetectors having the corresponding bandwidths. A decision on defectiveness of the weld is made by comparing the measured intensity signals and signals obtained for the reference welds with a normal structure.

Studies [7, 8] used values of the integrated intensity in several spectral bands as diagnostic features. As selection of the spectral bands is not a trivial problem, for this purpose the use was made of the automatic selection procedure based on experimental data. In that case the experimental data were two groups of spectra of the welding arc light. The first group was obtained for the welds with a normal structure, and the second — for welds containing defects.

The automatic selection was performed by using a specially developed algorithm based on the SFFS (Sequential Forward Floating Selection) algorithm. The experimental study showed the efficiency of the suggested procedure of selection of the diagnostic features for detection of defects forming as a result of oscillations of the welding current, variations in the arc length, non-uniform feeding of the shielding gas, and variations in width of the welding gap.

Study [8] describes the system developed for monitoring of the welding process, where a decision on the presence of defects is made by using the «multilayer perceptron» type ANN. Here the values of the intensity of a set of spectral bands selected by means of the above automation selection algorithm serve as a source of information for monitoring.

Studies [2, 9] suggested using the intensities of the spectral lines as diagnostic features. As established in study [2], the delay in feeding of a welding wire can be detected from a change in the intensity of argon spectral lines during the process of filler wire TIG welding. The system for monitoring of TIG welding of steel developed in study [9] uses signals of the intensities of the iron and hydrogen spectral lines for detection of defects in the welds. As shown by the experiments [9], the presence of tungsten inclusions and hydrogen in the weld metal, contamination of the metal surface with sand and non-uniformity of the shielding gas flow can be determined from a change in these signals.

The relationship between temperature of the welding arc plasma and quality of the welded joints was investigated in studies [8, 10, 11]. The temperature of the plasma was calculated from values of the intensity of several spectral lines of the shielding gas.

The experiments showed that by measuring the plasma temperature it is possible to detect such defects of the welds as burns-through and lacks of penetration, as well as the presence of the factors that have a negative effect on the quality of the welds (oscillations of the welding current, deflection of the welding torch from the joining line, and contamination of the metal surface with machine oil).

Study [10] suggested using the root-mean-square value of signal of the welding arc light spectrum as a diagnostic feature. The experiments showed that the value of this feature remains unchanged during the entire welding process at the absence of substantial deviation of the welding parameters from the rated ones. Formation of defects of the lack of penetration type is accompanied by decrease in the root-mean-square value, and in case of a burn-through there occurs a sudden change in this parameter. Marked fluctuations are fixed in the signal of the root-mean-square value in case of an edge displacement or deflection of the welding torch from the joining line.

In study [13] the spectral line profiles were approximated by the Lorentz function, and its parameters were used as diagnostic features to detect the perturbation actions appearing during the MAG welding process. Application of the integrated parameters of the spectral line profiles is explained by the fact that resolution of the fast-response digital spectrometers employed for real-time measurements is insufficiently high to fix the profiles of the individual lines located close to each other.

Because of averaging of the light intensity by discrete photosensitive elements of the spectrometer range, the digital signal of the spectrum comprises one wider intensity peak instead of several spectral lines. Such distortions cause decrease in the accuracy of measurement of the intensity of the individual spectral lines.

From this standpoint, the use of the integrated parameters of the spectral line profiles as diagnostic features is more preferable than the use of the intensity lines proper. The experiments proved that oscillations of the welding current, contamination of the metal surface in the welding location with paint and dirt can be detected from a change in the Lorentz function parameters.

The procedure was developed for identification of the metal transfer mode from the welding arc light spectrum in MIG/MAG welding [14] by the probability (Bayesian) decision-making technique. Statistical characteristics of the digital signal of the spectrum serve as primary parameters, on the basis of which the metal transfer mode is identified. According to the results of experimental verification of the procedure, the error in identification of the metal transfer mode was 5 %.

In plasma welding, the high-energy plasma flow makes a through hole in molten metal, which is im-mediately filled up. As a result, the through penetration weld is formed. To prevent burns-through and incomplete penetration of the welds, it is necessary to monitor the processes of appearance and disappearance of the through hole.

Study [15] describes the procedure developed for spectral analysis of the welding arc light, which can be used to detect the time points of appearance and disappearance of the through hole during the plasma welding process. Information on these time points is generated on the basis of analysis of variations in the intensity of the argon spectral lines.

The automatic seam guidance system was developed [3], compensating transverse deflections of the welding torch with respect to the longitudinally welded joint in TIG welding without groove preparation or with the V-groove. The source of information on deflections of the welding torch is a signal of the integrated intensity of the specified shielding gas spectral line. Oscillations of the intensity signal are fixed in movement along the joining line. Deflection of the welding torch from the joining line is calculated on the basis of the amplitude of oscillations of the intensity signal and values of time intervals between its local minima and maxima.

The team of German researchers and engineers developed a pilot sample of the system for automatic regulation of impulse MIG welding in argon atmosphere on the basis of the information on the welding arc light [16]. The system regulates input of the thermal energy to metal in each pulse of the welding current.

In impulse welding, the arc plasma temperature grows at a speed of several millions of Kelvin per second after the beginning of feeding of a pulse of the welding current. The pulse of the current is switched off when the arc plasma temperature reaches a certain value. The time point of switching off of the pulse is determined by measuring the integrated intensities of the arc light, I_m and I_g, in two corresponding spectral ranges Δ_m and Δ_g. The Δ_m range (approximately 260−550 nm) overlaps the region of the most intensive spectral lines of such metals as zinc, magnesium, aluminium, copper and iron, and the Δ_g range (approximately 650−950 nm) overlaps the region of the most intensive lines of the shielding gas (argon).

Arc light intensities I_m and I_g are measured by using two photodiodes. The difference of the measured intensities, $I_g − I_m$, monotonously decreases simultaneously with increase in the plasma temperature after switching on of the pulse of the welding current. After the $I_g − I_m$ difference decreases to the preset threshold corresponding to a certain maximal value of the plasma temperature, the regulation system feeds the control signal to switch off the pulse of the current. In the course of the tests the system developed provided stabilisation of the welding process at considerable deviations (±30 %) of the main and pulse currents from the rated values.

Therefore, at present the research and development efforts related to application of the spectral analysis for automation and monitoring of the welding process are at their initial stage. The suggested diagnostic features identified in spectrum of the welding arc light allow detection of defects in the welded joints and deviations of parameters of the welding process from the rated values. However, no investigations have been carried out as yet to confirm the high efficiency of the existing solutions required for their commercial application.

1. Kim, E.W., Allemand, C., Eagar, T.W. (1987) Visible light emissions during gas tungsten arc welding and its application to weld image improvement. *Welding Res. Suppl.*, **12**, 369–377.
2. Weglowski, M.S., Mikno, Z., Welcel, M. et al. (2007) Kontrola procesu spawania TIG w oparciu o promieniowanie luku spawalniczego. *Prz. Spaw.*, **12**, 15–19.
3. Li, P.G., Zhang, Y.M. (2000) Analysis of an arc light mechanism and its application in sensing of the GTAW process. *Welding Res. Suppl.*, **9**, 252–260.
4. Weglowski, M.S. (2007) Investigation on the arc light spectrum in GTA welding. *J. Achievements in Materials and Manufact. Eng.*, 20(**1**/**2**), 519–522.
5. Song, Y., Li, J. (1998) Spectral diagnostics of complex arc plasma. *China Welding*, 7(**1**), 53–59.
6. Kearney, F.M. *Optoelectronic weld evaluation system*. Pat. 4446354 USA. Int. Cl. B 23 K 9/095. Publ. 1984.
7. Garcia-Allende, P.B., Mirapeix, J., Conde, O.M. et al. (2009) Defect detection in arc-welding processes by means of the line-to-continuum method and feature selection. *Sensors*, **9**, 7753–7770.
8. Garcia-Allende, P.B., Mirapeix, J., Conde, O.M. et al. (2008) Arc-welding spectroscopic monitoring based on feature selection and neural networks. *Ibid.*, **8**, 6496–6506.
9. Bebiano, D., Alfaro, S.A. (2009) A weld defects detection system based on a spectrometer. *Ibid.*, **9**, 2851–2861.
10. Mirapeix, J., Fuentes, J., Davila, M. et al. (2009) Use of the plasma spectrum RMS signal for arc welding diagnostics. *Ibid.*, **9**, 5263–5276.
11. Mirapeix, J., Cobo, A., Conde, O. et al. (2006) *Non-invasive spectroscopic system for non-destructive arc welding analysis*. ECNDT.
12. Mirapeix, J., Cobo, A., Gonzalez, D.A. et al. (2007) Plasma spectroscopy analysis technique based on optimization algorithms and spectral synthesis for arc welding quality assurance. *Optics Express*, 15(**4**), 1884–1897.
13. Weglowski, M.S. (2009) Measurement of arc light spectrum in MAG welding method. *Metrology and Measur. Systems*, 16(**1**), 143–159.
14. Yun, S., Zhang, L., Han, G. et al. (2006) Bayesian decision-based pattern recognition on spectrum signal of metal transfer modes. *China Welding*, 15(**1**), 39–42.
15. Dong, Ch., Wu, L., Zhang, H. et al. (1999) Front side keyhole detection in plasma arc welding of stainless steel. *Ibid.*, 8(**2**), 102–110.
16. Heinz, G., Hofmann, F., Schopp, H. et al. (2009) Echtzeit-spektralregler fuer Impulsschweissmaschinen. *Schweissen und Schneiden*, **3**, 144–149.

NONDESTRUCTIVE TESTING OF WELDED JOINTS

IN-PROCESS QUALITY CONTROL OF WELDED PANELS OF ALLOY VT20 USING METHOD OF ELECTRON SHEAROGRAPHY

L.M. LOBANOV, V.A. PIVTORAK, E.M. SAVITSKAYA, I.V. KIYANETS and **V.V. LYSAK**
E.O. Paton Electric Welding Institute, NASU, Kiev, Ukraine

Application of modern method of nondestructive testing (NDT), i.e. electron shearography, for VT20 alloy titanium panels, manufactured with preliminary elastic tension, is considered. The efficiency of application of NDT of titanium panel without dismantling of fixture for tension is shown, thus allowing the immediate elimination of defects, if required.

K e y w o r d s : *arc welding, welded panels, titanium alloy, quality control, in-process control, electron shearography*

The manufacture of welded metal structures, characterized by a low cost, high reliability and strength under different service conditions, is closely connected with the development of effective methods of NDT of their quality. One of the challenging methods of quality control is the electron shearography which is characterized by such advantages as a visualization, no-contact, high sensitivity, feasibility of real time con-ductance of investigations of objects of intricate geometric shape and large sizes. Comparative simplicity of this method allows it to be applied in the solution of complex problems, connected with analysis of deformations, quality control, etc. Using the electron shearography it is possible to determine deformations without numerical differentiation of data. Moreover, the method is not sensitive to vibrations, i.e. it can be used in different industry branches during in-process control of quality of structures, made of metallic and composite materials [1–5].

At practical application of electron shearography for NDT of quality it is necessary to take into account the following assumptions which resulted from optical scheme of a shearography interferometer:

• sizes of objects being examined or their areas should be much smaller than the distance from source of laser light to the surface of object under examination;

• shear module is located normal to the object surface area being examined;

• direction of illumination of surface of examined object by a laser light is selected as close as possible to the normal of the object surface area being examined.

In this case, the following relationships are used on the shearogram for dark and light interference fringes [6]:

• for dark interference fringes

$$\frac{\partial w}{\partial x} = \frac{(2N + 1)\lambda}{4\delta x}, \qquad (1)$$
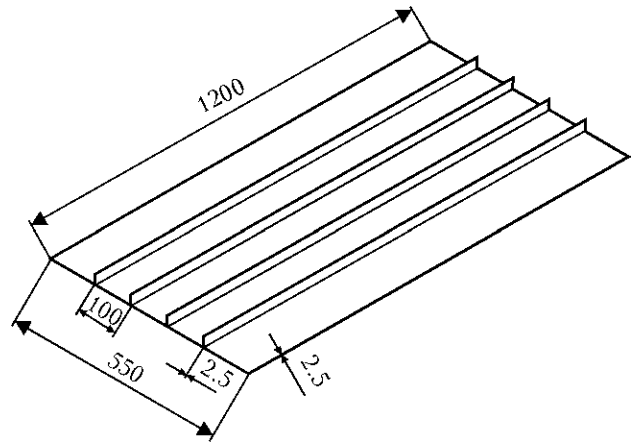
Figure 1. Sketch of welded panel manufactured of titanium alloy VT20

$$\frac{\partial w}{\partial y} = \frac{(2N + 1)\lambda}{4\delta y}; \qquad (2)$$

• for light interference fringes

Figure 2. NDT of quality of titanium panel 1 with stiffeners, manufactured under conditions of its preliminary elastic tension: a — titanium panel in loaded mechanical fixture after welding; b — pattern of interference fringes of area being examined; c — 3D pattern of deforming the panel area being examined; d — distribution of derivatives $\partial w / \partial x$ along the sections being examined; $A-A$ — section with a defect; $B-B$ — defect-free section

$$\frac{\partial w}{\partial x} = \frac{N\lambda}{2\delta x}, \qquad (3)$$

$$\frac{\partial w}{\partial y} = \frac{N\lambda}{2\delta y}, \qquad (4)$$

where N is the fringe order; λ is the wave length of laser light source; δx, δy are the shear dispacements, respectively, in the directions of axes ox, oy; $\partial w / \partial x$, $\partial w / \partial y$ are the derivatives from displacements along normal to the surface of object being examined.

Using equations (1)−(4) it is possible to make a direct estimation of off-plane deformation of object after determination of the fringe order.

Technology of NDT of quality with application of method of electron shearography was used for diagnostics of elements and sub-assemblies of structures manufactured of various structural materials [3].

At present, the welded thin-walled panels with stiffeners, manufactured of titanium alloys, find the wider spreading in aircraft and aerospace industry. Quality control of these panels is rather labor-consuming and causes certain difficulties. In this connection, the development of new methods of investigation of their quality remains urgent.

The method of electron shearography was used for NDT of quality of stringer panels made of high-strength titanium alloy VT20 of $1200 \times 550 \times 2.5$ mm in size (Figure 1). Four longitudinal stiffeners of 25 mm height and 2.5 mm thickness were welded-on to titanium sheet by slot welds. The distance between stiffeners was 100 mm. Welding of titanium panels was performed under the conditions of their preliminary tension. Here, the automatic argon arc welding with immersed arc and automatic argon arc non-consumable electrode welding along the layer of activated

Figure 3. NDT of quality of titanium panel 2 with stiffeners, manufactured under conditions of its preliminary elastic tension: a−d — the same as in Figure 2

flux were used. After welding the titanium panel remained in fixture in a state of tension.

NDT of quality of panels was performed in the following sequence. The examining area of weld of panel after tension was illuminated by a laser light and reflected light wave, characterizing the initial state of surface being examined, was recorded in the computer memory. Then, the examining area was blown with a hot air at temperature of about 50−70 °C during 25−40 s, thus leading to its deformation. Then the light wave, reflected from the deformed area of surface being examined, was also recorded in the computer memory. Using a special computer program the recorded optical information was processed up to obtaining the shearogram and 3D pattern of deforming the surface being examined.

The result of control of welded panel 1 of alloy VT20, welded by automatic argon arc welding with immersed arc, is presented in Figure 2. The shearogram of examined area of weld (Figure 2, b) shows a local change of pattern of interference fringes on the general background of deforming, that proves the presence of internal defects. The plotted 3D pattern of deforming (Figure 2, c) and curves of distribution of derivatives $\partial w / \partial x$ along the selected sections $A-A$ and $B-B$, respectively, of defective and defect-free ones (Figure 2, d) confirm the presence of defects on the area being examined (shown by arrow).

It should be noted that in examining area of panel a section $A-A$ is given in Figure 2, b, in which the local change of derivative has the highest value (the analysis of several sections was made and section was selected with the highest local value of derivative $\partial w / \partial x$).

The carried out X-ray control of quality of the examined area of weld of titanium panel of VT20 alloy showed the presence of clusters of pores of 0.2−0.4 mm in it.

In examination of welded titanium panel 2 the area of arc break was observed, where the concentration of deformations in the site of welding interruption was observed (Figure 3, b). The shearography quality
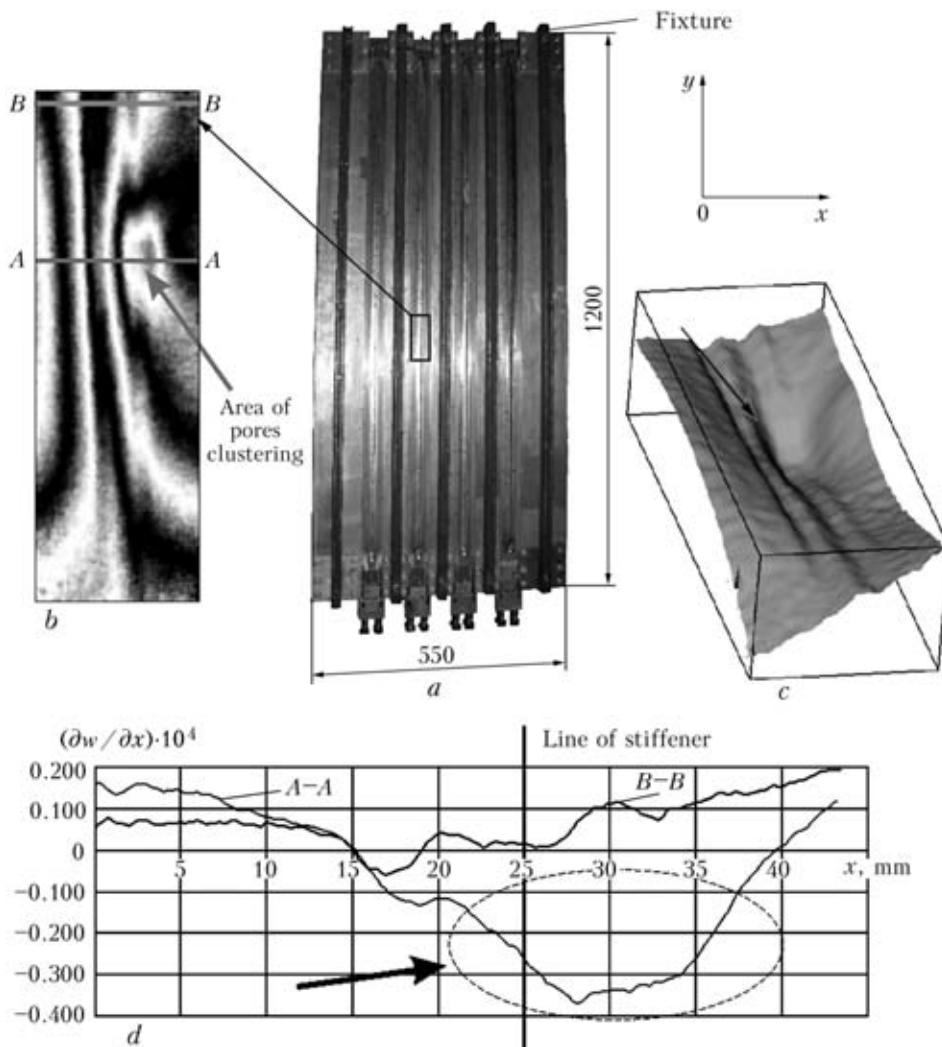

Figure 4. NDT of quality of titanium panel 3 with stiffeners, manufactured under conditions of its preliminary elastic tension: $a-d$ — the same as in Figure 2

Figure 5. NDT of quality of titanium panel 4 with stiffeners, manufactured under the conditions of its preliminary elastic tension: a–d — the same as in Figure 2

control was performed using the same parameters of heating as in the previous case.

Results of further processing of interference fringes up to obtaining of 3D pattern of deforming (Figure 3, c) and plotting of curves of distribution of derivatives $\partial w/\partial x$ along the sections A–A and B–B being examined (defective and defect-free areas of weld, respectively) (Figure 3, d) confirmed the presence of a local jump of derivative $\partial w/\partial x$ at the area of arc break during welding panel.

During NDT of quality of panel 3, welded by the automatic argon arc welding with immersed arc, the areas with an abrupt change of derivatives $\partial w/\partial x$ were also revealed. Results of quality control, obtained on one of them, are presented in Figure 4.

The 3D pattern of deforming the examining weld areas and curves of distribution of derivative $\partial w/\partial y$ along section A–A show a local area of an abrupt its change (shown by arrows) that proves the presence of defects in weld (Figure 4, c, d).

The X-ray control of examining weld area showed the cluster of pores of 0.2–1.0 mm sizes and inclusions of 0.3 and 0.8 mm sizes in it.

Figure 5, b–d shows, respectively, pattern of interference fringes, 3D pattern of deforming the examining area of weld of welded titanium panel 4, welded by the automatic argon arc welding with immersed arc, and distribution of derivatives $\partial w/\partial x$ along the sections A–A and B–B being examined at the area of weld after its repair using the manual arc welding.

It is seen visually that after the repair of defective weld area an abrupt local change of derivative $\partial w/\partial x$ is observed that characterizes the concentration of deformations in weld area, recovered by repair.

During welding of titanium panel 5 using the automatic argon arc welding with non-consumable electrode along the layer of activated flux, a weld area with a local concentration of deformations, caused by pore clustering, was also observed (Figure 6, b, c).

Distribution of derivatives $\partial w/\partial x$ along the sections A–A and B–B being examined is shown in Fi-
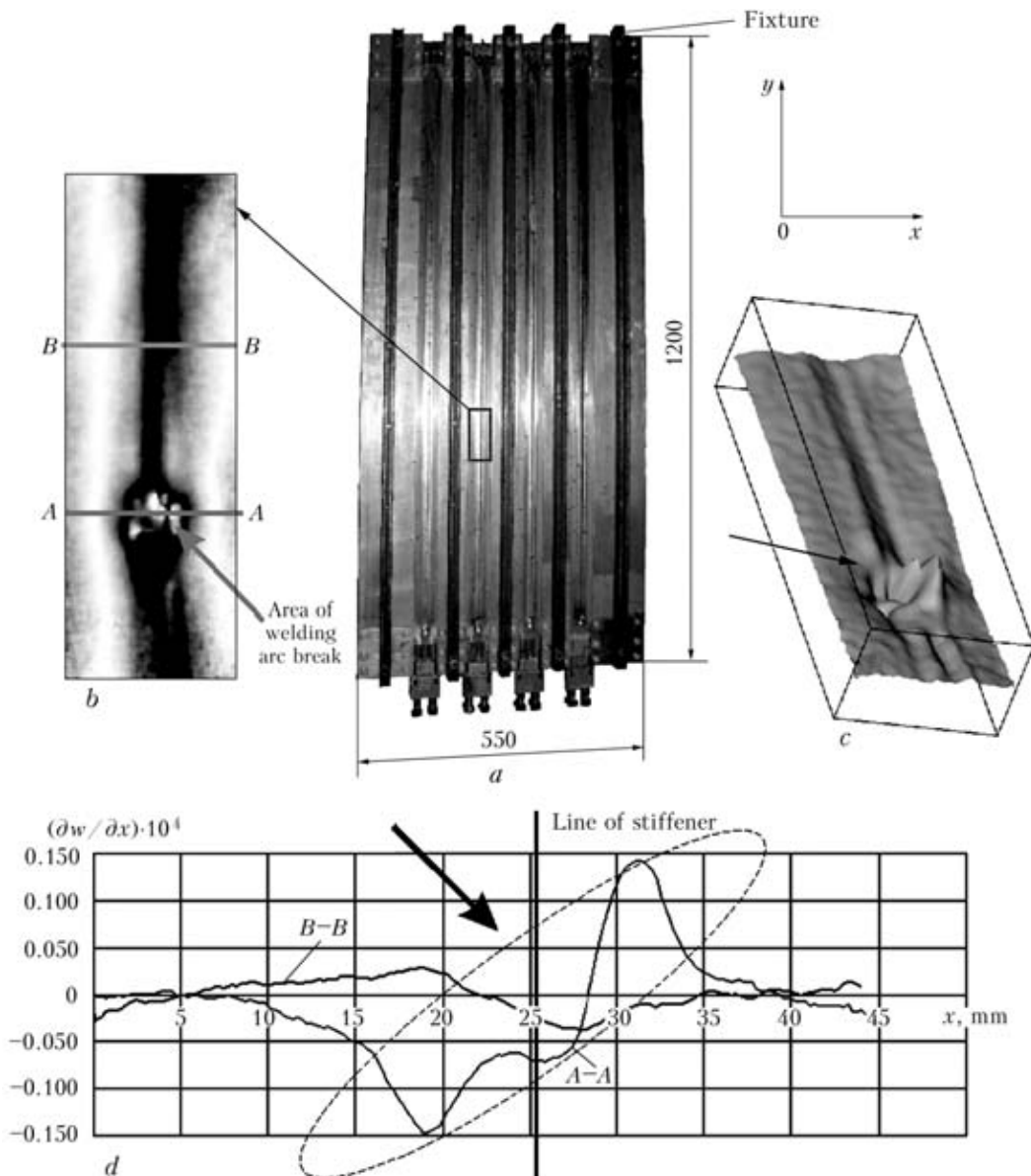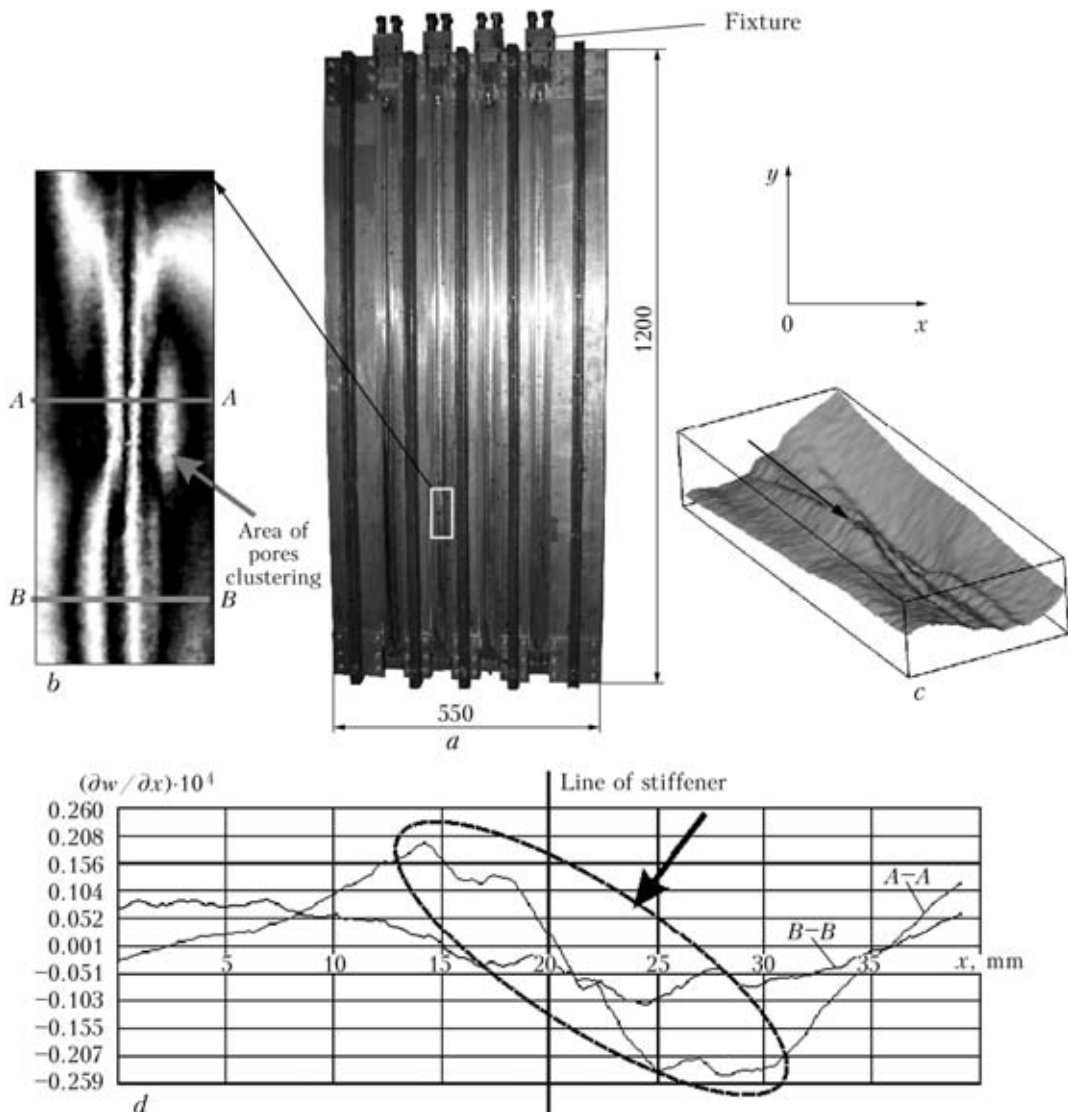
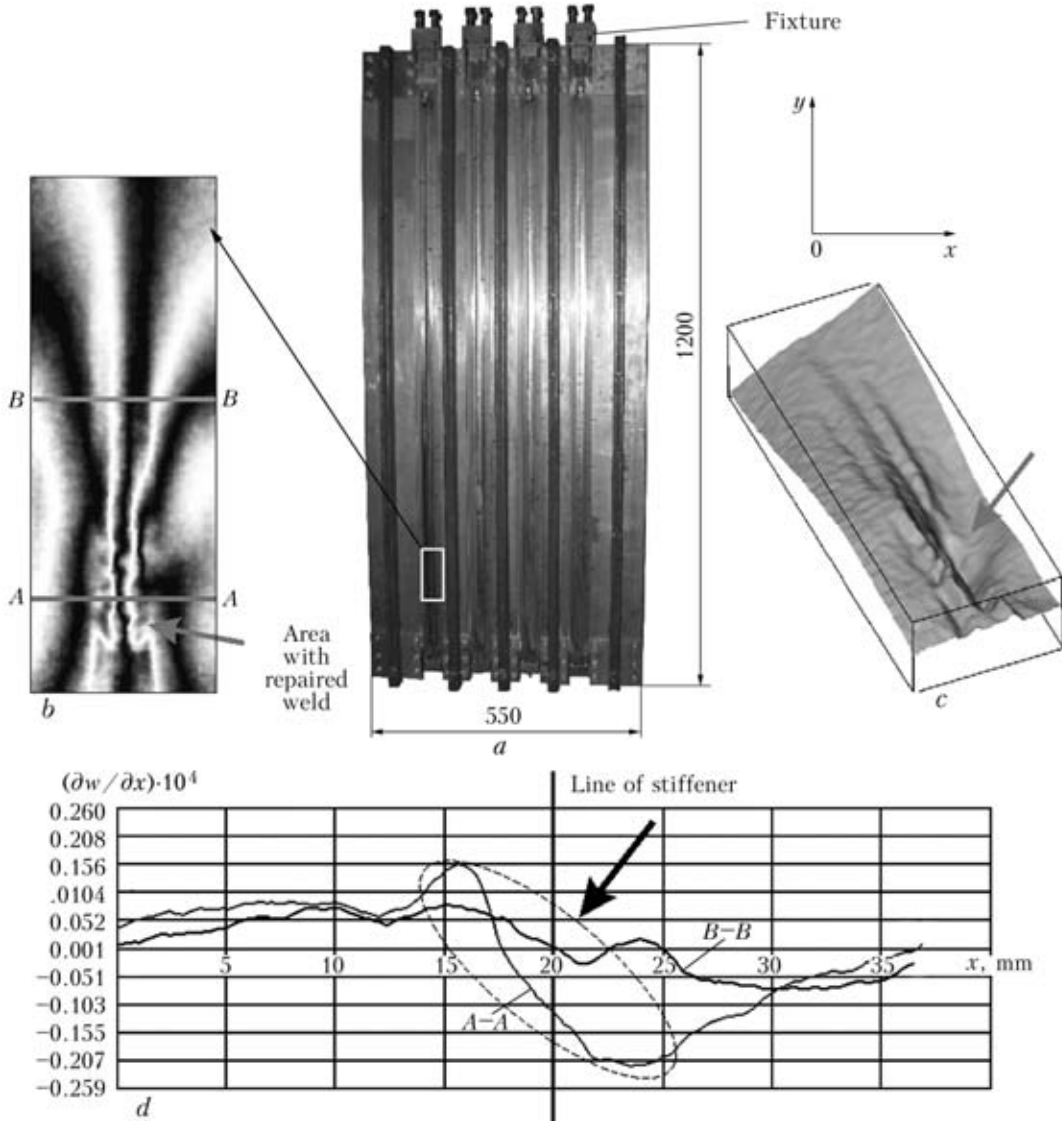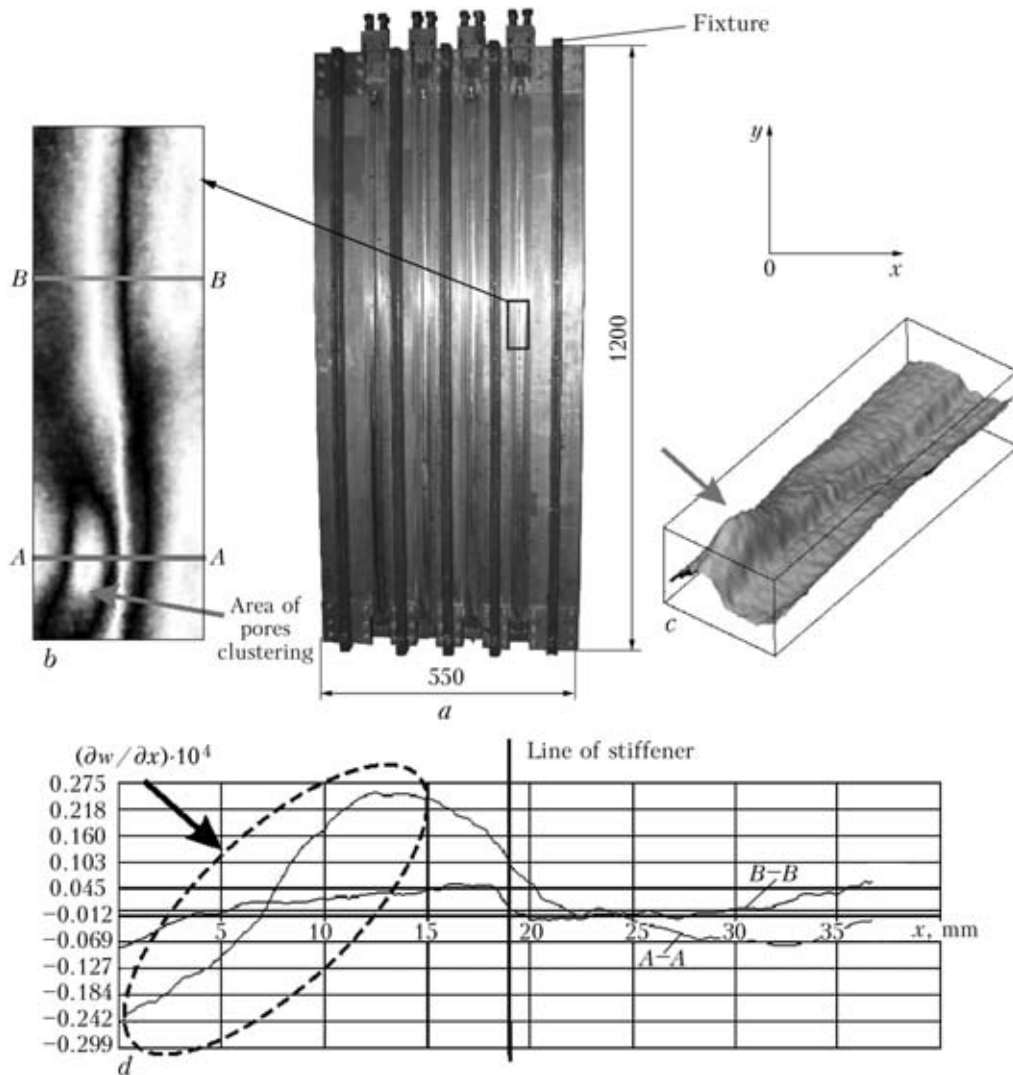**Figure 6.** NDT of quality of titanium panel 5 with stiffeners, manufactured under conditions of its preliminary elastic tension: *a–d* — the same as in Figure 2; *b* — pattern of interference fringes at the area of pores clustering

gure 6, *d*. An abrupt change of derivative $\partial w / \partial x$ in section *A–A* at the weld area being examined characterizes the presence of defects.

Thus, the carried out series of experiments on no-contact NDT of quality of welded titanium panels with stiffeners, manufactured of alloy VT20 and performed under the conditions of their preliminary tension, showed that the method of electron shearography allows in-process examination of quality of welded panels and revealing of defective areas of welds. It is especially important that the method allows revealing the defects without dismantling the fixture for tension of titanium panel and, when necessary, beginning at once their elimination.

During welding of titanium panels it is also necessary to take into account that the break of welding arc in making weld and manual repair welding of weld

areas cause the local concentration of deformations, that can lead to the reduction in their service life at the effect of service loads.

1. Rastogi, P.K. (2000) *Trends in optical nondestructive testing and inspection*. Amsterdam; Lausanne: Elsevier.
2. Lobanov, L.M., Pivtorak, V.A., Olejnik, E.M. et al. (2004) Procedure, technique and equipment for nondestructive shearographic testing of materials and elements of structures. *Tekhn. Diagnostika i Nerazrush. Kontrol*, **3**, 1–4.
3. Lobanov, L.M., Pivtorak, V.A., Savitskaya, E.M. et al. (2008) Diagnostics of elements and assemblies of structures using electron shearography method. *Ibid.*, **4**, 7–13.
4. Newman, J.W. (2005) Holographic and shearographic NDT. Application in aerospace manufacturing. *Materials Evaluation*, **7**, 746–750.
5. Collrep, J., Krupka, R., Siebert, T. (2007) Industrial applications of shearography for inspection of aircraft components. *NDT World Review*, 36(**6**), 28–31.
6. Hung, Y.Y., Ho, H.P. (2005) Shearography: an optical measurement technique and applications. *Materials Sci. and Eng.*, **49**, 61–87.

SINGLE- AND MULTIOPERATOR SYSTEMS FOR AUTOMATIC WELDING OF POSITION BUTT JOINTS OF NUCLEAR POWER PLANT PIPING

N.M. MAKHLIN[1], **A.E. KOROTYNSKY**[1], **V.A. BOGDANOVSKY**[1], **I.A. OMELCHENKO**[2] and **A.A. SVIRIDENKO**[3]

[1]E.O. Paton Electric Welding Institute, NASU, Kiev, Ukraine
[2]Expert Center «Transserviceengineering, Kiev, Ukraine
[3]OJSC «CheZaRa», Chernigov, Ukraine

The paper describes PWI activities on development and manufacture of orbital complexes for automatic welding of butt joints of 8–76 mm piping. These complexes became accepted for repair of equipment of power units of Ukrainian nuclear power plants.

Piping of NPP reactors is the basic element of NPP production strings [1]. According to the norms and rules of nuclear power engineering, the piping, operating predominantly under the conditions of exposure (in many cases simultaneously) to high temperatures, residual stresses and higher pressure of corrosive-aggressive heat carrier, are classified as a separate group of devices by their impact on NPP reliability and safety [1, 2]. Functions, performed by NPP power unit piping, complexity of their service conditions, cramped conditions in welding operation sites and limited access to these areas make high demands of quality, strength and corrosion resistance of welded joints on such piping [1–3]. Labour consumption for welding butt joints of NPP power unit piping is equal up to 40 % of all the labour consumption in NPP mounting and up to 60 % of total labour consumption for welding operations in reactor mounting. The main scope of the work (up to 80 %) is taken up by welding of butt joints of less than 100 mm diameter piping. Up to 60 % of the total number of butt joints are those of austenitic steel piping [1, 4, 5].

The majority of welded joints of NPP power unit piping are position butt joints, for which the dominating welding processes are manual argon-arc (TIG) welding using filler material, and automatic non-consumable electrode orbital welding (GTAW) with filler wire feeding or without it.

Manual TIG welding using filler material is characterized by relatively high technological flexibility that made this process accepted in mounting and particularly in repair of NPP power unit piping. Multioperator welding systems (MWS) are mostly used to perform manual TIG welding of piping and other reactor equipment, and much more seldom it is performed with single-operator specialized TIG welding machines. On the other hand, manual TIG welding has a number of significant disadvantages:

• involvement of a large number of highly qualified welders for performance of a considerable volume of welding operations in compressed terms (for instance, in mounting of just one power unit with WWER type reactor it is necessary to perform welding of not less than 41,000–60,000 butt joints of not more than 100 mm diameter piping) [5];

• required level of welded joint quality is not achieved, which results in their defect level reaching 15–45 % at first-attempt acceptance that necessitates repair of defective butt joints and in this connection, the inevitability of significant additional losses [4–6];

• machine time in TIG welding of piping butt joints (arcing duration) is usually equal to not more than 20 %, that does not allow reaching the required efficiency of the welding station [6].

Unlike manual TIG welding, the process of automatic orbital GTAW ensures:

• stable high quality and operational reliability of piping welded joints (at GTAW without filler wire the defect level at first-attempt acceptance does not exceed 4 %, that with filler wire — 7 %);

• not less than 4 times increase of welding operation efficiency;

• considerable reduction of duration of operator training in automatic welding (several months) compared to duration of training of a highly qualified welder in manual TIG welding (several years) [4–7].

Experience of operation of welded joints made with orbital automatic machines ODA (developed by R&D Institute of Mounting Technology — NIKIMT) on water and steam-water service lines of RMBK-1000 rectors, which have long ago passed the limit of their design service life without a single repair, provides convincing proof that the greatest effect from application of GTAW process is achieved as a result of many times reduction of the cost of repair of piping welded joints during their operation [7].

GTAW process using orbital complexes of ODA series and other models developed by NIKIMT, was applied with greatest success in mounting and repair of piping of NPP power units with channel reactors of RMBK type, the level of welding operation automation reaching 60 % [1, 4, 6, 7].

At present in Russia, Ukraine and in a number of other countries NPP power units are being constructed and will be constructed in the near future mainly with reactors of WWER and BN type, in mounting of which the level of automation of piping welding does not yet exceed several percent, that is attributable to a number of objective and subjective causes. These include absence or incomplete sets of modern orbital automatic machines, designed for typesizes of piping applied in the structures of local NPP power units, as well as equipment, devices and fixtures for sound preparation of piping butts for GTAW; established technologies of mounting up to 100 mm piping, according to which such piping in the absence of their working drawings, is mounted to suit job, without enlarging them into blocks; limited application of such advanced technologies of piping mounting as pack and cassette mounting methods, preliminary binding of the mounted heat engineering equipment by piping, etc., which make application of GTAW of site butt joints the most effective; absence of commercial production of GTAW equipment, designed for power supply from systems of centralized power supply of welding stations, widely used in mounting [1, 4, 5, 8].

Welding equipment market now offers a wide range of orbital automatic welding machines, developed and manufactured by foreign companies, for instance, POLYSOUDE (France), ESAB (Sweden), etc. They, however, require considerable operating costs, and, in the opinion of leading specialists in the field of automatic orbital welding, are markedly inferior to even earlier developed by NIKIMT automatic machines (for instance, ODA series) as to machine time resource, suitability for dimensions and interpipe spacing in local power units, technological capabilities (welding tube butt joints of thin-walled small diameter piping by the methods of autopressing or sequential penetration still have not been mastered in foreign countries), method of torch assembly cooling (all foreign models of orbital automatic welding machines envisage liquid cooling), repairability of automatic machine components [1].

Considering the scale of development of nuclear power engineering through upgrading and extension of residual life of operating and construction of new NPP power units with WWER type reactors, application of GTAW to perform more than 120,000 piping welded joints in each power unit appears to have no alternative, while development and mastering of commercial production of modern local orbital automatic welding machines, particularly for welding small-diameter piping (up to 100 mm), and fitting

the mounting organizations and repair units of NPP with such automatic welding machines and equipment for edge preparation are becoming ever more urgent tasks.

Single-operator ADTs 625 UZ.1, ADTs 626 UZ.1 and ADTs 627 UZ.1 automatic machines, developed at PWI, allow solving a certain part of these tasks. These machines are designed for orbital TIG welding without filler wire of position butt joints of piping of 8 to 76 mm diameter with up to 4 mm wall thickness from steels of austenitic or pearlitic classes or high alloys under the conditions of mounting and repair of power engineering facilities, including NPP and TPP, as well as in other industries.

The main technical parameters of ADTs 625 UZ.1, ADTs 626 UZ.1 and ADTs 627 UZ.1 automatic machines are given in the Table, and block diagram of automatic machines is shown in Figure 1. Each of the semi-automatic machines includes multifunctional power source ITs 616 UZ.1 for TIG welding, controller block (control system) ITs 616.20.00.000, remote control panel (operator panel) ITs 616.30.00.000, one of welding heads ADTs 627.03.00.000, ADTs 625.03.00.000 or ADTs 626.03.00.000, respectively, and ADTs 625.07.00.000 manifold.

ITs 616 UZ.1 power source ensures:

• formation of vertical («bayonette») external volt-ampere characteristics (VAC) necessary for the process of TIG welding;

• presetting of welding current values and time components of welding cycle by welding current and inert gas feed (duration of time intervals of «gas-to-welding», «smooth increase of welding current», «preheating», «smooth decrease of welding current», «gas after welding»);

• contactless excitation of welding arc by high-voltage breakdown of the arc gap;

• stabilization of set values of welding current and time parameters of welding cycle at the impact of external disturbances (mains voltage fluctuations, arc gap length variation, etc.);

• possibility of realization of the modes of automatic step-pulse welding, manual and automatic welding by modulated current, as well as cycles of welding in modes 2T, 4T and in special 4T-1 mode;

• possibility of remote control.

Power unit 1 (see Figure 1) of the power source includes power isolating transformer and power low-voltage rectifier, adjustable DC step-down converter (DC-DC converter) and welding current sensor. The main component of DC-DC converter control path is PWM-controller 2, to the control input of which a signal proportional to welding current setting voltage comes from control unit 3, while the signal proportional to welding current comes to its information input. Welding current is regulated by variation of setting voltage (setting), welding current and voltage being related by a straight linear dependence. Stabi-

Main technical characteristics of ADTs 625 UZ.1, ADTs 626 UZ.1 and ADTs 627 UZ.1 automatic machines

Parameter	ADTs 627 UZ.1	ADTs 625 UZ.1	ADTs 626 UZ.1
Welded piping diameter, mm	8−24	18−42	42−76
Range of welding speed regulation, m/h	1−20		
Tungsten electrode diameter (VL, VI or VT grades), mm	1.6	2.0; 3.0	
Greatest radial displacement of the torch, mm	15	16	20
Greatest displacement of the torch across the butt, mm	±0.1	±5.0	
Torch cooling	Gas		
Range of welding current adjustment, A	8−250		
Range of arc voltage adjustment, V	9−18		
Accuracy of welding current maintenance, %, not worse than	±0.2		
Accuracy of maintaining arc voltage, V, not worse than	±0.20	±0.15	
Position of electric drive of faceplate rotation	Parallel to pipe longitudinal axis		
Radius of rotating parts, mm, not more than	60	65	80
Method of arc length stabilization	Mechanical follower	ARAV	
Number of arc passes	1−4		
Weight of welding head, kg, not more than			
Consumed electric power (at welding current of 250 A), kV·A, not more than	5.7		

lization of this welding current value is ensured at the expense of application of negative feedback by welding current.

Control block *3* of welding power source generates signals which are used to control switching on and automatic switching off of arc excitation block *4* of

Figure 1. Block-diagram of orbital automatic machines ADTs 625 UZ.1, ADTs 626 UZ.1 and ADTs 627 UZ.1: *1* — power unit of welding power source; *2* — PWM-controller; *3* — control block of welding power source; *4* — arc excitation block; *5* — gas equipment; *6* — control circuit power unit; *7−9* — controller of welding cycle, rotation drive and ARAV, respectively; *10* — remote control panel (operator panel)

the power source; generation, adjustment and maintaining during welding the assigned values of all the settings and time parameters of current component of welding cycle for welding process modes and stages; control of gas equipment *5* of the power source that ensures control and adjustment of time parameters of gas component of welding cycle; generation of control signals required for functioning of welding cycle controller *7* included into the automatic machine control system.

Arc excitation block *4* is a voltage booster, with its output circuit connected in series into the welding circuit between the output of power source power unit *1* and electrode of the torch, mounted in the head of automatic welding machine, and is designed for generation of high voltage pulses, injected into the arc gap to perform contactless excitation of the welding arc at the initial stage of the welding process.

Power unit *6* of the power source generates stabilized and unstabilized direct current voltages, as well as decreased alternating current voltage, required for powering the control circuits, components and blocks of the power source, automatic machine control system, remote (operator) control panel, gas equipment, and welding head mechanism drives.

Power source ITs 616 UZ.1 belongs to welding power sources of «chopper» type, which have just as high dynamic characteristics and control capabilities, as the inverter-type welding power sources, the chopper-type power sources being somewhat inferior to welding inverters as to their weight and size characteristics. They, however, are significantly superior to the latter as to the characteristics of functional and
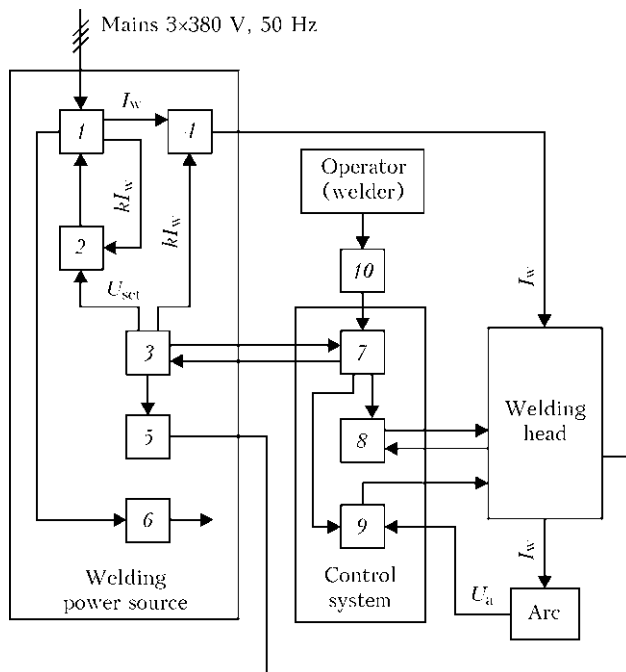
service reliability and repairability. This is attributable to the fact that compared to welding inverters, chopper-type power sources are characterized by a smaller number of stages of conversion of the energy flow supplied from the mains to the welding arc, location of welding current regulator in the low-voltage part of this flow, minimizing the risk of avalanche-like development of nonrestorable failures in case of an accident.

If required, ITs 616 U3.1 power source can be effectively used for realization of the processes of manual TIG welding, also with application of modes of welding by modulated current.

Automatic machine control system is designed for:
• generation of control signals of switching on, off and duration of functioning of the automatic machine components and mechanisms, in keeping with the assigned algorithms of performance of GTAW of position butt joints of pipelines;
• ensuring regulation and processing of feedback signals and maintaining during welding the programmed values of welding speed (speed of displacement of the torch with non-consumable electrode), arc gap length and number of arc passes;
• automatic performance of changes of welding cycle parameters (welding current, welding speed, direction of rotation of welding head faceplate), depending on the number of arc pass, as well as the stage of welding cycle.

The main functional blocks of automatic machine control system are controllers of welding cycle 7, rotation drive 8 and automatic regulator of arc voltage (ARAV) 9.

Welding cycle controller 7 ensures assigning of time parameters of GTAW cycle, as well as values of welding current, welding speed, number of arc passes, direction of its displacement, depending on diameter, material and wall thickness of welded piping.

Rotation drive controller 8 is designed for adjustment and maintaining during welding of assigned values of speed of rotation of welding head faceplate around the piping being welded through stabilization of the rotation speed of reduction gearmotor of welding head rotation drive through feedback using signals generated by reduction gearmotor encoder.

ARAV controller 9 ensures maintenance during welding of specified value of arc gap through automatic compensation of its deviations from the programmed value by correction of the vertical position of welding torch electrode relative to the surface of welded piping. Continuous-type ARAV, applied in the automatic machine, is a closed-loop system of automatic adjustment, based on application of proportionality of arc voltage to its length in non-consumable electrode welding [9, 10].

Control system of automatic machine functions together with the remote control panel (operator panel) incorporating the control, signaling and indication elements, ensuring:
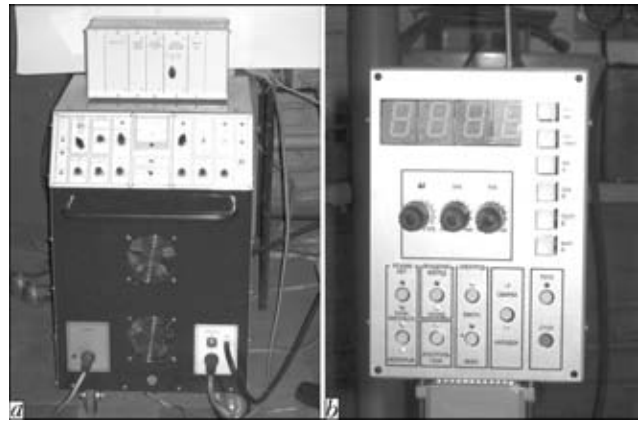
Figure 2. ITs 616 UZ.1 power source, ITs 616.20.00.000 control system (*a*) and ITs 616.30.00.000 remote control panel (*b*) of ADTs 625 UZ.1, ADTs 626 UZ.1 and ADTs 627 UZ.1 automatic machines

• selection of automatic machine operating mode;
• selection of control mode;
• selection of welding mode;
• setting the direction of rotation of welding head faceplate;
• assigning the direction of radial displacement of welding head electrode for setting up mode;
• preliminary control of inert gas flow rate;
• switching on/off of welding cycle;
• setting arc voltage;
• setting welding speed;
• readjustment of welding current during welding (by ±10 %);
• digital indication of pre-assigned and current values of welding current, arc voltage, speed of welding head faceplate rotation around the piping being welded (welding speed) and inert gas flow rate in amperes, volts, rmps and liters/minute, respectively.

Appearance of ITs 616 UZ.1 power source, control system and control panel of automatic machines ADTs 625 UZ.1, ADTs 626 UZ.1 and ADTs 627 UZ.1 is shown in Figure 2.

Welding heads ADTs 627.03.00.000, ADTs 625.03.00.000 and ADTs 626.03.00.000 for GTAW of piping of 8—24, 18—42, 42—76 mm diameters, respectively, have a design characteristic for put-on heads (Figure 3), with application of unified components and mechanisms. Head design allows performing its fast mounting on the piping being welded, removal by one welding operator and reliable fastening of the head case on the piping (that prevents its displacement as a result of jerks or vibration), and ensures the accuracy of head mounting on the piping (non-parallelism of welding head axis relative to piping radial axis is not more than 3°), reversing of faceplate rotation direction by a command from the automatic machine control system, possibility of transverse correction of torch electrode position relative to piping butt axis, laminar outflow of inert gas from the torch and reliable shielding of welding zone, fast replacement of worn tungsten electrode of the torch. Each of welding heads includes a case of lighter-weight design,

Figure 3. Appearance of welding heads: *1* — ADTs 627.03.00.000; *2* — ADTs 625.03.00.000; *3* — ADTs 626.03.00.000

mechanism of head clamping on the piping, faceplate rotating around the piping axis, mechanism of faceplate rotation (rotator), mounted on faceplate welding torch and actuator for vertical displacement of welding torch of ARAV system in ADTs 625.03.00.000, ADTs 626.03.00.000 heads and arc length stabilization system, using a follower in ADTs 627.03.00.000 head.

Stationary case of each welding head is the load-carrying structure for the mechanism of head clamping on the piping being welded and faceplate rotator. Head fastening on the piping being welded or its unfastening are performed using two clamping mechanism grips, enclosing part of the piping cylindrical surface, which are kinematically connected to the controlling lever. Faceplate rotator consists of reduction gear located inside the stationary case, and handle with built-in drive, which is a reduction gear motor with encoder. Rotator handle is parallel to piping axis, and can be fastened on the stationary case of the head in any of the two opposite directions relative to faceplate plane. Dimensions and design of the handles, as well as electric motors and encoders of rotator drives of all the heads are unified. Rotator drives of each of the heads differ just by the reduction ratio of reduction gear motors. Head rotators are made to have common kinematic diagram.

Output gear of rotator reduction gear carries a faceplate, on which ARAV actuator is mounted in ADTs 625.03.00.000 and ADTs 626.03.00.000 heads, and a lever with follower-stabilizer of arc length and torch with non-consumable electrode is mounted on ADTs 627.03.00.000 head. ARAV actuator incorporates a reversible reduction gear motor, the output shaft of which is connected through a tooth gear to a device of «screw-nut» type, the nut being built into the shoe moving along the screw. The shoe is rigidly connected to a bracket to which an insulator carrying a torch, is attached. The «ARAV−torch» assembly also includes a mechanism of transverse displacement,

allowing correction of electrode position across the butt being welded.

Torches of ADTs 625.03.00.000 and ADTs 626.03.00.000 heads are completely unified in their composition and structure, and differ only by long-term protection of the ceramic nozzle. The torch of ADTs 627.03.00.000 head differs from these heads by dimensions, case shape, collet for electrode fastening and location of branchpipe in it for connection of head current and gas supply.

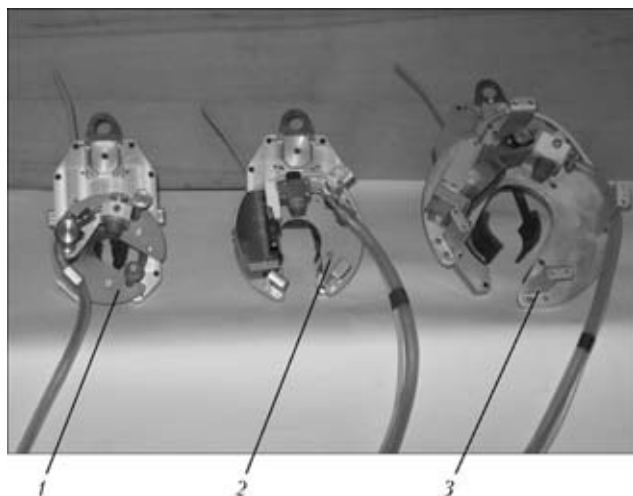Any of ADTs 627.03.00.000, ADTs 625.03.00.000 and ADTs 626.03.00.000 welding heads is connected to ITs 616 UZ.1 power source, ITs 616.20.00.000 control system, ITs 616.30.00.000 remote control panel and gas supply system through ADTs 625.07.00.000 manifold, which can be removed from the head for up to 15 m distance.

ADTs 627 UZ.1, ADTs 625 UZ.1 and ADTs 626 UZ.1 automatic machines enable two kinds of operation modes — «Setting up» and «Welding», two control methods — «Manual» and «Automatic», and three types of welding modes — «Continuous», «Pulsed» and «Modulated welding current».

«Setting up» operation mode of the automatic machine is used for control of functioning of welding head rotator and checking its alignment, checking the trajectory of torch rotation around the butt joint of the piping being welded, checking and regulation of non-consumable electrode extension and technologically substantiated length of the arc gap, pre-setting (assigning) the rotation speed of the torch with non-consumable electrode. A feature of «Setting up» operation mode is absence of welding current in the welding circuit. In «Setting up» operation mode and «Manual» control method of the automatic machine the moments of the start and stop of the torch rotation are assigned by operator commands using «Start» and «Stop» buttons on remote control panel ITs 616.30.00.000. In «Setting up» operation mode of the automatic machine and «Automatic» control method the moment of the start of torch rotation is also assigned by the operator, and rotation stopping is automatic at the moment of completion of the set cycle duration, in keeping with the selected number of rotations and with certain «overlapping» of the section of the start of rotation.

«Welding» operation mode of the automatic machine at «Continuous» mode type allows performing all the stages of the welding cycle for all of its components while maintaining during each pass of the arc (each complete revolution of the faceplate) constant values of welding current, arc voltage and faceplate rotation speed (welding speed), set for this pass.

In «Welding» mode of automatic machine and «Pulsed» mode type the process of step-pulse welding is realized, which is performed on two energy levels of welding current, following each other with set periodicity: «high» called pulse, and «low» called pause,

torch displacement (faceplate rotation) with the specified speed occurring only during time intervals, corresponding to welding current pause duration.

«Modulated current welding» mode is realized in «Welding» operation mode of the automatic machine and «Continuous» type mode, using «Modulation» mode of ITs 616 UZ.1 power source with current modulation being provided, and faceplate rotation speed during each pass being maintained constant at the level set for this pass.

To implement any of the three kinds of welding modes, it is possible to use, as in «Setting up» operation mode of the automatic machine, one of the two control methods — «Manual» or «Automatic». With «Manual» control method the start and end of the welding cycle are assigned by operator commands. With «Automatic» control method the start of the welding cycle is also assigned by the operator, while cycle completion occurs automatically, rotation of welding head faceplate being performed during time interval, the duration of which is a sum of durations of all the assigned arc passes (full revolutions of the faceplate around the piping being welded), duration of «overlapping» of the point of welding start and duration of smooth lowering of welding current («crater welding up»).

During earlier research [11, 12], it was found that in GTAW without filler wire of piping butts there exist mode regions, in which the respective relationships between welding current, arc voltage, welding speed and shielding gas flow rate provide the possibility of achieving the high and stable quality of welded joints. The same investigations have also revealed that to achieve a high quality of welds the maximum admissible deviation during welding by one of the mode parameters of GTAW of position butt joints of piping from the set values should not exceed ±14 % for welding current, ±13 % for arc voltage, ±10 % for welding speed and ±20 % for shielding gas flow rate, and at simultaneous introduction of disturbances by all the parameters of the mode the maximum admissible deviations by each parameter should not exceed ±2.5 %.

In ADTs 627 UZ.1, ADTs 625 UZ.1 and ADTs 626 UZ.1 automatic machines the above requirements by accuracy of maintaining during welding the assigned parameters of its mode are fully satisfied. This, as well as the circuit and design solutions incorporated into the automatic machines and their functional capabilities, allows realization of all the known technologies, including pulsed processes, GTAW of position butt joints of 8 to 76 mm piping with up to 4 mm wall thickness, as well as welding by the processes of autopressing, successive penetration and by a comparatively new process, which was called antipressing in Ukraine [12].

In 2008–2009 commercial manufacture of ADTs 627 UZ.1, ADTs 625 UZ 3.1 and ADTs 626 UZ.1

automatic machines was mastered in Ukraine that allowed beginning fitting nuclear power engineering enterprises and NPP repair units with these machines. An example of successful application of automatic machines of this series is their application in GTAW in helium atmosphere of sealing joints of a pipe with the end piece and plug (batch production at PP «Atomenergomash» of NNPC «Energoatom») of absorbers for containers of dry storage of spent fuel.

Pilot production trials of ADTs 627 UZ.1, ADTs 625 UZ.1 and ADTs 626 UZ.1 automatic machines showed that they can be effectively applied for GTAW of position butt joints of thin-walled piping both in repair of operating NPP power units, and in mounting of those under construction, as well as other power engineering facilities, the highest effectiveness of automatic machine application being achieved at piping enlargement into blocks.

On the other hand, wide application of GTAW in construction of power engineering facilities is restrained by a number of factors, including the features of mounting heat engineering equipment and piping of NPP power units, in particular, mounting undertime, need for concentration and simultaneous operation of tens of individual welding stations in a limited production area, specific potentially hazardous conditions of work performance, eliminating application of AC 220 and 380 V mains interconnections for power supply of welding and other process equipment [13]. This accounts for predominant application of systems of centralized power supply of manual arc (MMA) welding and manual TIG welding in mounting of NPP power units. Each of such MWS includes powerful multioperator welding rectifier with a flat external VAC, individual welding stations and main wiring connecting them. In most of the cases MMA and TIG welding modes are regulated by ballast resistances in the circuit of each individual station [9, 14]. The advantages of the existing MWS are a relatively safe voltage level in the main wiring, the value of which does not exceed the values of open-circuit voltage of multioperator welding rectifier (i.e. not more than 80 V), as well as simplicity, reliability and mobility of the welding station equipment, and its essential drawbacks are a pronounced dependence of welding current of each individual station on arc gap length and fluctuation of voltage in the mains powering the multioperator rectifier, mutual influence of welding stations at their simultaneous operation, absence of the possibility of maintaining the set parameters of process modes with the required accuracy and high power input in welding operations.

The noted disadvantages of the currently available MWS are totally absent in MWS based on electronic regulators of welding current for MMA and TIG welding, which provide not only a considerable increase of MWS efficiency (from 41 to not less than 83 % at MMA welding and from 21 to not less than 84 % in
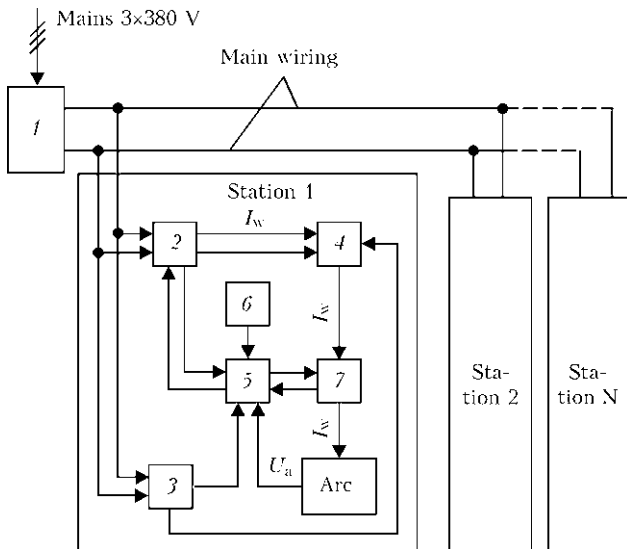
Figure 4. Block-diagram of multioperator welding system for automatic orbital welding (for designations see the text)

TIG welding), but also an essential expansion of technological capabilities, that is the prerequisite for improvement of welded joint quality [15, 16]. The properties and characteristics of welding current regulators for MWS for MMA and TIG welding enable development of MWS for GTAW of position butts of piping in mounting and repair of power engineering facilities.

One of such MWS, the block diagram of which is given in Figure 4, was developed at PWI on the base of components of ADTs 627 UZ.1, ADTs 625 UZ.1 and ADTs 626 UZ.1 automatic machines and upgraded welding current regulators RDG-201 UZ.1 for TIG welding.

As a centralized power source, MWS for GTAW uses multioperator welding rectifier *1* of VDM, VKSM, VMG series, or a similar one from those available, as a rule, in operating NPP and TPP power units and widely applied in mounting of the constructed power engineering facilities. Each individual station contains electronic regulator of welding current *2* and power unit of control circuits *3*, arc excitation block (AEB) *4*, control system *5*, remote control panel (operator panel) *6*, and welding head *7*, powered from the main wiring.

Upgraded regulator of welding current RDG-201 UZ.1, applied in MWS, has the same external VAC, dynamic properties and functional capabilities (except for ensuring arc excitation), as ITs 616 UZ.1 power source for TIG welding, and as to design of power components and control path RDG-201 UZ.1 welding regulator practically does not differ from DC-DC converter of power unit of this power source. Being part of MWS station equipment, welding current regulator RDG-201 UZ.1 ensures pre-setting of parameter values and realization of GTAW current and gas component in all the types of welding modes (continuous, step-pulse, modulated current welding). Technical characteristic of upgraded welding current regulator

RDG-201 UZ.1 is given below, and its appearance is shown in Figure 5.

If required, welding current regulator RDG-201 UZ.1 incorporated into MWS station equipment for GTAW can be also used for manual TIG welding (for instance, for tack welding, defect repair, etc.).

Multichannel block of control circuits *3* (see Figure 4) performs conversion of main wiring voltage into stabilized and non-stabilized DC voltages required for powering arc excitation block *4*, control system *5*, remote control panel (operator panel) *6* and drives of welding head actuators *7*. Main channels of control circuit power unit are reversible step-down DC-DC converters with an increased conversion frequency (up to 132 kHz), that allowed miniaturizing their structural dimensions and weight.

AEB *4* implements the circuit of thyristor generator of high-voltage pulses with resonance pumping [9], which has the secondary winding of its output pulse transformer connected in series into the welding circuit. High voltage pulses generated by AEB cause a breakdown of the gap between the welding head electrode and surface of piping being welded, that creates conditions for excitation of a stable arc discharge in this gap.

**Specification of upgraded
welding current regulator RDG-201 UZ.1**

Supply voltage (main wiring voltage), V 52–88
Rated welding current, A 200
Range of welding current regulation, A, not more than:
    lower value 8
    upper value 260
Greatest deviation of welding current from specified
value at supply voltage fluctuations (main wiring
voltage) up to ±25 % of rated 70 V value, %,
not more than 2
Range of regulation of the duration, s:
    smooth increase of welding current 1–5
    «preheating» of welding area 1–5
    pulses (pauses) of welding current in the mode of
    modulated current welding 0.10–2.25
    smooth decrease of welding current («crater»
    welding up) 1–5
    gas purging («gas-to-welding» time interval) 5–25
    gas blowing («gas-after-welding» time interval) 5–25
Efficiency (at rated welding current), %, not less
than 80
Overall dimensions, mm, not more than ..... 515 × 281 × 353
Weight, kg, not more than 24

Used as control system *5*, operator panel *6* and welding head *7* of MWS station equipment are ITs 616.20.000 control system, ITs 616.30.00.000 control panel, and depending on diameter of welded piping, one of welding heads ADTs 627.03.00.000, ADTs 625.03.00.000 or ADTs 626.03.00.000.

Upgraded welding current regulator RDG-201U Z.1, control system ITs 616.20.00.000, control panel ITs 616.30.00.000 and manifold for connection of the welding head service lines, included into the composition of MWS station equipment for GTAW, are designed as monoblock structures with the control circuit power unit built into the control system structure, and AEB and inert gas flow meter are built into the

manifold structure. To ensure compactness and mobility and ease of station equipment operation and storage, one of the possible design solutions can be placing and fastening the welding current regulator and control system in a mobile structure, which is an equipment rack fitted with wheels.

Maximum length of welding circuit for individual MWS stations for GTAW and automatic machines ADTs 627 UZ.1, ADTs 625 UZ.1 and ADTs 626 UZ.1, which ensures a sound process of automatic orbital welding of position butt joints of piping, is equal to 60 m.

A feature of MWS for automatic orbital welding is the possibility of simultaneous operation of individual stations for GTAW and manual TIG welding stations under the condition that the load current of multioperator welding rectifier does not exceed the admissible value, here both electronic regulators and ballast resistances can be used at manual TIG welding stations for welding current adjustment.

Loading capability of multioperator welding rectifier, when using ballast resistances as station regulators was determined from relationship [9]

$$N = \frac{I_{2r}}{k_0 I_{d\,r}\sqrt{DC/100}}, \qquad (1)$$

where N is the greatest number of stations, which can be connected to multioperator rectifier; I_{2r} is the rated secondary current (load current) of multioperator rectifier; k_0 is the coefficient of simultaneous operation of stations; $I_{d\,r}$ is the rated welding current of the individual station; DC is the duty cycle of individual station, %.

When electronic regulators of welding current are used in MWS, the loading capability of multioperator rectifier is determined by the following formula [16]:

$$N = \frac{\eta I_{2r}\, U_{2r}}{k_0 I_{d\,r} U_{d\,r}\sqrt{DC/100}}, \qquad (2)$$

where η is the efficiency of electronic regulator; U_{2r} is the rated secondary working voltage of multistation rectifier; $U_{d\,r}$ is the rated arc voltage (welding voltage).

If MWS includes both additional stations with electronic regulators of welding current, and stations with ballast resistances, determination of loading capacity of multioperator rectifier is performed by the following expression:

$$N = \eta\, \frac{(I_{2r} - n I_{d\,r}^1)\sqrt{\dfrac{DC}{U_{2r}}}}{k_0 I_{d\,r}\, U_{2r}\sqrt{\dfrac{DC}{100}}}, \qquad (3)$$

where n is the number of stations with ballast resistances; $I_{d\,r}^1$ is the rated welding current of the station with ballast resistance.

Figure 5. Appearance of welding current regulator RDG-201 UZ.1 for TIG welding

Comparative characteristics of loading capacity of MWS can be illustrated by the following example. When MWS uses multistation welding rectifier VDM-1001, in which rated secondary current $I_{2r} = 1000$ A and rated secondary voltage $U_{2r} = 60$ V, at $k_0 = 0.65$, rated welding current of individual station $I_{d\,r} = 200$ A and 60 % duty cycle, loading capacity is equal to:

• 10 TIG or MMA welding stations for the variant of application of ballast resistances as station welding current regulators;

• 26 stations for manual TIG welding or GTAW with application of electronic regulators of welding current;

• 10 manual TIG welding or GTAW stations in the case when MWS composition includes 4 stations with ballast resistances and 6 TIG welding or GTAW stations, if MWS incorporates 5 stations with ballast resistances.

CONCLUSIONS

1. Development and mastering of commercial production of ADTs 627 UZ.1, ADTs 625 UZ.1 and ADTs 626 UZ.1 automatic machines for orbital welding without filler wire allows fitting mounting organizations and repair units and enterprises of power engineering industry by modern local equipment, which enables realization of both well-established and new technologies of automatic welding of position butt joints of thin-walled piping of 8 to 76 mm diameter from steels of austenitic and pearlitic classes and high alloys in mounting and repair of power engineering facilities.

2. Application of commercially produced electronic regulators of welding current in MWS not only significantly widens the technological capabilities, and improves the technico-economic characteristics of such systems, but also is the necessary condition for con-

struction of MWS for automatic orbital welding, in particular by upgrading the currently available MWS, thus opening up the prospects for a considerable increase of the level of automation in welding position butt joints of piping in mounting of the constructed power units of NPP, TPP and repair of operating ones, as well as other major power engineering facilities.

3. Achievement of a high level of unification of components of ADTs 627 UZ.1, ADTs 625 UZ.1 and ADTs 626 UZ.1 automatic machines for GTAW and use of these components in MWS station equipment for automatic orbital welding enable effective and flexible operation of such automatic machines, narrowing the range and reducing the number of equipment units, required for fulfillment of welding operations in mounting and repair of power engineering facilities, lowering of operating costs for this equipment, and acceleration of personnel training.

4. Further development of single- and multioperator systems for GTAW is expansion of their functional and process capabilities by improvement of control system of automatic machines and MWS station equipment at the expense of development of a bank of typical welding modes and application of microprocessors and non-volatile memory.

In conclusion the authors believe it to be necessary to note that development and design of the above single- and multioperator systems for automatic orbital welding was performed with active and direct participation of engineers V.Yu. Buryak, N.S. Fedorenko, V.L. Kobryansky, A.G. Skirta, E.V. Kunkina, D.S. Oliyanenko, retrofitting of GTAW technologies and developed of equipment — engineers V.M. Gavva, A.D. Cherednik, A.V. Tkachenko, and mastering of this equipment production — engineers O.I. Korkach, V.N. Andrejchenko, V.E. Ivanov,

A.U. Mnukhin, V.P. Tishchenko, G.I. Pisarev, V.M. Zolotov, V.S. Pavlovsky.

1. Grinenko, V.I., Roshchin, V.V., Khavanov, V.A. et al. (2008) To problem of automation of site welding of nuclear power plant pipelines. *Tekhnologiya Mashinostroeniya*, **8**, 48—51.
2. *PN AE G-7-008—89*: Rules of design and safe operation of equipment and pipelines of nuclear power plants.
3. *PN AE G-7-009—90, PN AE G-7-010—90*: Equipment and pipelines of nuclear power plants. Welding and surfacing. Fundamentals.
4. Belkin, S.A., Shefel, V.V. (1985) Automatic argon-arc welding in mounting of nuclear power plant piping. *Energ. Stroitelstvo*, **11**, 43—46.
5. Galyshev, V.K. (1988) Application of automatic welding in mouting of piping of Zaporozhskaya nuclear power plant. *Ibid.*, **3**, 9—10.
6. Belkin, S.A. (1988) On progress of mechanized welding program of butt joints of pipelines of up to 150 mm diameter. *Ibid.*, **3**, 3—4.
7. Shefel, V.V. (1988) State-of-the-art and prospects of development of small-sized pipe-welding equipment. *Ibid.*, **12**, 3—4.
8. Sidorenko, V.F., Kuskov, M.F., Zubova, N.F. (1988) Improvement of mobility of automatic pipe-welding machine. *Ibid.*, **6**, 42—43.
9. (1986) *Arc welding equipment*: Refer. Book. Ed. by V.V. Smirnov. Leningrad: Energoatomizdat.
10. Gladkov, E.A. (2006) *Control of processes and equipment in welding*: Refer. Book. Moscow: Akademiya.
11. Poloskov, S.I., Bukarov, V.A., Ishchenko, Yu.S. (2000) Influence of parameter deviation in argon-arc welding of position pipe butts on quality of welded joints. In: *Abstr. of All-Russian Sci.-Techn. Conf. on Welding and Related Technologies*. Moscow: MEI (TU), 22—25.
12. Bukarov, V.A. (2002) Technology of automatic shielded-gas arc welding. In: *Transact. of NIKIMT on Welding in Nuclear Industry and Power Engineering*. Vol. 1. Moscow: IzdatAT, 149—210.
13. Roshchin, V.V., Khavanov, V.A., Akulov, L.I. et al. (2002) Site welding of equipment and metal structures of nuclear reactors. *Ibid.*, 81—118.
14. Bulkin, P.Ya., Donskoj, A.V. (1985) *Multistation welding systems*. Leningrad: Sudostroenie.
15. Korotynsky, A.E., Makhlin, N.M., Bogdanovsky, V.A. (2002) About design of electronic controllers of welding current for multistation welding systems. *The Paton Welding J.*, **12**, 16—24.
16. Makhlin, N.M., Korotynsky, A.E., Bogdanovsky, V.A. et al. (2004) Electronic controllers of welding current for multistation welding systems. *Svarochn. Proizvodstvo*, **5**, 13—18.

WAYS OF INCREASING THE TECHNOLOGICAL EFFICIENCY OF RECTIFIERS FOR MECHANIZED WELDING AND SURFACING (Review)

I.I. ZARUBA[1], **V.V. ANDREEV**[1], **V.I. STEPAKHNO**[2] and **V.A. KORITSKY**[2]
[1]E.O. Paton Electric Welding Institute, NASU, Kiev, Ukraine
[2]Pilot Plant for Welding Equipment of the E.O. Paton Electric Welding Institute, NASU, Kiev, Ukraine

Presented is the information on modern methods used to control the short-circuit current in transient processes caused by electrode metal transfer in mechanised CO_2 welding.

Keywords: *mechanised arc welding, consumable electrode, welding current, direct current, welding throttle*

In mechanised dip-transfer CO_2 welding, short-circuit current $I_{sh.-c}$ can be limited with a throttle or resistor in the DC circuit at a flat or gently sloping volt-ampere characteristic of the welding power source, or by using a power transformer with developed scattering in the welding rectifier [1, 2]. In this case the shape of the curve of $I_{sh.-c}$ depends on its limitation method (Figure 1).

Earlier, the simple multiple-operator power system was developed on the basis of inertialess limitation of $I_{sh.-c}$ with a resistor [3]. Compared to the inertia limitation of $I_{sh.-c}$, e.g. with a throttle, the inertialess method facilitates the initial excitation of the arc, this being particularly important for welding using the electrode wire with a diameter of 2 mm or more.

Methods used for limitation of $I_{sh.-c}$ in flat CO_2 welding are described in study [4]. In CO_2 welding of vertical and overhead welds the difference in the $I_{sh.-c}$ limitation methods is especially pronounced. It was established that the lower the amplitude value of $I_{sh.-c}$, the lower is the metal spattering. In flat welding, the minimal amplitude of $I_{sh.-c}$ is limited only by the process stabilisation condition [5].

In vertical and overhead welding, the $I_{sh.-c}$ value is chosen primarily on the basis of the metal transfer mode and weld formation. The higher the amplitude value of $I_{sh.-c}$ (up to a certain limit), the higher is the pulse towards a workpiece received by the electrode metal drop and pool, this being favourable for holding them on the vertical and overhead surfaces. So, there is an obvious contradiction between the requirements to decrease of spattering (minimal $I_{sh.-c}$) and ensuring of formation of the vertical and overhead welds (maximal $I_{sh.-c}$).

Welders often neglect spattering and operate at high amplitude values of $I_{sh.-c}$. As proved by practice, the best results are achieved with the inertia method of limitation of $I_{sh.-c}$. In case of the inertialess limitation of the current with a ballast rheostat the drops

grow in size, this hampering their transfer into the pool and deteriorating the weld formation.

As a rule, the drops shift towards the lateral surface of an electrode, as at their initial contact, when the contact area is smaller than the section area of the neck between the electrode and a drop, the electrodynamic force is directed from the pool to the electrode, thus preventing transfer of the drops. The bulk of the drops are repelled from the pool. However, they do not loose link with the electrode and, being replenished with new portions of the liquid metal, grow in size. Subsequent contacts are accompanied by the same phenomena until a drop set in an intensive oscillatory motion by pushes of the electrodynamic force

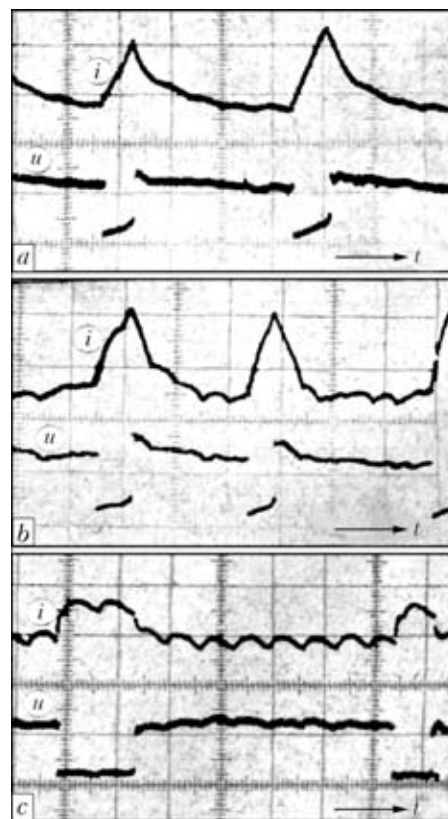**Figure 1.** Current and voltage oscillograms with the short-circuit current limited with throttle (*a*), slope of external characteristic of welding rectifier the transformer of which has a developed scattering (*b*), and with resistor (*c*) [2]
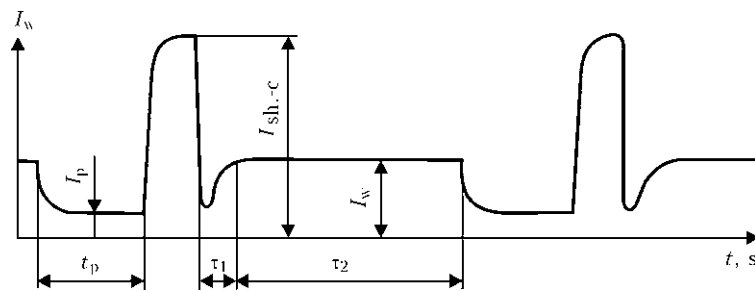
Figure 2. Oscillogram of current in dip-transfer welding using a thyristor key: τ_1 — duration of pause in flow of the welding current by the moment of bridge disruption; τ_2 — electrode melting duration; t_p — duration of the pause before short-circuiting

detaches from the electrode and flies away or collides with the pool with a major part of its surface and is absorbed by the latter, which happens more rarely in welding in the vertical position.

In flat welding, formation of a big drop does not affect formation of the weld, as the gravity force favours its movement to the electrode tip and, in the majority of cases, to the pool. To decrease the electrodynamic force that repels the drop from the pool at the first moment of their contact it is necessary to decrease $I_{sh.-c}$. However, the value of $I_{sh.-c}$ should be sufficient to generate a corresponding pulse for subsequent pressing of the drop to the pool. These requirements are not met when $I_{sh.-c}$ is limited with a ballast rheostat.

In search for optimal solutions, in 1985 associates of the E.O. Paton Electric Welding Institute and Tomsk Polytechnic Institute conducted experiments by using a thyristor key [6] and suggested a dip-transfer arc welding method, the point of which consists in controlling the current in transient processes caused by metal transfer (Figure 2).

In welding with the DC power source comprising a throttle in its welding circuit, the current is decreased momentarily for a period of t_p before short-circuiting of the arc gap. At the moment of beginning of a short-circuit the throttle is shunted by the resistor, this leading to a sudden growth of the current from the minimal to peak value. The dramatic increase of the short-circuit current causes growth of the electrodynamic force directed from the electrode to the weld pool and tending to accelerate transfer of the electrode metal to the weld pool due to the pinch-effect along the electrode melting line. This causes reduction of the short-circuit duration from $(4-5) \cdot 10^{-3}$ s (the average short-circuit duration with the throttle present in the welding circuit) to $(1.5-2.0) \cdot 10^{-3}$ s.

When a bridge between the weld pool and non-melted part of the electrode reaches its critical size ($U_a = 6-8$ V), the welding current is abruptly decreased to 20–40 A for $(0.2-0.4) \cdot 10^{-3}$ s (τ_1 in Figure 2). At the expiration of pause duration τ_1 the welding current is again increased. As this takes place, the throttle, the presence of which increases elasticity of the arc and improves its burning stability in a period of electrode melting, τ_2, and decrease of the current before a short-circuit, t_p, is again connected to the current circuit (see Figure 2).

Such conditions lead to a substantial decrease in the arc gap and size of a drop of the metal transferred to the pool. Reduction of the short-circuit duration makes it possible to increase the electrode wire feed speed and, accordingly, the productivity of the welding process, its stability being maintained at a high level and the value of open-circuit voltage $U_{o.-c}$ being kept insignificant.

In the middle of the 1990s the above arc welding method was further developed in the «Lincoln Electric» STT (Surface Tension Transfer) process for welding of the root welds [6].

The STT process is a successor of the conventional process of mechanised gas-shielded welding, where metal is transferred through short-circuits of the arc gap. However, STT is radically different from it in the possibility of directly controlling conditions of transfer of the electrode metal into the weld pool, which is provided due to a high-speed inverter circuit of the power source, special electron microprocessor module that forces the required level of the welding current, and feedback loop that dynamically traces variations in the arc voltage. During the entire cycle of transfer of the drop into the weld pool the value of the welding current strongly depends on the phase of formation of the drop and its subsequent transfer to the pool. The transfer phase is identified by processing the values of the voltage continuously taken from the arc gap.

Particularly for this process «Lincoln Electric» developed the 225 A inverter power source Invertec STT II [7], which realises the welding current waveform control technology. Invertec STT II differs from the conventional welding power sources, as it is a source with neither flat nor steeply drooping characteristic. The device is fitted with the feedback that traces the main phases of the drop transfer and immediately responses to the processes occurring between the electrode and weld pool by changing the value and waveform of the welding current.

It should be noted that the STT process equipment is rather expensive and requires appropriate service conditions. The same refers to the process with a minimal heat transfer, i.e. CMT (Cold Metal Transfer) developed by «Fronius» [8]. The metal transfer process occurs due to reversion of the electrode wire feed at the moment of the short-circuit formation, which

favours the drop detachment. In this case the short-circuit current is insignificant, thus providing metal transfer with a minimal spattering.

At present this technology is applied in the cases where a decreased, flexibly adjusted heat input is required. In operation with thin and ultra thin sheets a very high productivity of the welding process allows filling up the wider gaps. Low dilution with the base metal opens up new possibilities and provides special advantages.

Main peculiarities of the process are as follows:

• adjustment of the short arc exclusively in the power source;

• new dynamic inverting circuit;

• very quick digital regulation of the process;

• considerable decrease of the power peak in re-ignition of the arc;

• substantial decrease of heat transfer at the melting stage.

Acceleration of transfer of the drop to the pool by way of forced switching off of the current in the circuit at the first and last short-circuit phases allows the productivity of the process to be increased. However, practical utilisation of the key elements in the mechanised welding units is difficult so far because of complexity of the devices and high cost of the main elements of the circuit. Therefore, the better candidates are comparatively inexpensive devices, such as throttles, which are used to fit up commercial rectifiers for mechanised welding and surfacing. As shown by our investigations, the similar results can be obtained using no sophisticated systems for incorporation of feedbacks.

We paid attention to the effect of the energy accumulated in the throttle and welding circuit at short-circuiting of the arc gap on the subsequent arc excitation and electrode melting intensity. It turned out that the forced control of this energy by means of the internal feedback makes it possible to obtain the positive results on the quality of the weld formation and metal losses. It is enough to control the energy of the throttle to minimise the arc length and, hence, the size of the electrode metal drops after short-circuiting.

In dip-transfer CO_2 welding the spattering of metal depends to some extent on the arc voltage, as size of the drop and energy of explosion of the bridge are proportional to the length of the arc gap [9]. Therefore, the trend to performing welding under conditions with a low arc voltage is not always technologically justified. As shown by observations, when the short-circuit current is limited with the throttle, the electromagnetic energy stored in it in a growing part of the transient process after disruption of the bridge causes a dramatic increase of the arc gap due to intensive melting of the electrode, which can be seen in typical oscillograms of the arc voltage. We investigated the possibility of controlling and stabilising the length of the arc gap by proportioning of the energy input into the arc after short-circuiting. For this we
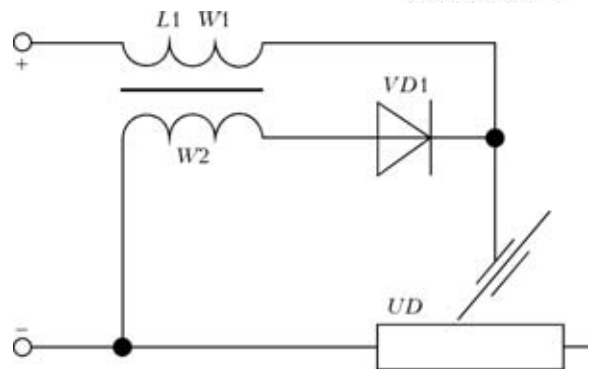

Figure 3. Electric circuit of the throttle with diode in the control winding circuit

developed and tested a special throttle, the electric circuit of which is shown in Figure 3 [10].

Throttle $L1$ comprises power winding $W1$ connected in series to the welding circuit, auxiliary winding $W2$, magnetic core, and diode $WD1$ in the auxiliary winding circuit, the diode being connected through a cathode to the electrode when welding is performed at a reverse polarity current, and the end of winding $W2$ being connected to a workpiece. When welding is performed at a straight polarity current, connection of the diode is changed.

The device operates under transient conditions caused by closing of the arc gap by the molten metal drops. Increase of the power winding current is accompanied by increase of the auxiliary winding current, which is summed up with the main current. Dramatic decrease of the welding current after disruption of the liquid bridge between the electrode and the weld pool is caused by a change in the resultant magnetic flux of the throttle at a stage of growth of the welding current, as well as in the throttle inductance value.

This causes a more dramatic short-time increase of the current in a short-circuiting period, which leads to active constriction of the molten electrode metal bridge and its destruction. This is accompanied by a substantial reduction of duration of the short-circuits and increase in their frequency (Figure 4). The metal transfer becomes of a spray type. Dramatic decrease of the current after short-circuiting provides a minimal length of the arc gap.

At present, such throttles are used to fit up welding rectifiers VS-650SR manufactured by the Pilot Plant for Welding Equipment of the E.O. Paton Electric Welding Institute [11]. Unlike traditional welding rectifiers, owing to an original throttle with internal feedback this source provides stabilisation of the length of the arc gap and size of the drops of the transferred metal in dip-transfer gas-shielded welding, which considerably improves the weld formation and quality of welding in all spatial positions with a minimal spattering of the electrode metal (Figure 5).

Also, we developed variants of designs of the device with a thyristor in the control winding circuit [12]. The use of the thyristor control in the throttle allows a substantial decrease in the rate of growth of the
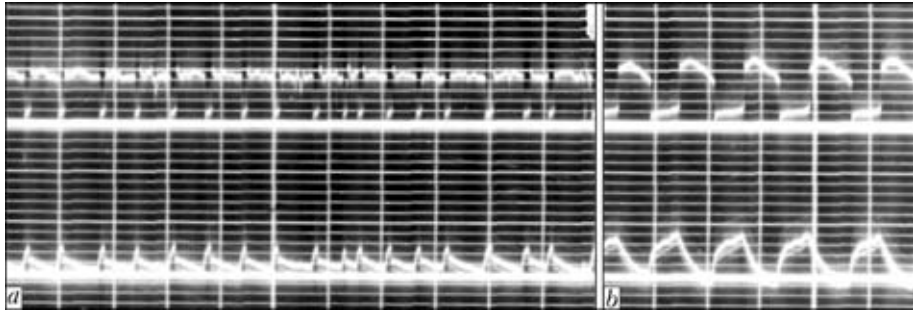
Figure 4. Oscillograms of arc voltage and welding current (U_a = 20 V, I_w = 100 A, $U_{o.-c}$ = 26 V, $D_{e.w}$ = 1.2 mm): a — throttle with internal feedback; b — throttle without internal feedback
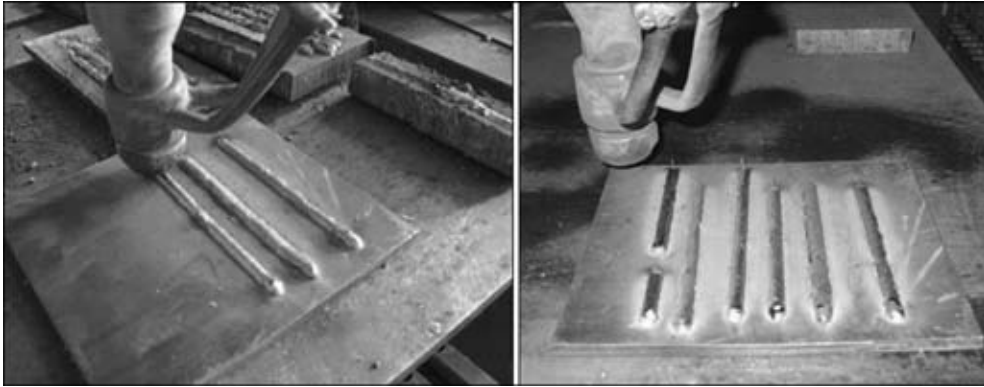

Figure 5. Appearance of deposited beads in CO_2 welding using rectifier with the throttle fitted with internal feedback

current at the beginning of a short-circuit, this ensuring reliable coalescence of the drop with the molten metal pool. Owing to the thyristor control, the maximal value of the short-circuit current can be optimised to a certain degree and selected so that it provides reliable disruption of the liquid bridge between the drop and electrode, as well as transfer of the drop to the pool.

At the same time, this regulation can decrease the maximal value of the short-circuit current, thus limiting the energy of explosion of the liquid bridge and reducing the probability of an outburst of the drop outside the weld pool. All this adds to reduction of the metal spattering factor. Accelerated decrease of the welding current after the end of a short-circuit reduces overheating of metal and burn-out of alloying elements, this being of a high technological importance in a number of cases. Connection of a low constant voltage source in series to the throttle control winding and thyristor offers a much wider possibility for controlling the energy of the welding throttle in transient processes due to regulation of the level and waveform of the short-circuit current.

Therefore, upgrading of the throttles of commercial welding rectifiers by fitting them with a special additional winding of the internal feedback provides a technological effect comparable with such in welding by using the expensive equipment.

The key advantages of the device include simplicity, targeted utilisation of the electromagnetic energy stored by the throttle and improvement of the quality of welding. Welding by using the internal feedback in the throttle provides a spray transfer of the electrode

metal at its low losses for formation of fumes and spattering, reduction of burn-out of alloying elements and oxidation of the electrode metal because of the reduced time of dwelling of the molten metal drop in the arc zone, improvement of stability of the welding process and arc burning, self-regulation of the level of $I_{sh.-c}$, reduction of the time of $I_{sh.-c}$, increase in frequency of $I_{sh.-c}$, and quality welding in all spatial positions.

1. Zaruba, I.I., Andreev, V.V. (1978) Peculiarities of methods applied for limiting of the shirt-circuit current in CO_2 welding. *Avtomatich. Svarka*, **1**, 16–19.
2. Zaruba, I.I., Bargamen, V.P., Andreev, V.V. et al. (1973) Influence of the shirt-circuit current limitation method on formation of vertical and overhead welds in CO_2 welding. *Ibid.*, **4**, 64–67.
3. Lebedev, V.K., Medvedenko, N.F., Zaruba, I.I. (1967) Investigation of multiple-operator power supply systems for CO_2 welding. *Ibid.*, **10**, 40–44.
4. Zaruba, I.I. (1970) Mechanism of metal spattering in arc welding. *Ibid.*, **11**, 12–16.
5. Zaruba, I.I. (1971) Condition of stability of the short-circuit welding process. *Ibid.*, **2**, 1–4.
6. Zaruba, I.I., Saraev, Yu.N., Knyazkov, A.F. et al. *Method of dip-transfer arc welding and device for its realization.* USSR author's cert. 1310140. Int. Cl. B 23 K 9/00. Publ. 15.05.87.
7. Ioffe, Yu.E., Kvasov, F.V. (1997) New «Lincoln Electric» high-tech systems for automatic welding. *Svarochn. Proizvodstvo*, **4**, 40–43.
8. Lebedev, V.A. (2010) Tendencies in development of mechanized welding with controlled transfer of electrode metal (Review). *The Paton Welding J.*, **10**, 37–44.
9. Zaruba, I.I. (1970) Electric explosion as a cause of metal spattering. *Avtomatich. Svarka*, **3**, 14–18.
10. Lebedev, V.K., Zaruba, I.I., Andreev, V.V. et al. *Welding throttle.* USSR author's cert. 694308. Int. Cl. B 23 K 9/00. Publ. 30.10.79.
11. Stepakhno, V.I., Andreev, V.V., Koritsky, V.A. (2011) Power supplies for arc welding and surfacing with improved operational characteristics. *Vagon. Park*, **5**, 26–30.
12. Zaruba, I.I., Andreev, V.V., Moskovich, G.N. et al. *Device for stabilization of welding current in DC dip-transfer welding.* USSR author's cert. 1087282. Int. Cl. B 23 K 9/00. Publ. 23.04.84.

STATE-OF-THE-ART AND PROSPECTS OF MARKET OF STEEL AND WELDING EQUIPMENT IN CHINA (Review)

O.K. MAKOVETSKAYA

E.O. Paton Electric Welding Institute, NASU, Kiev, Ukraine

Generalized data on the state-of-the-art in the ferrous metallurgy and welding engineering industries of China in a period of 2009−2010 are presented, and prospects of their further development are considered.

Steel production. Stable and high rate of the annual average growth of economy of around 10 % remains in the country since 1978 (beginning of the performance of economic reform in China). Steel production is also constantly rising. The annual average increase of steel production made around 7 % in the 1980s, 10 % in the 1990s, and more than 20 % since 2000. 626.6 mln t of steel was manufactured in China in 2010 that exceeded the total output of 15 countries being leading world producers of steel (Table 1). Portion of China in the world steel production has risen from 5.1 in 1980 up to 44.2 % in 2010 during 30 years [1].

High rates of industrialization and urbanization, significant investments in the key branches of Chinese economy, related with high metal consumption such as machine building, motor car, ship, civil and industrial construction, first of all, stipulate the increase of steel production and consumption. Volume of steel consumption in China has risen 3.5 times during ten years since 2001 till 2010 and exceeded 600 mln t in 2010. An index of consumption per capita increased 3.4 times for the same period and made 445.2 kg in 2010 [1, 2].

More than 95 % of steel produced in China is consumed in the domestic market. China exported around 42 mln t in 2010 and imported 17 mln t of finished steel products. Industrial and civil engineering (56 %), machine building (18 %), motor car (6 %), ship (3 %) construction and power engineering (2 %) are the main steel consuming industries in China. Necessity of Chinese economy in a high-quality steel production constantly rises [3].

One of the relevant issues of modern China is an increase of efficiency and competitiveness of ferrous metallurgy. Planned reforming of the industry has been performed since 2004, after «Plan of development of ferrous metallurgy in China up to 2020» was stated. The tasks on solving of a problem of excessive production capacities, fragmentation, technical reequipment of the industry, stimulation of export and environment pollution were set in a state plane of development of Chinese economy for 2011−2015. It is

planned to increase a portion of ferrous metallurgy in GDP of the country up to 4 % in 2011 according to the plan indices. At that, steel production capacity is planned to be reduced up to 500 mln t [4, 5].

The total capacities of the PRC on melting of raw steel increased more than 4 times since 2000 to 2009 and achieved 743 mln t that makes 80.4 % from a global addition of capacities for this period according to evaluation of the World Steel Association.

At present time the steel making capacities are 20−30 % higher than the level of actual consumption. It was planned to stop running of the blast furnaces of less than 300 m^3 in volume, converters and electric furnaces up to 20 t in 2010. Stop of running of the blast furnaces of less than 400 m^3 in volume and converters and electric furnaces of less than 30 t are expected during 2011. The out-of-date blast furnaces of total capacity of around 100 mln t/year are to be stopped during 2010−2011. As a result of reform the ten largest state companies will control the steel making capacities to 60 % in 2015 and 70 % in 2020 according to the intended plan. The portion of the five

Table 1. Countries of the world − the main producers of steel in 2010

Country	Rank	Volume of steel production, mln t	Portion in world production, %
China	1	626.65	44.2
Japan	2	109.60	7.7
USA	3	80.59	5.7
Russia	4	67.02	4.7
India	5	66.85	4.7
Republic of Korea	6	58.45	4.0
Germany	7	43.82	3.0
Ukraine	8	33.56	2.4
Brazil	9	32.82	2.3
Turkey	10	29.00	2.0
Italy	11	25.75	1.8
Taiwan	12	19.64	1.4
Mexico	13	17.04	1.2
Spain	14	16.31	1.1
France	15	15.42	1.0

largest steel making companies was equal 32.6 % in 2010 in total output of steel along the country. It increase up to 45 % is planned in 2011.

Construction of the state-of-the-art large metallurgical plants allowed increase the steel output as well as changed a structure of steel making technology and products manufactured in China, promoted implementation of the energy saving technologies. Significant success was achieved in the area of environment control [6]. The last open-hearth furnace was stopped in China in 2001. The portion of steel making in oxygen steel-making converters made 90.2 % (565.4 mln t) in 2010 and it was 9.8 % for the arc furnaces (61.3 mln t). The portion of steel making by means of continuous casting made 97.9 % (613.7 mln t) in 2010. Specific emissions in the atmosphere are reduced 3 times in steel making by means of a converter method in comparison with the open-hearth method. Metal consumption reduces up to 15 % and specific pollutant emissions in the atmosphere decrease 2.5 times during the process of continuous steel making. Significant increase of output of hot-rolled stock is observed. 796.3 mln t of hot-rolled stock were manufactured in China in 2010 and portion of a flat section exceeded that of a rolled one in structure of its production for the first time in 2007. 362.9 mln t of rolled and 408.1 mln t of flat sections were produced in China in 2010. Table 2 shows the data on production of some main types of metal products in China for different years [1].

It is planned that the quality of 60 % of the end steel products, manufactured by the leading large and medium steel making enterprises, will comply with the world standards as a result of technical reequipment of this industry, and Chinese enterprises will be able to satisfy the internal demand in the main types of end steel products by 90 %. One of the main priorities of the industry is to master a production of new types of steel products and goods with a high added value. The Chinese Central Government appro-

priated around 25 bln of yuans (approximately 4 bln of dollars) for technical reequipment and support of research studies in the industry in 2011.

«Norms of production and running of ferrous metallurgy enterprises» were published by Chinese government in 2010. They determined the specific parameter standards of production and equipment as well as measures of environment protection for metallurgical enterprises. In particular, production of 1 t of steel requires that a blow of foul water does not exceed 2 m^3, atmospheric emission of dust are to be 1 kg and emission of sulfur dioxide should make 1.8 kg according to the norms of environment protection. A technology of dry quenching [7, 8] should be obligatory used at the medium and large metallurgical enterprises for reduction of electricity consumption and pollution of the environment.

Rise of a competitiveness of Chinese ferrous metallurgy [5] is the final aim of implementation of the measures directed to power saving and reducing of emissions, optimizing of commercial structure, increasing of production and closing of outdated capacities.

Welding engineering. Portion of China in the world welding market made 23 % (3.1 bln of dollars) [9] in 2010 according to ESAB evaluation. China takes the first place in the world on the output and consumption of welding consumables. Volume of the Chinese market of welding engineering increased by 14 % in comparison to 2009. Output of welding consumables made around 2.5 thou t in 2009 and volume of welding consumable market in value terms for China was around 1.1 bln of dollars [9]. Table 3 shows the data on output of the main welding consumables in China in 2004−2009.

Structure of welding consumable production in China rapidly changes: production of solid wire and flux-cored wire increases and that for the welding electrode reduces.

Coated electrodes for manual arc welding made around 60 % of all being manufactured in China in 2009 and 40 % of that was welding wires (25 % — solid and 15 % — flux-cored wire).

Output of welding consumables in China will achieve 3.5−4.0 mln t in 2015 according to forecast of China Iron and Steel Research Institute. At that, portion of production of coated electrode for manual arc welding reduces to 22 % , rising of solid wire for CO_2 welding up to 50 % and flux-cored wire up to

Table 2. Output of the finished steel products in China, mln t

Type of products	2004	2009	2010
Rolled section	162.9	332.5	362.9
Flat section	127.7	307.7	408.1
Light-section profile (≤ 80 mm)	21.9	39.1	42.5
Rolled stock of round section for reinforcement of concrete structures	57.7	121.5	131.0
Other types of products from hot-rolled sections	23.1	55.4	69.0
Rod	50.2	96.7	105.5
Metal coated plate and strip	6.0	20.7	28.5
Pipes and fittings	21.2	–	57.7
Welded pipes	13.0	30.4	32.4

Table 3. Production of welding consumables in China, thou t

Welding consumables	2004	2005	2006	2007	2009
Electrodes	1100	1200	1250	1300	1450
Wire	400	480	560	650	1050
Total	1550	1750	1900	2050	2500

Table 4. Export and import of welding and filler materials, thou t (numerator), mln USD (denominator)

Welding consumables	Export			Import		
	2008	2009	2010	2008	2009	2010
Coated electrodes and wire (without solid wire), total	323.7/422.3	336.0/347.4	315.6/352.4	53.0/300.1	51.9/245.0	56.5/293.6
Including:						
coated electrodes for arc welding	191.9/173.8	247.3/191.0	239.7/187.5	6.9/53.5	4.2/35.3	6.0/49.5
brazing consumables	17.1/37.5	20.9/34.8	21.7/43.5	11.6/149.6	11.0/125.4	12.4/161.4
flux, auxiliary materials	19.6/18.5	17.5/14.7	16.0/14.4	23.0/93.5	19.6/84.8	23.6/108.0
Welding consumables, total	360.4/478.3	374.4/396.9	353.3/410.3	85.6/543.2	82.5/455.2	92.5/563.0

15 % are to be observed, amount of wire for submerged arc welding will be around 12 % and materials for nonconsumable electrode welding preserve on 1 % level [1].

Construction, machine building, power engineering (construction of oil and gas pipelines), shipbuilding, railway transport are the main industries consuming welding consumables in China. 40—50 % [11] is a portion of consumption of welding consumables in building.

Export of welding consumables was significantly reduced in 2009 due to the economy crisis, however, indices of export of welding consumables turned to the pre-crisis level already in 2010. The volume of export of welding consumables in China in kind terms more than 4 times higher of the volume of import, however, the volume of import almost by 40 % exceeds the volume of export of welding consumable and filler materials in value terms. China had a negative trade balance in studied group of products in 2010 as well as in the pervious years.

Table 4 gives the data on the volume of export and import of welding consumables and filler materials in value and in kind terms according to the COMTRAD database of United Nations Organization [12]. Analysis of a group of consumables, containing alloyed solid welding wire (code 7217), has no representation in the paper, since COMTRAD database classifies the production on a six-unit code and 721710 class (wires and strips) does not represent a subclass on solid welding wires (positions seven and eight).

Coated electrodes make the main portion of export of welding consumables (45 % in indices of in value terms and almost 70 % in kind terms). The volume of export of coated electrodes constantly rises. Flux-cores wire (30 %), consumables for gas welding (21 %) and for brazing (26 %) form the main portion in structure of the import.

Main types of welding equipment. Serial devices for alternating current arc welding; equipment for direct current arc welding; automatic and semi-automatic machines; machines for resistance welding; special welding and cutting automated equipment can be referred to this type of production, manufactured in China.

The output of electric welding equipment in value terms for China in 2009 made 2.9 bln of dollars that is lower of that in 2008 by 12 %. The output of welding equipment increased up to 3.4 bln of dollars in 2010 during after crisis period. In future the year-on-year increase of production of welding equipment will make 11.2 % up to 2012 on estimate of the Chinese experts. The output of welding equipment in value terms is expected to exceed 4.2 bln of dollars [13] in 2012.

Production of low-class equipment (alternating current welding transformers for arc welding) dominates in the structure of production of Chinese welding equipment, however, a portion of its annual increment is insignificant (around 5—6 %) and constantly decreasing. In contrast, a portion of production of highly technological and power-saving equipment, i.e. inverter power sources for direct and pulse current welding, automatic and semi-automatic equipment with digital control rises steadily (see Figure). Portion of the inverter power sources in value terms during production of welding equipment made 28 % in 2010 that was by 60—70 % lower than that in the developed countries. Increase to 39 % [13] of the portion of inverter power sources in the production structure is expected to 2012.
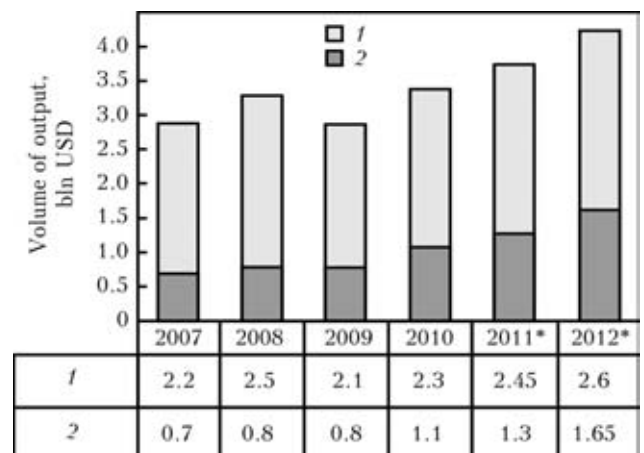
Volume of output of welding equipment in value terms in China: *1* — traditional equipment; *2* — inverter sources; * — forecasting data

Table 5. Export and import of electric welding equipment, mln USD

Equipment	Export			Import		
	2008	2009	2010	2008	2009	2010
Electric equipment for welding, brazing, cutting, surfacing in total	583.467	476.617	798.439	1044.182	751.004	1099.107
Electric solderers	36.053	32.056	47.053	6.072	4.670	7.982
Machines and devices for brazing	6.661	4.190	10.681	36.390	34.565	59.265
Machines and devices for automatic resistance welding	36.288	52.483	106.767	195.114	98.498	198.886
Other machines and devices for resistance welding of metals	90.275	51.782	58.460	42.914	13.632	35.387
Automatic equipment for arc welding	25.620	14.586	22.544	131.511	140.192	137.360
Other machines and devices for arc welding	139.373	122.394	250.212	19.040	19.040	13.436
Electric machines and devices for laser and / or another beam or plasma-arc welding; electric machines and devices for thermal metal spraying	119.991	124.805	168.741	481.122	336.917	497.283
Spare parts of machines and devices for brazing, welding or thermal metal spraying	129.205	74.319	133.977	131.918	109.092	142.678

The annual need of China in arc welding equipment counts approximately 380 thou pcs, among them 25 % make the equipment for CO_2 metal-arc welding (MAG) [11].

The level of automation and robotization of welding production rises. Necessity in the robots for arc welding is rated in 2.4−2.5 thou units. Welding robots are widely used not only in motor car construction, but also in machine building, construction and transport machine building (railway and electric transport).

There is an increase of application of the cutting equipment. 2 thou units make the annual necessity in gas, plasma and laser cutting equipment. The main portion (around 95 %) is the machines for plasma and gas cutting. Around 70 % of internal market of cutting equipment is provided by Chinese producers. 30 % make a portion of import of this type of equipment from Japan and EC countries. Necessity in equipment for water-jet cutting is also significant. Annual demand in this type of equipment makes around 500 pcs.

Chinese production supplies 60−70 % of welding equipment to internal market. This index has not changed since 2007 as a result of advancing increase of the steel and metal structure production. Therefore, preservation of a significant volume of import of welding equipment with annual increment is quite natural and has exceeded 1 bln of dollars in 2010.

There is an increase of import of welding robots in China. Japan (80 %), Germany, Austria and Switzerland are the main suppliers. The import of welding robots for arc welding from Japan made 1,765 pcs in 2009 (it increased by 12.1 % in relation to 2008). 400 pcs for spot welding and 150 pcs for laser welding, mainly, for microelectronics (production of mobile phones and computers) [11] were purchased in 2009.

The data on volume of the external trading of Chinese electric welding equipment in 2008−2010 according to the information from the COMTRAD database of the UNO [12] represented in Table 5.

Export of electric welding equipment rises with a substantial rate having the advantage in price. In a period of 2008−2010 the export of electric welding equipment increased by 40 % and import by 5 % regardless the world crisis as can be seen from Table 5. Most of developed countries of the world, including USA, Canada, Germany, France, Russia, Japan, Korea etc. export these production. The equipment for arc welding (direct and alternating current power sources) dominates in the structure of export of Chinese electric welding equipment with 24 %. The equipment for plasma-arc welding and cutting make 20 % and spare part are 22 %. China mainly imports highly technological electric welding equipment for electron beam and laser welding, arc, resistance automatic welding and semi-automatic welding.

Opening of the national internal market and appearance of the leading producers of welding engineering, i.e. Lincoln Electric, General Electric, ESAB, Osaka Transformer Company (OTC), KUKA, Termadyne, Miller etc. in it are tightly related with the rapid development of Chinese welding industry in the XXI century. This allows reorganizing the national welding industry in the country, arranging production of the most state-of-the-art foreign welding engineering, implementing modern methods of management of own production, significantly increasing the level of welders' training.

ESAB Company from Switzerland, the largest in the world producer of welding engineering, actively entered in the Chinese market in 2005. They created company «Shanghai−ESAB Welding & Cutting Systems China Ltd.» for production of welding engineer-

ing and opened a plant for manufacture of automatic welding and cutting equipment. The first ESAB plant on production of solid and flux-cored welding wire with production capacity of 40 thou t of welding wire per year was launched in China in 2006. Another plant on production of welding consumables — flux-cored wire was started in 2008. Capital investments in this enterprise made 30 mln of dollars. Production capacity of the enterprise is 10 thou t of flux-cored wire per year [14].

American company «Lincoln Electric» opened its first plant on production of solid and flux-cored wire in 1989. Today they have five plants on production of welding consumables and filler materials (flux-cored and solid wire, fused flux) and automatic welding equipment in China. Construction of a plant on production of new grades of wires for MIG welding as well as new plant on welding flux manufacture [15] were started in 2010.

National welding industry of China counts more than 1000 enterprises. These are mainly small and medium concerns with the annual output up to 160 thou of dollars. More than ten national industrial companies and companies, for example, Nantong Sanjiu Welding Machine Co. Ltd., Shougang Group, Chengdu Hanyan Weida Automatic Welding Equipment Co. Ltd., Shanghai DONSUN Welding Group Co. Ltd. with annual output around 10 bln of RMB (around 1.6 bln of dollars) exist in the country. These are, as a rule, the large scientific-and-production complexes. Their activity covers the whole range of product life cycle: from development to after-sale service, including staff training.

Reorganization of the industrial enterprises is performed and conditions for increase of a number of large-scale and serial production enterprises are developed for the purpose of increasing the competitiveness of Chinese welding industry in the world market and growing the export of production in the country. Taking into account the peculiarities of small and medium enterprises, the emphasis is made on creation of small, but strictly specialized companies, which can be termed «unique».

Enterprises are obliged to increase a rate of technological reequipment and promote development of the new products due to competitiveness rise. Significant number of enterprises appeared in the welding industry of China which can invest costs in the investigations and development of new technologies and products. Thus, for example, the first national robot for spot welding «165 spot-welding robot» [16] was developed and implemented into production as a result of the joint project of Institute of Robotics Technology of Harbin Institute of Technology and motor-car giant Chery Automobile Co.

Chinese specialists note that «the era of small profit» is to come in China in the nearest future. The increase of the profit due to low cost of raw materials and salaries has been already exhausted. Implementation of high technologies, methods of enterprise management and rise in qualification of workers and staff are the single possible way of profit increase at the enterprises.

1. (2011) *Steel Statistical Yearbook 2011*. Brussels: Worldsteel committee on economic studies.
2. (2011) Review of ferrous metallurgy of China in a period of 2010. *Chyorn. Metallurgiya*, **4**, 88−95.
3. Hong, Y., Mu, Y. (2010) China's steel industry: an update. *EAI Background Brief*, 501(**1**).
4. (2010) China steel industry and its impact on United States. Issues for Congress. *CRS Report for Congress*, **8**, 28.
5. Yusheng, J. (2011) Trends of development of China's ferrous metallurgy. *Chyorn. Metallurgiya*, **1**, 5−9.
6. Pokhodnya, I.K., Kotelchuk, A.S. (2010) Advance of ferrous metallurgy and welding consumables production in PRC (Review). *The Paton Welding J.*, **4**, 30−33.
7. (2011) China's 12th five-year plan: iron and steel. *KPMG*, **4**, 7.
8. (2011) Decrease in CO_2 emissions in ferrous metallurgy. *Novosti Chyornoj Metallurgii za Rubezhom*, **1**, 94−98.
9. (2010) *Chapter International plc*: Annual report.
10. Welder branch of view, to seize the changes in market demand, it is the key to the development. *http:www.feipush.com/news/*
11. (2010) Chinese market a fast demand recovery advances. *The Japan Welding News for the World*, 14(**51**), 3−4.
12. United Nations Statistics Division — Commodity Trade Statistics Database (COMTRADE). *http:comtrade.un.org*
13. China inverter welding and cutting equipment industry report, 2010−2011 by ResearchInChina. *www.pr-inside.com/china-inverter-welding-and-cutting-equipment-r2627494.htm*
14. Welding-machine-industry-China-step-step-enhance-competitiveness of enterprises. *http://www.sourcejuice.com*
15. (2010) *Strong... and growing stronger*: Annual report. Lincoln Electric.
16. China's first 165 kilograms class successful application of spot welding robot. *http://www.sourcejuice.com*

SYSTEM OF VIDEO OBSERVATION OF THE PROCESS OF TIG WELDING OF TITANIUM STRUCTURES

V.A. KOLYADA

E.O. Paton Electric Welding Institute, NASU, Kiev, Ukraine

A system for video observation of the process of narrow-gap TIG welding of titanium structures at currents of up to 500 A was developed. Video observation system is equipped with the means for automatic control of photoreceiver sensitivity, depending on the intensity of welding arc radiation.

Recently, the scope of application of titanium alloys in different industries has considerably increased, particularly in aircraft construction and shipbuilding. In shipbuilding industry the process of narrow-gap multilayer MIAB welding of 20−100 mm thick titanium structures became widely accepted. In order to control this welding process, the welding machine operator requires feedback devices, ensuring visual observation of the welding zone, which is difficult because of small dimensions of the gap, and varying intensity of light radiation of the arc. As a consequence, in this case it is rational to use machine vision means for realization of visual observation. Standard systems of video observation are not suitable for solving this task, as the functions of automatic adjustment of signal amplification or final adjustment of lens aperture cannot provide an adequate solution of the problem of photoreceiver oversaturation at a high level of external light radiation.

PWI developed a system of video observation of the process of TIG welding of titanium structures, fitted with elements of adaptation to the level of light radiation of the welding arc. The system is a monochromatic digital videocamera with an integrated microprocessor controller. Special light filters are mounted between the videocamera lens and photoreceiver matrix. Standard TV signal in PAL format is used as the output signal. Microprocessor controller is applied for analysis of the obtained images, automatic fine tuning of operating mode of photoreceiver matrix and generation of output TV signal. Also realized is the scaling function, allowing selection of a region in the image that corresponds to the welding zone, and representing it in the form of full-screen frames.

Digital images, generated using the photoreceiver matrix, have a limited dynamic range of pixel intensity, dependent on the digit capacity of analog-digital converters of photoreceiver cells. At insufficient level of external lighting the images can have zero or ex-

tremely low brightness. Here, pixel intensity will be in the vicinity of the dynamic range lower limit. At the same time, exceeding the photoreceiver matrix saturation limit can be observed at a high level of lighting, i.e. pixel intensity will correspond to the upper limit of the range. In both the cases, visual quality and information content of the generated images are extremely low. Thus, stabilization of visual quality of output TV signal requires maintaining a high brightness of images, while avoiding any significant oversaturation of photoreceiver matrix.

Light radiation of the weld pool in TIG welding of titanium structures is characterized by considerable fluctuations of intensity, reduction of which requires controlling videocamera operation mode. Videocamera exposure time e, which determines the total sensitivity of the photoreceiver, was selected as the control signal. Maximum intensity of any of image pixels, i_{max}, depends on the level of photoreceiver lighting L and value of parameter e, assigned in the previous cycle of videocamera operation:

$$i_{max}[n] = l_{max}[n]e[n-1]k_1,$$
$$I_{min} \le i_{max}[n] \le I_{max}, \quad l \ge 0, \quad E_{min} \le e[n] \le E_{max}, \tag{1}$$

where n is the cycle number; $l_{max} \in L$ is the maximum level of lighting of one of the photoreceiver cells; $k_1 > 0$ is the videocamera gain factor; $l_{max} > 0$, $I_{min} \ge 0$ are the upper and lower limits of the general dynamic range of pixel intensity; $E_{max} > 0$, $E_{min} > 0$ are the limits of exposure variation, respectively.

If the value in the right-hand part of equation (1) is equal to or exceeds I_{max}, this leads to saturation of photoreceiver matrix pixels. The quantity of pixels with maximum intensity can be assigned in the following form:

$$m_{max}[n] = i_s[n]k_2[n], \quad i_s \ge 0, \tag{2}$$

where $i_s[n] = l[n]e[n-1]k_1 - I_{max}$; $k_2[n] \ge 0$ is the coefficient dependent on distribution of light radiation intensity of the observed object.

From expressions (1) and (2) it follows that the videocamera is a non-linear object, for automatic control of which it is rational to apply an optimum or adaptive approach [1]. Parameters $I_{max}[n]$ and
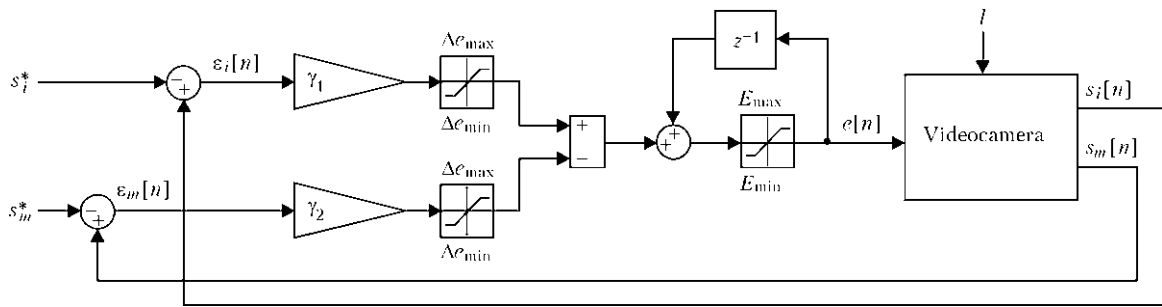
Figure 1. Schematic of automatic regulator for stabilization of image visual quality (for designations see the text)

$m_{\max}[n]$ are independent. Therefore, regulator feedback should be represented by two signals, one of which characterizes the current brightness of the image, and the other — the saturation level of the photoreceiver. Brightness index is calculated as

$$s_i[n] = \frac{I_{\max} - i_{\max}[n]}{I_{\max}}. \tag{3}$$

Level of photoreceiver saturation is determined as follows:

$$s_m[n] = \frac{m_{\max}[n]}{M}, \tag{4}$$

where M is the total number of image pixels.

Quality control criteria for minimizing the instant value of errors, has the following form:

$$J(e) = \varepsilon^2[n] + \varepsilon_m^2[n] = (s_i[n] - s_i^*)^2 + \\ + (s_m[n] - s_m^*)^2 \to \min, \tag{5}$$

where s_i^*, s_m^* are the setting impacts.

At zero s_i^*, s_m^* values and fixed aperture, minimization of error by brightness index is achieved by extension of videocamera exposure, while minimizing

the error by saturation level, contrarily, is achieved by its lowering. To find an optimum solution, a gradient method was selected [2], in keeping with which the equation of discrete regulator will be written as follows:

$$e[n] = e[n-1] + \nabla J(e) = e[n-1] + \\ + \gamma_1 \varepsilon_i[n] - \gamma_2 \varepsilon_m[n], \tag{6}$$

where $\gamma_1 > 0$, $\gamma_2 > 0$ are the error gain factors.

Schematic of synthesized automatic regulator is shown in Figure 1. Value of gain factor γ_1, γ_2 was pre-determined by simulation in MatLab environment, and was additionally precised experimentally. Minimizing of control error was taken as the main criterion of regulator setting up, as considerable overregulation can lead to oscillatory process (image blinking). Additional limitations from $\Delta e_{\min}$ up to $\Delta e_{\max}$ are also imposed on the amplitude of the change of control signal $e[n]$.

Logic of regulator operation at $s_i^* = 0$, $s_m^* = 0$ is illustrated using Figure 2. At the initial moment of time at $l[0] > 0$ an error by brightness index $\varepsilon_i[n]$ arises. In subsequent steps exposure $e[n]$ increases up to reaching the upper limit of brightness range
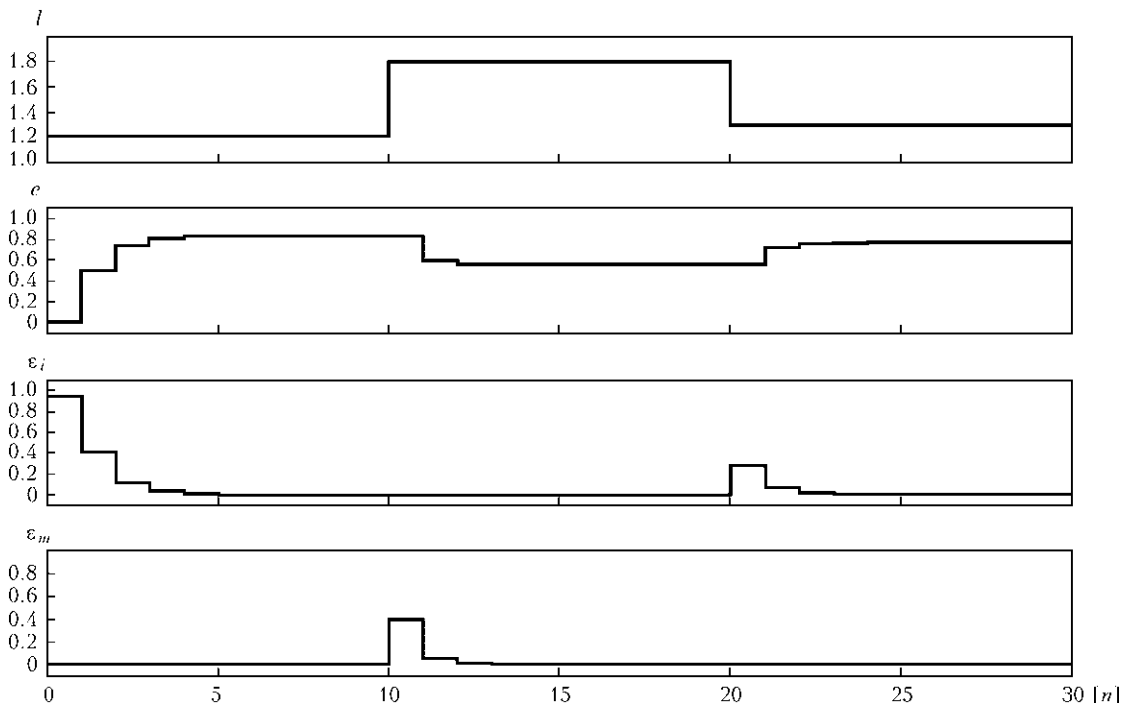

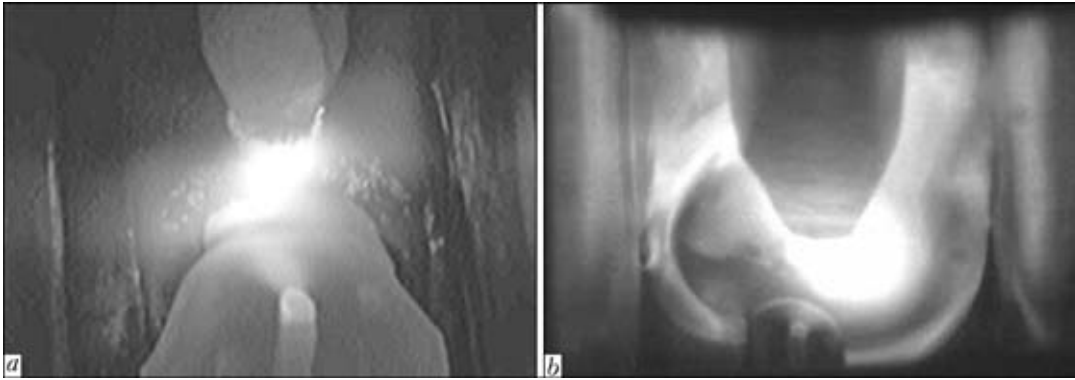**Figure 2.** Behaviour of automatic regulator at variation of external lighting of photoreceiver

Figure 3. Examples of generated images of TIG welding zone at welding current of 100 (*a*) and 500 (*b*) A

$(i_{max}[n] \to I_{max})$. At saturation of photoreceiver matrix $(\varepsilon_m[n] > 0)$ videocamera exposure gradually decreases and so on. Thus, stabilization of visual quality of the image near the saturation boundary is ensured. If required, assigning $\Delta e_{min} = 0$, $s_i^* > 0$ and/or $s_m^* > 0$, we can provide a certain zone of regulator insensitivity to variation of external lighting.

At zero or low external lighting the exposure increases up to reaching the upper level E_{max}, and at the same time it is possible to increase the total image brightness to the maximum. The range of effective stabilization of image visual quality can be adjusted using the lens aperture.

To improve visual perception of the TV signal, gamma-correction of output images is applied elementwise. Increase of gamma-correction coefficient allows enhancing the contrast and intelligibility of image dark areas, not making the light details of the frame too contrast or bright.

During experiments it was established that the developed video observation system provides an acceptable level of detalization of output TV signal for the entire range of welding currents (110–500 A), and allows the welding operator a sufficient degree of control of the welding process. All the necessary objects are clearly visible in Figure 3: electrode, welding arc, groove walls, liquid metal region.

The video observation system was introduced as standard equipment of the machine for TIG welding of titanium of VT20 and VT6 grade. The proposed approach to control of photoreceiver sensitivity can be applied for development of systems of video observation of any objects, which are characterized by a considerable range of variation of light radiation intensity.

1. Aleksandrov, A.G. (1989) *Optimal and adaptive systems*. Moscow: Vysshaya Shkola.
2. Tsypkin, Ya.Z. (1968) *Adaptation and training in automatic systems*. Moscow: Nauka.